

EFFECT OF PARTICLE SIZE ON HEAT OF HYDRATION OF POZZOLAN-  
INCORPORATED CEMENTS

A THESIS SUBMITTED TO  
THE GRADUATE SCHOOL OF NATURAL AND APPLIED SCIENCES  
OF  
MIDDLE EAST TECHNICAL UNIVERSITY

BY  
MEHMET KEMAL ARDOĞA

IN PARTIAL FULFILLMENT OF THE REQUIREMENTS  
FOR  
THE DEGREE OF MASTER OF SCIENCE  
IN  
CIVIL ENGINEERING

JUNE 2014



Approval of the thesis:

**EFFECT OF PARTICLE SIZE ON HEAT OF HYDRATION OF  
POZZOLAN-INCORPORATED CEMENTS**

submitted by **MEHMET KEMAL ARDOĞA** in partial fulfillment of the  
requirements for the degree of **Master of Science in Civil Engineering**  
**Department, Middle East Technical University** by,

Prof. Dr. Canan Özgen

Dean, Graduate School of **Natural and Applied Sciences**

Prof. Dr. Ahmet Cevdet Yalçiner

Head of Department, **Civil Engineering**

Prof. Dr. Mustafa Tokyay

Supervisor, **Civil Engineering Dept., METU**

Assoc. Prof. Dr. Sinan Turhan Erdoğan

Co-supervisor, **Civil Engineering Dept., METU**

**Examining Committee Members:**

Prof. Dr. İsmail Özgür Yaman

Civil Engineering Dept., METU

Prof. Dr. Mustafa Tokyay

Civil Engineering Dept., METU

Assoc. Prof. Dr. Sinan Turhan Erdoğan

Civil Engineering Dept., METU

Assoc. Prof. Dr. Mustafa Şahmaran

Civil Engineering Dept., Gazi University

Asst. Prof. Dr. Çağla Meral

Civil Engineering Dept., METU

**Date: 19.06.2014**

**I hereby declare that all information in this document has been obtained and presented in accordance with academic rules and ethical conduct. I also declare that, as required by these rules and conduct, I have fully cited and referenced all material and results that are not original to this work.**

Name, Last name : Mehmet Kemal Ardoğa

Signature :

## **ABSTRACT**

### **EFFECT OF PARTICLE SIZE ON HEAT OF HYDRATION OF POZZOLAN INCORPORATED CEMENTS**

Ardoğa, Mehmet Kemal

M. Sc., Department of Civil Engineering

Supervisor: Prof. Dr. Mustafa Tokyay

Co-supervisor: Assoc. Prof. Dr. Sinan Turhan Erdoğan

June 2014, 109 pages

Hydration reactions, the chemical reactions between cement and water are exothermic. The determination of the heat of hydration and rate of heat evolution of cement are extremely important to understand the hydration mechanism.

In this study, clinker and gypsum rock were ground after adding natural pozzolan (trass) with various proportions until a specific fineness value and different cements were obtained. These cements were divided into particle size groups with a sonic sifter and the heat of hydration and rate of heat evolution of each cement group were investigated over a 2-day period. In addition, chemical analyses and particle size distribution analyses were performed with the goal of trying to understand whether there was a connection between cement average particle size, pozzolan content and heat of hydration and the rate of heat evolution periods, or not.

It is found that, the addition of a small amount natural pozzolan enhances 2-day heat of hydration of cement due to its nucleation effect. However, in the case where higher amounts of pozzolan are used, the hydration heat decreases because of the dilution effect. Moreover, other possible reasons for the changes in rates of heat

evolution of different cement groups are predicted to be the alteration in  $\text{Ca}^{2+}$  concentration and dispersion effect. It is shown that fine size groups are more reactive than the coarse size groups during hydration. Using the particle size distributions and chemical analyses of size groups, the behavior of the unsieved cement sample can also be estimated.

Keywords: cement, natural pozzolan, particle size, hydration, heat of hydration.

## ÖZ

### **TANE BOYUTUNUN PUZOLAN İÇEREN ÇİMENTOLARIN HİDRATASYON İSİSİNE ETKİSİ**

Ardoğa, Mehmet Kemal

Yüksek Lisans, İnşaat Mühendisliği Bölümü

Tez Yöneticisi: Prof. Dr. Mustafa Tokyay

Ortak Tez Yöneticisi: Doç. Dr. Sinan Turhan Erdoğan

Haziran 2014, 109 sayfa

Çimento ile su arasındaki kimyasal reaksiyonlar olan hidrasyon tepkimeleri ekzotermiktir. Çimentonun hidrasyon ısı ve ısının oluşum hızının tespiti, çimento hidrasyon mekanizmasını anlamak için son derece önemlidir.

Bu çalışmada, klinker ve alçı taşı, değişik oranlarla doğal puzolan (tras) katıldıktan sonra belli bir inceliğe kadar öğütülmüş ve farklı çimentolar elde edilmiştir. Bu çimentolar sonik eleyici ile parçacık büyüklük gruplarına ayrılmış ve 2 günlük zaman diliminde her çimento grubunun hidrasyon ısıları ve hidrasyon ısı yayılım hızları araştırılmıştır. Ek olarak, kimyasal analizleri ve parçacık büyüklük analizleri, çimento ortalama parçacık büyüklüğü, puzolan miktarı ile hidrasyon ısı ve hidrasyon ısı yayılım hızı aşamaları arasında bir ilişkinin olup olmadığının anlaşılmasına çalışılması amacı ile yapılmıştır.

Az miktarda doğal puzolan ilavesinin 2 günlük çimentonun hidrasyon ısını, çekirdeklenme etkisi nedeniyle, arttırdığı bulunmuştur. Ancak, yüksek miktarda puzolan kullanıldığı durumda ise, hidrasyon ısı, seyrelme etkisi yüzünden azalmıştır. Ayrıca, değişik çimento gruplarının ısı yayılım hızlarındaki değişimlerin

diğer olası nedenlerinin  $\text{Ca}^{2+}$  konsantrasyonundaki deęişim ve saçılım etkisi olduęu tahmin edilmektedir. İnce büyüklük gruplarının, hidratasyon sırasında iri büyüklük gruplarından daha etkin olduęu gösterilmiştir. Büyüklük gruplarının parçacık büyüklük dağılımları ve kimyasal analizleri kullanılarak, elenmemiş çimento örneğinin davranışı da tahmin edilebilmiştir.

Anahtar kelimeler: çimento, doğal puzolan, parçacık büyüklüğü, hidratasyon, hidratasyon ısısı.



To My Family,

## ACKNOWLEDGEMENTS

Firstly, I would like to express my deepest appreciation to my supervisor Prof. Dr. Mustafa Tokyay and my co-supervisor Assoc. Dr. Sinan Turhan Erdoğan for their support, criticism, guidance and supervision during the preparation of this thesis.

Secondly, I would like to thank to my parents, O. Nedim and Safiye Neşe, and my brother Armağan for their great support and patience. In addition, I want to acknowledge the support of my aunts, R. Aysel and Nazife Coşkunyel and my cousin N. Erce Batur.

For their great support, I should express my great appreciation to Prof. Dr. İsmail Özgür Yaman and Prof. Dr. Turhan Y. Erdoğan.

Special thanks go to my friend Hasan Eser for his wonderful support, help and motivation during the preparation of the thesis. Moreover, for their support and help, I would like to thank to Murat Şahin, Meltem Tangüler, Burhan Aleessa Alam and Cuma Yıldırım.

I want to express my gratitude to my friends, Utku Albostan, Mert Bilir, Abdullah Demir, Alireza Sassani, Mahdi Mahyar and Okan Koçkaya for their motivation.

For their great cooperation, I should thank to R&D Laboratories of Turkish Cement Manufacturers Association (TCMA).

Last but not least, this study or other similar studies would not have been possible without the heroism of our ancestors. I would like to express my gratitude to Mustafa Kemal Atatürk, İsmet İnönü and their fellow fighters.

## TABLE OF CONTENTS

ABSTRACT .....	v
ÖZ .....	vii
ACKNOWLEDGEMENTS .....	x
TABLE OF CONTENTS .....	xi
LIST OF TABLES .....	xv
LIST OF FIGURES .....	xvii
LIST OF ABBREVIATIONS .....	xx
CHAPTERS	
1. INTRODUCTION .....	1
1.1 General.....	1
1.2 Objective and Scope .....	3
2. LITERATURE REVIEW .....	5
2.1 General.....	5
2.2 Portland Cements .....	5
2.2.1 Raw Materials .....	6
2.2.2 Production Stages.....	6
2.2.3 Oxides and Their Notation .....	7
2.2.4 Bogue Equations .....	8
2.2.5 Impurities.....	9
2.2.6 Chemical Reactions.....	9
2.2.6.1 Products of Chemical Reactions.....	10
2.2.6.2 Hydration of Clinker Compounds .....	11
2.2.6.2.1 Hydration of Calcium Silicates Phases.....	11

2.2.6.2.2 Hydration of Aluminate Phases .....	11
2.2.6.2.3 Hydration of Ferrite Phases .....	12
2.2.7 Mineral Admixtures .....	12
2.2.7.1 Types of Mineral Admixtures .....	13
2.2.7.1.1 Natural Mineral Admixtures .....	13
2.2.7.1.2 Artificial Mineral Admixtures .....	14
2.2.7.2 Production of Pozzolanic Cements .....	15
2.2.7.3 Pozzolanic Reaction in Cements .....	16
2.2.7.4 Advantages .....	17
2.2.8 Types of Portland Cements .....	17
2.2.9 Other Cement Types .....	19
2.3 Heat of Hydration in Cement .....	19
2.3.1 Introduction .....	19
2.3.2 Heat Evolution Rate and Its Stages .....	20
2.3.2.1 Pre-induction Period .....	21
2.3.2.2 Dormant (Induction) Period .....	22
2.3.2.2.1 Impermeable Layer Hypothesis .....	22
2.3.2.2.2 Other Hypotheses .....	22
2.3.2.3 Acceleration Period .....	23
2.3.2.4 Post-Acceleration Period .....	23
2.3.3 Factors Influencing Heat of Hydration and Rate of Heat Evolution .....	23
2.3.3.1 Fineness .....	23
2.3.3.2 Mineral Admixtures .....	24
2.3.3.3 Chemical Composition .....	27
2.3.3.4 Water Amount .....	28
2.3.3.5 Temperature .....	29
2.3.3.6 Particle Size Distribution .....	29
2.3.3.7 Chemical Admixtures .....	29

2.3.4 Methods to Measure Heat of Hydration .....	30
2.3.4.1 Solution Method .....	30
2.3.4.2 Semi-adiabatic Method .....	30
2.3.4.3 Isothermal Calorimeter Method .....	30
2.3.5 Significance of Determining Heat of Hydration.....	31
2.3.5.1 Rate and Degree of Hydration.....	31
2.3.5.2 Temperature .....	32
2.3.5.3 Chemical Composition.....	33
2.3.5.4 Strength.....	34
2.3.5.5 Setting Time .....	34
2.3.5.6 Shrinkage .....	35
3. EXPERIMENTAL PROCEDURE .....	37
3.1 General.....	37
3.1.1 Materials.....	38
3.2 Grinding of cements .....	38
3.3 Size Grouping of Cements .....	39
3.4 Measurement of the Particle Size Distribution of Cements.....	42
3.5 Measurement of Heat of Reaction of Cements .....	42
4. RESULTS AND DISCUSSION.....	45
4.1 General.....	45
4.2 Mass fractions of Cement Groups .....	45
4.3 Particle Size Distributions of Cement Groups .....	47
4.4 Grinding Time of Cement Groups.....	51
4.5 48-h Heat of Hydration of Cement Samples.....	52
4.6 Rate of Heat of Hydration of Cement Samples.....	56
4.6.1 First Peaks of Rate of Heat of Hydration of Cement Samples .....	61
4.6.2 Dormant (Induction) Period of Rate of Heat of Hydration of Cement Samples .....	65

4.6.3 Second (Main) Peak of Rate of Heat of Hydration of Cement Samples ...	69
4.7 Estimating the Contribution of Trass Incorporation on Early Heat Evolution of Cement Samples .....	73
4.8 Estimating the Heat Evolution Characteristics of the Original Cement from the Size Groups .....	78
4.9 Summary.....	88
5. CONCLUSIONS .....	91
5.1 General .....	91
5.2 Recommendations for Future Studies .....	93
REFERENCES.....	95
APPENDICES.....	101
A. Cumulative Particle Size Distributions of Cements .....	101
B. A Calculation Example About Estimating the Contribution of Trass Incorporation on Early Heat Evolution .....	105
C. A Calculation Example About Estimating the Heat Evolution Characteristics of the Original Cement from the Size Groups .....	107

## LIST OF TABLES

### TABLES

Table 2.1. The raw materials for calcereous and argillaceous materials for cement production (Bogue, 1955; ACI, 2001) .....	6
Table 2.2. The percentage values of oxide in a typical portland cement and cement chemistry notations (Erdoğan, 2010) .....	8
Table 2.3. The names, chemical notations and notations with respect to cement chemistry of clinker compounds (Erdoğan, 2010) .....	8
Table 2.4. The possible main products of hydration reactions (Erdoğan, 2010) .....	10
Table 2.5. Some natural pozzolans, their chemical compositions and geological origins (Lohtia and Joshi, 1995) .....	14
Table 2.6. Some artificial pozzolans and their chemical compositions (Erdoğan, 2010) .....	14
Table 2.7. Properties of different pozzolanic cements containing natural pozzolans for the same fineness with respect to their production stages .....	15
Table 2.8. Types of cements with respect to their clinker compound contents (ACI, 2001) .....	18
Table 2.9. EN cement types (TS EN 197 – 1) .....	18
Table 2.10. Heat of hydration of Portland cement clinker compounds at the given age (J/g) (Mehta and Monteiro, 2006; Odler, 2004) .....	28
Table 3.1. Chemical analysis of the materials used in experiments .....	38
Table 3.2. Charge properties of laboratory ball mill .....	38
Table 3.3. Percentage and mass of the raw materials used in each cement group before grinding process .....	39
Table 3.4. Designation of the subgroups of cements .....	40
Table 3.5. Chemical analysis results of 0P cements .....	41
Table 3.6. Chemical analysis results of 3P cements .....	41
Table 3.7. Chemical analysis results of 11P cements .....	41

Table 3.8. Chemical analysis results of 22P cements.....	42
Table 4.1. Mass fractions of the raw materials in each cement group after grinding.....	46
Table 4.2. For each cement, the grinding time for required specific surface .....	51
Table 4.3. 48-hour heat of hydration of cements .....	54
Table 4.4. The time and rate of heat of hydration values of cement samples during dormant period .....	65
Table 4.5. Time of occurrence of second peak .....	69
Table 4.6. Maximum rate of heat of hydration values during second peak .....	70
Table 4.7. The estimated and actual time values for the emergence of second peak.....	87
Table C.1. The values for 48-h heats of hydration, 24-h rates of heat of hydration and clinker and gypsum contents observed in 3P cements .....	101
Table C.2. The particle size distribution of 3PO.....	101



## LIST OF FIGURES

### FIGURES

Figure 2.1. The heat evolution curve of a cement at a constant temperature (20 °C) and w/c = 0.375, adapted from (Lawrence, 2004).....	20
Figure 2.2. The rate of hydration heat curve of a typical portland cement (Odler, 2004) .....	21
Figure 2.3 Schematic representation of the hypothesis of hydration enhancement by fine admixtures (Lawrence et al., 2003) .....	27
Figure 3.1 Parts of a sieve stack .....	40
Figure 4.1. Particle size distributions of original groups of cement samples.....	48
Figure 4.2. Particle size distributions of 0-10 µm size groups of cement samples....	48
Figure 4.3. Particle size distributions of 10-35 µm size groups of cement samples...	49
Figure 4.4. Particle size distributions of 35-50 µm size groups of cement samples...	49
Figure 4.5. Particle size distributions of 50-2000 µm size groups of cement samples. ....	50
Figure 4.6. 48-hour cumulative heat of hydration of 0P cements .....	52
Figure 4.7. 48-hour cumulative heat of hydration of 3P cements. ....	52
Figure 4.8. 48-hour cumulative heat of hydration of 11P cements .....	53
Figure 4.9. 48-hour cumulative heat of hydration of 22P cements .....	53
Figure 4.10. 48-hour heat of hydration of cements vs. its size subgroups.....	54
Figure 4.11. Rate of heat evolution of original groups in the 48 hours .....	56
Figure 4.12. Rate of heat evolution of 0-10 µm size groups in the 48 hours.....	57
Figure 4.13. Rate of heat evolution of 10-35 µm size groups in the 48 hours.....	57
Figure 4.14. Rate of heat evolution of 35-50 µm size groups in the 48 hours.....	58
Figure 4.15. Rate of heat evolution of 50-2000 µm size groups in the 48 hours .....	58
Figure 4.16. Rate of heat evolution of 0P cements in the 48 hours.....	59

Figure 4.17. Rate of heat evolution of 3P cements in the 48 hours .....	59
Figure 4.18. Rate of heat evolution of 11P cements in the 48 hours.....	60
Figure 4.19. Rate of heat evolution of 22P cements in the 48 hours.....	60
Figure 4.20. Rate of heat evolution of 0P cements in the first minutes.....	61
Figure 4.21. Rate of heat evolution of 3P cements in the first minutes.....	61
Figure 4.22. Rate of heat evolution of 11P cements in the first minutes.....	62
Figure 4.23. Rate of heat evolution of 22P cements in the first minutes.....	62
Figure 4.24. The first peak times of cements.....	63
Figure 4.25. Maximum values of rate of heat of hydration for the first peak.....	63
Figure 4.26. Rate of heat evolution of 0P cements during dormant period .....	66
Figure 4.27. Rate of heat evolution of 3P cements during dormant period .....	66
Figure 4.28. Rate of heat evolution of 11P cements during dormant period.....	67
Figure 4.29. Rate of heat evolution of 22P cements during dormant period.....	67
Figure 4.30. Rate of heat evolution of 0P cements during second peak .....	71
Figure 4.31. Rate of heat evolution of 3P cements during second peak .....	71
Figure 4.32. Rate of heat evolution of 11P cements during second peak .....	72
Figure 4.33. Rate of heat evolution of 22P cements during second peak .....	72
Figure 4.34. Normalized heat of hydration of pozzolanic cement groups and the actual heat of hydration of the non-pozzolanic cement for original groups .....	75
Figure 4.35. Normalized heat of hydration of pozzolanic cement groups and the actual heat of hydration of the non-pozzolanic cement for 0-10 $\mu\text{m}$ size groups .....	75
Figure 4.36. Normalized heat of hydration of pozzolanic cement groups and the actual heat of hydration of the non-pozzolanic cement for 10-35 $\mu\text{m}$ size groups ...	76
Figure 4.37. Normalized heat of hydration of pozzolanic cement groups and the actual heat of hydration of the non-pozzolanic cement for 35-50 $\mu\text{m}$ size groups ...	76
Figure 4.38. Normalized heat of hydration of pozzolanic cement groups and the actual heat of hydration of the non-pozzolanic cement for 50-2000 $\mu\text{m}$ size groups	77
Figure 4.39. Heat of hydration of 0P cements .....	80
Figure 4.40. Heat of hydration of 3P cements .....	80
Figure 4.41. Heat of hydration of 11P cements .....	81

Figure 4.42. Heat of hydration of 22P cements.....	81
Figure 4.43. Measured vs calculated heat of hydration for 0P cements .....	82
Figure 4.44. Measured vs calculated heat of hydration for 3P cements .....	82
Figure 4.45. Measured vs calculated heat of hydration for 11P cements .....	83
Figure 4.46. Measured vs calculated heat of hydration for 22P cements .....	83
Figure 4.47. Measured / calculated heat of hydration vs time graph for 0P, 3P, 11P and 22P cements .....	84
Figure 4.48. Rate of heat evolution for 0P cements .....	85
Figure 4.49. Rate of heat evolution for 3P cements .....	85
Figure 4.50. Rate of heat evolution for 11P cements.....	86
Figure 4.51. Rate of heat evolution for 22P cements.....	86
Figure 4.52. Measured / calculated rate of heat evolution graph for 0P, 3P, 11P and 22P cements.....	87
Figure A.1. The cumulative particle size distribution of 0P cements.....	101
Figure A.2. The cumulative particle size distribution of 3P cements.....	102
Figure A.3. The cumulative particle size distribution of 11P cements.....	102
Figure A.4. The cumulative particle size distribution of 22P cements.....	103

## **LIST OF ABBREVIATIONS**

ACI:	American Concrete Institute.
ASTM:	American Society for Testing and Materials.
CEN:	European Committee for Standardization.
DEF:	Delayed ettringite formation.
EN:	European Norms.
HH:	Heat of hydration.
PSD:	Particle size distribution.
RHE:	Rate of heat evolution.
TCMA:	Turkish Cement Manufacturers' Association.
TS:	Turkish Standards.
w/c:	water to cement ratio.

## **CHAPTER 1**

### **INTRODUCTION**

#### **1.1 General**

Concrete essentially consists of cement, aggregates and water. To improve certain properties of fresh and hardened states of concrete, chemical admixtures and mineral additives can be added. Immediately after mixing, the state of concrete becomes plastic (the shape of concrete can be reformed), and it is called fresh concrete. Chemical reactions between cement and water start when they come into contact with each other. As the reactions proceed, fresh concrete transforms into hardened concrete and concrete gains rigidity. After this point, its shape can not be changed.

Cement is the binding material of aggregates in concrete. The chemical reactions, called hydration, occur due to the interaction between cement and water and with time, the products from these exothermic reactions can give a binding property to cement, and therefore concrete.

All over the world, due to reasons such as economics, lower environmental impact or higher durability characteristics of concrete, some mineral additives are used in the production of cement and “blended cement” is produced by one of two different methods: Intergrinding and separate blending. Cements from these two different processes have different properties like compressive strength and setting time due to their different homogeneity and average particle sizes. For the same fineness value, interground cements can have a higher setting time and a lower energy requirement

than separately blended cements depending on the type of mineral addition. (Erdem et al., 2006; Erdoğan et al., 1999).

In general, mineral admixtures, depending on their origins, can be natural or artificial and different pozzolans can affect concrete properties in different ways even if their origins are the same. Natural pozzolans, generally originated from volcanic rocks, can be obtained from nature while artificial ones are the by-products of different industries. Since in the past, Anatolia has suffered many volcanic activities, Turkey is one of the richest countries in the world from the point of possible natural pozzolan deposits (Erdoğan et al., 2009). One of the most common types of natural pozzolans used in cement and concrete industry is trass in Turkey. Trass is a volcanic tuff which is transformed from volcanic glass by hydrothermal activity (Mehta and Monteiro, 2006). Although the name trass is being used for every type of natural pozzolan in Turkey, it refers to only one single type (Erdoğan et al., 2009). The general usage of trass is as a replacement of cement, instead of an additive for concrete. The use of trass provides not only the reduction of cost because of lower clinker usage, but also decreases the environmental impact of cement and hence, concrete (Erdoğan et al., 2009).

The reactions between cement and water are exothermic. They produce some amount of heat called heat of hydration. Heat of hydration on short term can be influenced by fineness, particle size distribution and clinker characteristics of cement, impurities and mineral additive content (Erdoğan et al., 2009).

If the fineness of a cement is higher, the surface area of this cement becomes higher also. Because, the reactions start from the surface of the cements grains, from the very beginning, the amount of the finer cement which reacts with water in a unit time is excessively higher than for coarser cements (Erdoğan, 2010). Therefore, the heat of hydration and rate of heat evolution increase due to enhancing rate of hydration.

According to past studies, due to the different grindability of two different materials (the clinker and the mineral additive), the particle size distribution curves should be also considered besides the fineness value of cements (Uzal and Turanlı, 2003).

Various clinker compounds have different rates of heat evolution and heat of hydration in the same time periods. Per one gram, alite and aluminate phases produce more heat than belite and ferrite phases (Mehta and Monteiro, 2006). Moreover, the rates of heat evolution of these compounds are also different than each other (Erdoğan, 2010). The proportion of these compounds will affect the hydration; and consequently, the rate of heat evolution.

Impurities will be considered as an important factor while determining the heat of hydration. Change in the amount of sulfate results in fluctuations in the maximum rate of heat evolution and heat of hydration (Odler, 2004).

The rate of heat evolution curve of a typical cement has a number of peak points. There are several theories to explain these points. The most widely accepted one is the impermeable layer hypothesis (Odler, 2004) referring to an impervious deposit of C-S-H gel on the surface during the beginning of the hydration.

Determination of the heat of hydration is important for fresh concrete operations. During mixing, transporting, casting and finishing of concrete, the temperature of concrete can rise. In extreme weather cases, like hot or cold weather concrete, the heat may be the most important parameter affecting the properties of concrete. Extreme weather cases can influence the mechanical properties of concrete (Erdoğan, 2010).

Various methods are used to measure the heat of hydration produced by the reactions between cement and water. Isothermal conduction calorimetry method is considered as a better choice among the others due to its easiness, repeatability and reproducibility (Arndt et al., 2007; Siler et al., 2012). According to ASTM C 1702, the related standard, in isothermal calorimetry, cement and water are combined at constant temperature, and the heat is measured.

## **1.2 Objective and Scope**

The objective of this study is to determine the differences in the heat of hydration and rate of heat of hydration evolution using the different size groups of pozzolan-incorporated cements. For this purpose, the effects of particle size distributions,

clinker and addition amounts in each particle size group, 0-10  $\mu\text{m}$ , 10-35  $\mu\text{m}$  35-50  $\mu\text{m}$  and 50-2000  $\mu\text{m}$ , on heat of hydration and rate of heat evolution are investigated. Analyzing these effects separately, the effects of using of trass as an additive in a cement on the hydration process is investigated.

Chapter 1 contains general information about the study. It also describes the objective and scope of the thesis. Chapter 2 presents a review of the literature on cement, mineral admixtures, heat of hydration of cements, factors influencing the heat of hydration of cements, and the significance of prediction the heat of hydration of cement. The experimental procedure followed, the chemical and physical properties of raw materials and cements, and an explanation of the experiments carried out form Chapter 3. Chapter 4 presents the results of experiments. A discussion of results is also given in this chapter. Finally, in Chapter 5, the study, discussion of results and conclusions are summarized. Recommendations for further studies are also given.



## **CHAPTER 2**

### **LITERATURE REVIEW**

#### **2.1 General**

Portland cement has been used for decades due to its binding property. During the reactions of water and portland cement particles, portland cement gains this property and releases heat. The amount of heat released and the rate of heat evolution can give important information about the properties of the cement, and hence the concrete (Erdoğan, 2010).

#### **2.2 Portland Cements**

Cements are binder materials which react with water. Despite the fact that nowadays there are many types of cements used all over the world, for years the most popular one has been the ordinary portland cement produced from only clinker and gypsum (Erdoğan, 2010).

Portland cement is a construction material used all over world. Since it resembled the rocks on the isle called Portland, and had been patented with the name of this isle, it is known as portland cements. Since it is a hydraulic binder (it can set and harden under water and it is stable in aqueous media), it has been used in reinforced concretes and mortars in different construction applications.

The binding material in concrete is cement. The main properties of concrete like strength and durability of concrete are determined by the products of the hydration of cement.

For several purposes like increasing the durability of concrete, and changing the hydration characteristics of concrete, supplementary cementitious materials can be utilized in cement and concrete industry.

### 2.2.1 Raw Materials

Portland cements are produced from calcerous and argillaceous material. Calcerous and argillaceous raw materials which are suitable for cement production can be seen in Table 2.1 (Bogue, 1955; ACI, 2001). The most commonly used one for calcerous materials is limestone and for argillaceous materials is clay (Kuleli, 2009).

Table 2.1. The raw materials for calcerous and argillaceous materials for cement production (Bogue, 1955; ACI, 2001).

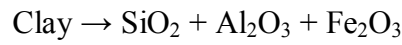
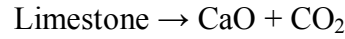
Calcerous Material		Argillaceous Material	
Limestone	Marl	Clay	Blast furnace slag
Cement rock	Marine Shells	Shale	Ashes
Chalk	Alkali Waste	Slate	Cement rock

### 2.2.2 Production Stages

In order to obtain the required properties of cement, the proportioning of the raw materials is important. Firstly, raw materials are pulverized and they are mixed with specific mass proportions. The proportions of the materials can be determined with respect to the desired properties of final product, their chemical compositions and materials mixed (Kuleli, 2009).

The mixing processes can be done by two different methods: dry process and wet process. In the dry process, the mixture is heated in a rotary kiln without adding any water. But, in the wet process, to make the mixture more homogeneous, water is added to the mix, but the required energy for heating is higher than in the dry process

due to this addition. In both processes, the mixed material is burned in rotary kiln at about 1500 °C. Excess water and gases like carbon dioxide are removed by the effect of temperature. The raw materials decompose into their oxides with the effect of heat in rotary kiln, but because of the impurities, there can be some other oxides like MgO, FeO, SO<sub>3</sub> etc. In the process called “clinkering” in the rotary kiln, certain chemical reactions start and the product called “clinker” are obtained (Kuleli, 2009).



After burning, the clinker is cooled, and mixed with a specific amount of a source of calcium sulfate (anhydrite, hemihydrate, gypsum) in order to control the setting time of cement paste. The material is pulverized to meet the requirements given in related standards. The final product is called ordinary portland cement. It can have a specific amount of minor additions according to TS EN 197-1 (<5 % by mass of total cement).

### **2.2.3 Oxides and Their Notation**

The oxides in cement depend on the percentage values of oxides in raw materials. The typical values of oxides can be seen in Table 2.2. The cement chemistry notation is also provided (Erdoğan, 2010).

During the clinkering process, various clinker compounds form from the oxides in raw materials (CaO [C], SiO<sub>2</sub> [S], Fe<sub>2</sub>O<sub>3</sub> [F] and Al<sub>2</sub>O<sub>3</sub> [A]). The clinker compounds and their names are shown in Table 2.3 (Erdoğan, 2010). C<sub>3</sub>S (alite) and C<sub>2</sub>S (belite) are named “calcium silicates”. In addition to these, in cement chemistry, water is shown with “H” and carbon dioxide is shown as with “C̄”.

Table 2.3 also shows the typical percentage amount of clinker compounds of ASTM Type I cement (ACI, 2001).

Table 2.2. The percentage values of oxide in a typical portland cement and cement chemistry notations of oxides (Erdoğan, 2010).

Oxides	Percentage (%)	Cement Chemistry Notation
CaO	63.6	C
SiO <sub>2</sub>	20.7	S
Al <sub>2</sub> O <sub>3</sub>	6.0	A
Fe <sub>2</sub> O <sub>3</sub>	2.4	F
SO <sub>3</sub>	2.1	$\bar{S}$
MgO	2.6	M
Na <sub>2</sub> O	0.1	N
K <sub>2</sub> O	0.9	K
Free CaO	1.4	Free C

Table 2.3. The names, chemical notations and cement chemistry notations of clinker compounds (Erdoğan, 2010).

Clinkering Compound	Chemical Notation	Cement Chemistry Notation	ASTM Type I Compounds Amount (%)
Alite	3CaO.SiO <sub>2</sub>	C <sub>3</sub> S	49
Belite	2CaO.SiO <sub>2</sub>	C <sub>2</sub> S	25
Aluminate (Celite)	3CaO.Al <sub>2</sub> O <sub>3</sub>	C <sub>3</sub> A	12
Ferrite	4CaO.Al <sub>2</sub> O <sub>3</sub> .Fe <sub>2</sub> O <sub>3</sub>	C <sub>4</sub> AF	8

#### 2.2.4 Bogue's Equations

The oxides coming from the raw materials convert to clinker compounds in the rotary kiln. To calculate the percentage of clinker compounds, certain methods like X-ray diffraction or photomicrograph methods can be used. But, the most common practice is Bogue's Equations. There are few assumptions in order to use Bogue's Equations (Erdoğan, 2010):

- 1- The chemical reactions reach equilibrium and cooling process can not change this condition.
- 2- There are no impurities and all of the oxides react only with each other.
- 3- The products are pure.

With the assumption of the ratio of  $A / F \geq 0.64$  (by mass), Bogue's Equations are shown in Eqn. 2.1 – 2.4. All parameters in the equations are in mass fraction.

$$\begin{aligned} \% C_3S = & (4.071 \times \% CaO) - (7.600 \times \% SiO_2) - (6.718 \\ & \times \% Al_2O_3) - (1.430 \times \% Fe_2O_3) - (2.852 \\ & \times \% SO_3) \end{aligned} \quad (\text{Eqn. 2.1})$$

$$\% C_2S = (2.867 \times \% SiO_2) - (0.7544 \times \% C_3S) \quad (\text{Eqn. 2.2})$$

$$\% C_3A = (2.650 \times \% Al_2O_3) - (1.692 \times \% Fe_2O_3) \quad (\text{Eqn. 2.3})$$

$$\% C_4AF = (3.043 \times \% Fe_2O_3) \quad (\text{Eqn. 2.4})$$

### 2.2.5 Impurities

There can be some substances or oxides in the kiln besides the oxides forming clinker compounds due to the impurities in raw materials. These can affect the properties of concrete depending on their contents in cement. In the presence of free lime, which can not form any clinker compounds, it can increase the volume expansion and produce higher heat values during hydration (Erdoğan, 2010).

### 2.2.6 Chemical Reactions

Impurities and main clinker compounds can react with water, ambient carbon dioxide and each other for a long time after the hydration starts.

During the mixing of cement and water, there occur chemical reactions between the clinker compounds, gypsum and water. These reactions are called “hydration”. There are two main hydration mechanisms in the hydration of cement: a solid-state reaction and a through-solution hydration. Solid state hydration is also called topochemical hydration. In this mechanism, which governs at later ages, the chemical reactions occur mainly at the surface of cement particles. But, this mechanism is recessive in early ages. According to through-solution method, the compound dissolves into the

solution and the reactions take place dominantly in the solution (Mehta and Monteiro, 2006).

The mechanism does not depend on only the age of cement but also the clinker compounds. Calcium silicates, aluminates and ferrite hydration have different hydration products and different hydration rates (Erdoğan, 2010).

### 2.2.6.1 Products of Chemical Reactions

The reaction of cement compounds with water can give different products. While the clinker compounds can give C-S-H gel, calcium hydroxide, ettringite, and calcium alumino monosulfo hydrate, the product of the reaction of hemihydrate and anhydrite. In addition, with internal reactions, products like calcium carbonate or alkali-silica gel which is the product of the reaction between reactive silica in aggregates and alkalis in cement can occur. The main products and their abbreviations with respect to cement chemistry can be seen in Table 2.4 (Erdoğan, 2010).

Table 2.4. The possible main products of hydration reactions (Erdoğan, 2010).

<b>Products</b>	<b>Chemical Notation</b>	<b>Cement Chemistry Notation</b>
C-S-H Gel	$3\text{CaO} \cdot 2\text{SiO}_2 \cdot 3\text{H}_2\text{O}$	$\text{C}_3\text{S}_2\text{H}_3$
Calcium Hydroxide	$\text{Ca}(\text{OH})_2$	CH
Ettringite	$3\text{CaO} \cdot \text{Al}_2\text{O}_3 \cdot 3\text{CaSO}_4 \cdot 32\text{H}_2\text{O}$	$\text{C}_6\text{A}\bar{\text{S}}_3\text{H}_{32}$
Calcium Alumino Monosulfo Hydrate	$3\text{CaO} \cdot \text{Al}_2\text{O}_3 \cdot \text{CaSO}_4 \cdot 12\text{H}_2\text{O}$	$\text{C}_4\text{A}\bar{\text{S}}\text{H}_{12}$
Gypsum Rock	$\text{CaSO}_4 \cdot 2\text{H}_2\text{O}$	$\text{C}\bar{\text{S}}\text{H}_2$
Calcium Carbonate	$\text{CaCO}_3$	$\text{C}\bar{\text{C}}$

Tobermorite and calcium hydroxides are formed from the reactions between water and calcium silicates. The reactions of  $\text{C}_3\text{S}$  and  $\text{C}_4\text{AF}$  can form ettringite and calcium

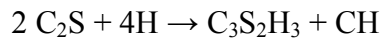
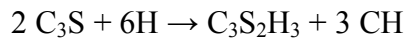
alumino monosulfo hydrate. Due to reactions of free lime, there can be some amount of calcium carbonate, also (Erdoğan, 2010).

#### **2.2.6.2 Hydration of Clinker Compounds**

The hydration processes of clinker compounds are different. To investigate the reactions, it is necessary to divide the reacted compounds into three parts; calcium silicates, aluminate and ferrite phases.

##### **2.2.6.2.1 Hydration of Calcium Silicates Phases**

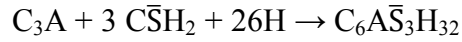
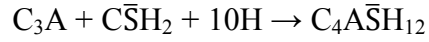
The hydration processes of the two calcium silicates are similar. The main product is C-S-H gel which provides the strength and durability of concrete. C-S-H gel can be similar to tobermorite or jennite depending on the ratio of C/S ratio. While a ratio lower than 1.5 leads to tobermorite-like structure, in the cases where the C/S greater than 1.5, the structure of the products is like jennite (Lothenbach et al., 2011). The other product of this reaction is calcium hydroxide. The main difference between the two different calcium silicate hydration processes is the amount of products and the amount of water they consume during hydration. Also, their hydration rates are not similar. The hydration rate of C<sub>3</sub>S is assumed to be higher than that of C<sub>2</sub>S (Erdoğan, 2010).



##### **2.2.6.2.2 Hydration of Aluminate Phases**

The products of the hydration of aluminates without gypsum are C<sub>3</sub>AH<sub>13</sub> and C<sub>2</sub>AH<sub>8</sub>. These are called hydrogarnets. But, these products are not stable; they convert to stable cubic hydrogarnets (C<sub>3</sub>AH<sub>6</sub>) (Erdoğan, 2010).

Because the reactions are very rapid and influence the setting time, a specific amount of calcium sulfate is added to clinker. The products are calcium alumino monosulfohydrate ( $C_4A\bar{S}H_{12}$ ) and ettringite ( $C_6A\bar{S}_3H_{32}$ ) (Erdoğan, 2010).



In the case of available water and gypsum, calcium alumino monosulfohydrate can be converted to ettringite even after hardening of concrete and the formation of ettringite can cause internal stresses and cracks due to the lower tensile strength of concrete (Erdoğan, 2010).

#### **2.2.6.2.3 Hydration of Ferrite Phases**

The hydration process of ferrite phase is similar to that of the aluminate phase. Without gypsum, the hydration products are  $C_3AH_6$  and  $C_3FH_6$  (Czernin, 1962).



With gypsum, the hydration process is similar to hydration of aluminate phase with gypsum. The main products are  $C_4(A,F)\bar{S}H_{12}$  and  $C_6(A,F)\bar{S}_3H_{32}$ . In addition to these, some amount of  $(A,F)H_3$  can be formed (Erdoğan, 2010).

#### **2.2.7 Mineral Admixtures**

Some mineral admixtures used to improve cement or concrete are also called pozzolans. Pozzolans usually are not binding materials by themselves, but they gain this property when mixed with water and lime. But, certain kinds of pozzolans like



ground granulated blast furnace slag, which is a by-product of iron and steel industry, have some binding property due to their higher CaO contents (Erdoğan, 2010). In ASTM C 219, a pozzolan is defined as:

*“a siliceous or siliceous and aluminous material, which in itself possesses little or no cementitious value but will, in finely divided form and in the presence of moisture, chemically react with calcium hydroxide at ordinary temperatures to form cementitious hydrates.”*

Mineral admixtures are used in different ways. Firstly, they can be mixed with lime directly as in ancient times. Alternatively, they can be used as mineral additives in concrete. Finally, as a cement replacement material, they can be added to cement in the production. These cements are called “pozzolanic cements” in TS EN 197-1.

#### **2.2.7.1 Types of Mineral Admixtures**

Although it is difficult to classify mineral admixtures, since they can be very different with respect to their chemical compositions, mineralogical natures, and geological origins; generally, mineral admixtures can be divided into two groups with respect to their origin. The mineral admixtures obtained from nature, are called “natural mineral admixtures” and those obtained from industry are called “artificial mineral admixtures”.

##### **2.2.7.1.1 Natural Mineral Admixtures**

The origins of almost all natural mineral admixtures (natural pozzolans) are volcanic rocks and minerals (Mehta and Monteiro, 2006). But, there are some kinds of pozzolans of sedimentary origin, too (Massazza, 2004). Volcanic-origin pozzolans are formed from cooling of magma with air or water. The other type of natural pozzolan, sedimentary origin pozzolan, originates from the sedimentation of clays and diatomaceous earths. Due to their different chemical compositions, origins and crystal structure, there exist many types of natural pozzolan. In Table 2.5, the chemical compositions of different natural pozzolans and their origins can be seen (Lohtia and Joshi, 1995).

Table 2.5. Some natural pozzolans, their chemical compositions and geological origins (Lohtia and Joshi, 1995).

	<b>Geological Origin</b>	<b>SiO<sub>2</sub></b>	<b>Al<sub>2</sub>O<sub>3</sub></b>	<b>Fe<sub>2</sub>O<sub>3</sub></b>	<b>CaO</b>	<b>MgO</b>	<b>Na<sub>2</sub>O</b>	<b>K<sub>2</sub>O</b>
<b>Santorini Earth</b>	Volcanic	65.1	14.5	5.5	3.0	1.1	2.6	3.9
<b>Rheinisch Trass</b>	Volcanic	52.1	18.3	5.8	4.9	1.2	1.5	5.1
<b>Diatomaceous Earth</b>	Sedimentary	86.0	2.3	1.8	-	0.6	0.4	-

#### 2.2.7.1.2 Artificial Mineral Admixtures

This type of mineral admixture is the by-product of an industrial process. Different types of industries produce different types of artificial mineral admixtures. Granulated blast furnace slag from ferrous industries, silica fume from silicon metal industries, fly ash from combustion of coal is produced. Especially, in developed countries, where the industry is advanced, and since they are common, it is preferred to use artificial mineral admixtures as pozzolans in cement and concrete. In Table 2.6, the chemical compositions of different artificial pozzolans are shown (Erdoğan, 2010).

Table 2.6. Some artificial pozzolans and their chemical compositions (Erdoğan, 2010).

	<b>SiO<sub>2</sub></b>	<b>Al<sub>2</sub>O<sub>3</sub></b>	<b>Fe<sub>2</sub>O<sub>3</sub></b>	<b>CaO</b>	<b>MgO</b>	<b>Na<sub>2</sub>O</b>	<b>K<sub>2</sub>O</b>
Granulated Blast Furnace Slag	34.0-41.0	13.0-19.0	0.3-2.5	34.0-41.0	3.5-7.0	-	-
Class C-Fly Ash	23.1-50.5	13.3-21.3	3.7-22.5	11.5-29.0	1.5-7.5	0.4-1.9	-
Class F-Fly Ash	43.6-64.4	19.6-30.1	3.8-23.9	0.7-6.7	0.9-1.7	0-2.8	-
Silica Fume	93.0-95.0	0.4-1.4	0.4-1.0	0.6-1.0	1.0-1.5	0.1-0.4	0.5-1.0

### 2.2.7.2 Production of Pozzolanic Cements

If pozzolans are mixed with cement before the preparation of concrete, this type of cement is called pozzolanic cement and there are two types of pozzolanic cement with respect to their production method.

The first is separately-blended pozzolanic cement where pozzolan and the mix of clinker and gypsum are ground separately and then mixed with each other. The other one is interground cement. The mixture of gypsum, clinker and pozzolan is put in a mill and ground together.

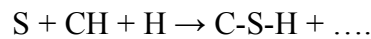
The dependance of various properties of different pozzolanic cements containing natural pozzolans of the same fineness or their production methods can be seen in Table 2.7. The differences between the two types of cement can be due mainly to relatively coarser clinker particles. In interground cements, where the raw materials are ground together, the hardest material to grind is usually the clinker (a few mineral admixtures like slag are harder than clinker (Kuleli, 2009). During the grinding process, clinker particles grind the softer materials, trass and gypsum. Thus, the average particle size of clinker is relatively greater, those of gypsum and trass are relatively smaller compared with separately-blended cements. In addition to this, the homogeneity of interground cements is higher than separately-blended ones. This fact can also affect properties (Erdem et al., 2006).

Table 2.7. Properties of different pozzolanic cements containing natural pozzolans for the same fineness with respect to their production stages.

Property	Seperately-Blended Cements	Interground Cements	Reference
Clinker particle size	Finer	Coarser	(Erdem et al., 2006)
Setting time	Shorter	Longer	(Erdem et al., 2006)
Strength of mortars	Lower	Higher	(Erdem et al., 2006)
Energy requirement for grinding	Higher	Lower	(Erdoğan et al., 1999)

### 2.2.7.3 Pozzolanic Reaction in Cements

The binding medium of many historical monuments constructed few centuries ago is based on this reaction. A mix of natural pozzolan, lime and water was used as the binding material. From the reaction of lime with water, calcium hydroxide (slaked lime) is produced. The silica in pozzolans reacts with calcium hydroxide and water and produces the main binding constituent of concrete, C-S-H gel (Erdoğan, 2010).



The pozzolanic reaction occurring in cements is similar to that of the mix of lime, natural pozzolan and water. From the hydration of clinker compounds, calcium hydroxide is formed as a by-product of the hydration. Using calcium hydroxide, the pozzolanic reactions occur in the presence of water. With this reaction, the constituent calcium hydroxide, which decreases the durability of concrete due to the possible reaction of it with other agents, is consumed, and the constituent C-S-H gel, which increases the strength of concrete, is produced (Erdoğan, 2010).

According to the related standards (ASTM C 618), for a mineral addition to use as a pozzolanic material in cement, its activity index should be determined. The ratio of the strength of the control mix (without any addition of mineral admixture) to the strength of test mixture should be higher than 75 % at 7 days or 28 days (Erdoğan, 2010).

According to the literature, the factors affecting pozzolanic activity are the summation of the contents of silica, alumina and iron oxide, amorphousness of the pozzolanic material, and fineness of the particles (Erdoğan, 2010). In spite of that, the sources refer that, due to the heterogeneity of pozzolan materials and complex reactions, this activity index shows only general trends of the related pozzolan (Massazza, 2004).

#### **2.2.7.4 Advantages**

Pozzolans are replaced with cement in concrete for various purposes. First of all, the cost of pozzolans per unit weight is lower than cement; it can be found in nature easily. Secondly, it can increase the workability of concrete, due to its fineness, it can absorb extra water, so that it can reduce bleeding of concrete or due to relatively slower pozzolanic reactions than hydration, it can increase setting time so that there can be more time to cast the concrete. Also, especially for certain kinds of pozzolans, for the same slump, the required water can be changed. If a very fine pozzolan like silica fume is used, the water requirement is increased. In addition, thirdly, it affects heat of hydration of the remaining cement. Fourthly, the addition of pozzolan may increase the durability and strength of concrete (Mehta and Monteiro, 2006). Moreover, it reduces the permeability of concrete, it can be used as a filler material to fill the capillary pores (Çavdar and Yetgin, 2004). Since pozzolanic reactions consume calcium hydroxide, the amount of calcium hydroxide which can be harmful decreases. Its density is typically lower than clinker, so when used in concrete instead of some amount of clinker, it increases the volume and increases the workability of concrete. Finally, because of their lower CO<sub>2</sub> emissions, the environmental impact of pozzolan-containing cements is lower than that of clinker (Mehta and Monteiro, 2006).

#### **2.2.8 Types of Portland Cements**

American and European standards divide the cements with respect to different aspects.

According to ACI, ASTM cements can be divided with respect to their clinker compound content (ACI, 2001). The types and the approximate percentages of clinkering oxides of typical cements can be seen in Table 2.8 (Erdoğan, 2010). European norms name cements based on the mineral admixture they incorporate and its content. The types, according to EN 197-1, can be seen in Table 2.9.

Table 2.8. The types of cements with respect to their clinker compound contents (ACI, 2001).

Type of cement	C <sub>3</sub> S	C <sub>2</sub> S	C <sub>3</sub> A	C <sub>4</sub> AF
Type I	49	25	12	8
Type II	46	29	6	12
Type III	56	15	12	8
Type IV	30	46	5	13
Type V	43	36	4	12

Table 2.9. EN cement types (TS EN 197-1).

Main types	Notation of the 27 products (types of common cement)		Composition (percentage by mass <sup>a</sup> )										Minor additional constituents
			Main constituents										
			Clinker	Blast-furnace slag	Silica fume	Pozzolana		Fly ash		Burnt shale	Limestone		
						natural	natural calcined	siliceous	calcareous				
			K	S	D <sup>b</sup>	P	Q	V	W	T	L	LL	
CEM I	Portland cement	CEM I	95-100	—	—	—	—	—	—	—	—	—	0-5
CEM II	Portland-slag cement	CEM II/A-S	80-94	6-20	—	—	—	—	—	—	—	—	0-5
		CEM II/B-S	65-79	21-35	—	—	—	—	—	—	—	—	0-5
	Portland-silica fume cement	CEM II/A-D	90-94	—	6-10	—	—	—	—	—	—	—	0-5
	Portland-pozzolana cement	CEM II/A-P	80-94	—	—	6-20	—	—	—	—	—	—	0-5
		CEM II/B-P	65-79	—	—	21-35	—	—	—	—	—	—	0-5
		CEM II/A-Q	80-94	—	—	—	6-20	—	—	—	—	—	0-5
		CEM II/B-Q	65-79	—	—	—	21-35	—	—	—	—	—	0-5
	Portland-fly ash cement	CEM II/A-V	80-94	—	—	—	—	6-20	—	—	—	—	0-5
		CEM II/B-V	65-79	—	—	—	—	21-35	—	—	—	—	0-5
		CEM II/A-W	80-94	—	—	—	—	—	6-20	—	—	—	0-5
		CEM II/B-W	65-79	—	—	—	—	—	21-35	—	—	—	0-5
	Portland-burnt shale cement	CEM II/A-T	80-94	—	—	—	—	—	—	6-20	—	—	0-5
		CEM II/B-T	65-79	—	—	—	—	—	—	21-35	—	—	0-5
	Portland-limestone cement	CEM II/A-L	80-94	—	—	—	—	—	—	—	6-20	—	0-5
		CEM II/B-L	65-79	—	—	—	—	—	—	—	21-35	—	0-5
		CEM II/A-LL	80-94	—	—	—	—	—	—	—	—	6-20	0-5
		CEM II/B-LL	65-79	—	—	—	—	—	—	—	—	21-35	0-5
	Portland-composite cement <sup>c</sup>	CEM II/A-M	80-88	12-20									0-5
		CEM II/B-M	65-79	21-35									
CEM III	Blastfurnace cement	CEM III/A	35-64	36-65	—	—	—	—	—	—	—	—	0-5
		CEM III/B	20-34	66-80	—	—	—	—	—	—	—	—	0-5
		CEM III/C	5-19	81-95	—	—	—	—	—	—	—	—	0-5
CEM IV	Pozzolanic cement <sup>c</sup>	CEM IV/A	65-89	—	11-35					—	—	—	0-5
		CEM IV/B	45-64	—	36-55					—	—	—	0-5
CEM V	Composite cement <sup>c</sup>	CEM V/A	40-64	18-30	—	18-30			—	—	—	—	0-5
		CEM V/B	20-38	31-49	—	31-49			—	—	—	—	0-5

<sup>a</sup> The values in the table refer to the sum of the main and minor additional constituents.

<sup>b</sup> The proportion of silica fume is limited to 10 %.

<sup>c</sup> In Portland-composite cements CEM II/A-M and CEM II/B-M, in pozzolanic cements CEM IV/A and CEM IV/B and in composite cements CEM V/A and CEM V/B the main constituents other than clinker shall be declared by designation of the cement (for examples, see Clause 8).

### **2.2.9 Other Cement Types**

Besides portland cement and pozzolanic cements, there can also be different cements categorized with respect to their special usage and their chemical admixture contents. The special cements noted by ACI are expansive cements, white cements, masonry cements, mortar cements, oil well cements, plastic cements, and rapid-setting cements (ACI, 2001).

## **2.3 Heat of Hydration in Cement**

### **2.3.1 Introduction**

In concrete, the heat produced is the result of cement water reactions. It is affected by rate of hydration, therefore; the factors affecting the rate of hydration also affect the rate of heat of hydration evolution and cumulative heat evolution up to a certain time.

The reactions between cement and water are exothermic, in other words, they produce heat during hydration. This heat is called “heat of hydration”. The cumulative heat of hydration of typical cement at a short time period can be seen in Figure 2.1. Heat of hydration depends on the age of concrete. With passing time, the cumulative heat of hydration increases until hydration reactions stop due to the consumption or loss of all water or cement. Heat of hydration is typically measured as “heat energy evolved per unit mass of cement” in units of cal/g or J/g. The heat mainly comes from the hydration of cement clinker compounds. Portland cements are produced at high temperatures, so the products are unstable at ambient conditions and are in a high-energy state. During the hydration process, the energy is released and the compounds reach a low-energy state (Mehta and Monteiro, 2006).

Due to high heat of hydration, the temperature of concrete can even reach about 80 °C (ACI, 2001). There can be various problems about the hot core of a concrete block. Excessive temperature rise can cause thermal cracks, changes in the microstructure of hydrated cement paste and changes in the compositions of hydration products. Excessive temperature can cause the inner part of concrete to expand, but outer parts in contact with air expand less. As a result of this and due to lower tensile strength of concrete, expansion cracks can occur. At elevated

temperatures, in concrete, the amount of larger pores, which affect the permeability of concrete, is seen to be higher than at lower temperatures, although the total pore volume at elevated temperatures is lower (Nanayakkara, 2011). Elevated temperatures not only increase the permeability of concrete, but also due to changes in microstructure, change its mechanical properties. It can reduce ultimate strength. In addition, delayed ettringite formation (DEF) can occur. Higher temperatures can cause ettringite to form calcium alumino monosulfo hydrate. With water, they react to form ettringite again and form expansion cracks, at later ages of concrete (Nanayakkara, 2011).

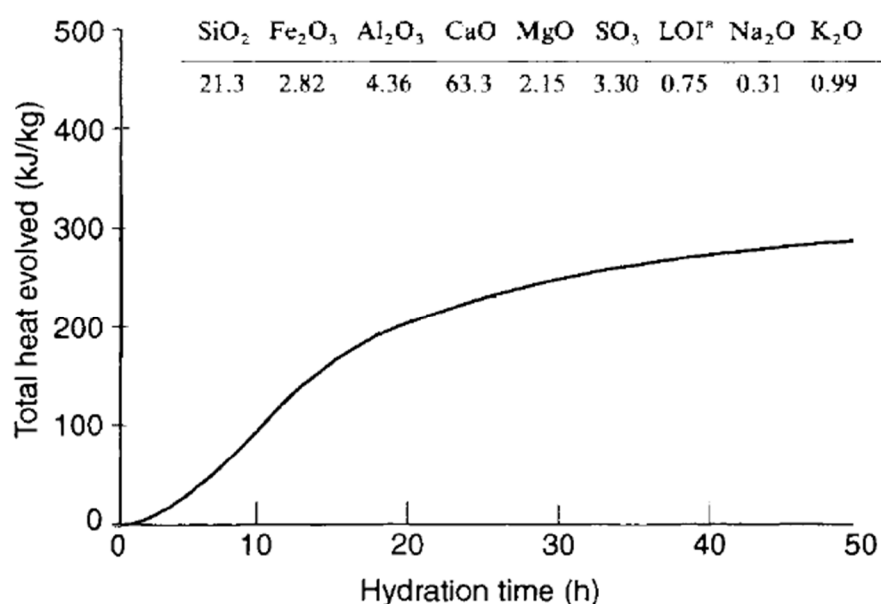


Figure 2.1. The heat evolution curve of a cement at a constant temperature (20 °C) and w/c = 0.375, adapted from (Lawrence, 2004).

### 2.3.2 Heat Evolution Rate and Its Stages

The rate of heat evolution vs. time curve of a typical portland cement is shown in Figure 2.2. In the rate of heat evolution graph, there are two main peaks. The first peak occurs in the first 10 minutes and its value is higher than the second peak. To



better understand the mechanism of hydration, the rate vs. time curve can be divided into four stages.

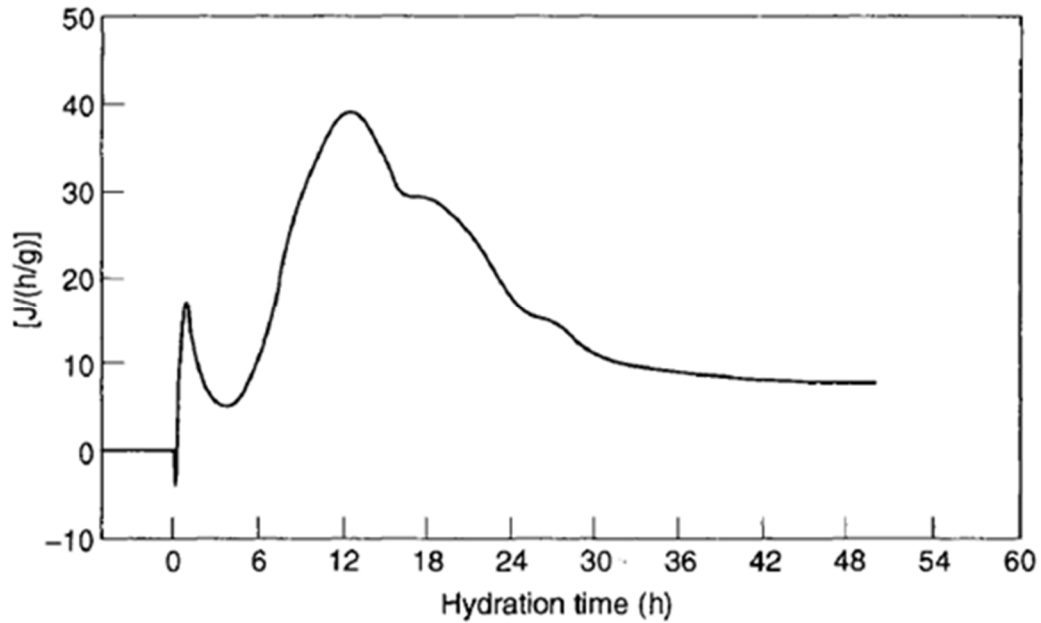


Figure 2.2. The rate of hydration heat curve of a typical ordinary portland cement (Odler, 2004).

### 2.3.2.1 Pre-induction Period

This period including the first peak occurs in the first minutes after the contact of water with cement particles. In the first minutes, ionic compounds dissolve into the solution. Sulfate ions dissolve in liquid phase completely within seconds. Calcium sulfate dissociate into  $\text{Ca}^{2+}$  and  $\text{SO}_4^{2-}$  ions until the saturation point. Among the clinker compounds, about 2 to 10 percent of the total  $\text{C}_3\text{S}$  amount dissolves and produces hydrates whose C/S ratio is lower than that of  $\text{C}_3\text{S}$ , so it affects the amounts of  $\text{Ca}^{2+}$  and  $\text{OH}^-$  in the solution. In case of  $\text{C}_2\text{S}$ , the process is similar to  $\text{C}_3\text{S}$  hydration.  $\text{C}_3\text{A}$  and  $\text{C}_4\text{AF}$  react with  $\text{Ca}^{2+}$  and  $\text{SO}_4^{2-}$  ions and yield ettringite phase. Rapid heat liberation is due to the rapid hydration of  $\text{C}_3\text{S}$  and  $\text{C}_3\text{A}$ . The reaction

between hemihydrate and water can also contribute to the initial first peak (Odler, 2004).

#### **2.3.2.2 Dormant (Induction) Period**

The induction period also called the dormant period occurs in the first few hours after the pre-induction period. After very rapid hydration, the hydration slows down and the hydration of all clinker compounds continues very slowly and after a while the rate of heat evolution increases. In this stage, it is known that the calcium hydroxide concentration reaches its maximum and starts to decline. But, the sulfate concentration remains since, the decrease of sulfate in liquid during the formation of ettringite phases, is compensated by the dissolution of calcium sulfate (Odler, 2004). The reason behind the slowing down of the heat evolution rate is not well understood, there are some possible reasons discussed in literature.

##### **2.3.2.2.1 Impermeable Layer Hypothesis**

This hypothesis proposes that a first stage product which is formed on the surface of the cement grain during hydration acts as a barrier and prevents water from penetrating through to the cement particle. For this reason, the rate of hydration and correspondingly, the rate of heat evolution slows down. After the change of initially formed C-S-H gel (phase transformation or ageing of C-S-H), it becomes more porous and it allows water to penetrate. The reason why the nature of the product changes is not obvious (Odler, 2004).

##### **2.3.2.2.2 Other Hypotheses**

In electrical double layer hypothesis, initial  $C_3S$  dissolution causes a surface layer rich in  $SiO_2$  and which adsorbs  $Ca^{2+}$  ions. This creates an electric double layer and prevents water from penetrating through to the cement particle. This decreases the rate of hydration (Odler, 2004).

According to the nucleation hypothesis, supersaturation of the liquid phase with respect to calcium hydroxide impedes dissolution of  $C_3S$  and causes the products (C-S-H gel and CH) to nucleate (Odler, 2004).

### **2.3.2.3 Acceleration Period**

This period takes places typically between 3 and 12 hours after mixing. The increasing rate of the hydration forms the second peak. The noticeable hydration of  $C_2S$  can be seen. Due to the formation of crystalline calcium hydroxide, the concentration of  $Ca^{2+}$  decreases. Moreover, the calcium sulfate is finished and Aft continues to be formed,  $SO_4^{2-}$  concentration declines (Odler, 2004).

### **2.3.2.4 Post-Acceleration Period**

The amount of unreacted cement particles decreases and that of products increases. The rate of hydration is controlled mainly by diffusion (Odler, 2004). This period continues until cement particles are fully hydrated or there is not enough water for hydration.

## **2.3.3 Factors Influencing Heat of Hydration and Rate of Heat Evolution**

Rate of hydration, therefore the rate of heat evolution can be affected by many factors. Almost all cement-related factors affecting the ultimate strength of concrete affect hydration, and correspondingly, the heat of hydration (Odler, 2004).

### **2.3.3.1 Fineness**

Fineness is one of the factors influencing the rate of hydration. Fineness reflects the average particle size (Erdoğan, 2010). Greater fineness implies smaller particle size. While the cement particle size decreases, in the beginning of hydration, water can react with cements at their surfaces in unit time, their cores can not be hydrated since they have not been introduced with water, yet. But, the unhydrated cement amount of finer cements is relatively less than that of the coarser cements. Thus, the heat of the hydration at early ages and rate of heat evolution of finer specimens are higher than coarser cements (Odler, 2004; Binici et al., 2007). But, later, since all the cement particles including their cores, have started to react with water, fineness can not change the value of heat of hydration (ACI, 2001). Fineness can control the early hydration, but it can not control the post-acceleration period; post acceleration period is independent of fineness (Mostafa and Brown, 2005).

### 2.3.3.2 Mineral Admixtures

The chemical characteristics of mineral admixtures added to cement are significant in determining the rate of heat evolution and heat of hydration of the cement in both the short and long run. Pozzolanic reactions can change the characteristics of the heat evolution curve (Massazza, 2004). Very reactive pozzolans like silica fume, metakaolin, nano silica and certain natural pozzolans etc. can contribute to the heat of hydration of the concrete for even several days by forming their hydration products (Rahhal et al., 2012). Moreover, certain mineral additions can change the length of the periods seen in rate of heat evolution curve. Massazza stated that natural pozzolans and microsilica can accelerate the hydration of  $C_3S$  reducing the induction period and increasing the value of the second peak of the rate of heat evolution curve (Massazza, 2004). Lawrence et al. (2005) showed that fly ash, used as a mineral addition, delays the hydration of the cement due to its chemical composition, particle size distribution and reactivity. Moreover, fly ash can cause the dormant period to lengthen (Massazza, 2004). Also, Gutteridge and Dalziel (1990) showed that fine calcium carbonate, added to cement as a mineral addition, during the first four hours, can cause a delay in the hydration, while it can have an accelerating effect on the hydration after 24 hours.

Mineral admixtures such as ground granulated blast furnace slag and class-C fly ash used in the cement and concrete industry, besides their pozzolanic reactivities, can have self-cementitious properties due to their higher lime contents. In an alkaline environment, slag is reacted with calcium hydroxide which comes from hydration of calcium silicates of the clinker portion of cement and water (Erdoğan, 2010; Wang, 2011). Hassett and Eylands (1997) found that a mix of class-C fly ash and water reacts to produce heat. The reactions producing heat may change the characteristics of the heat of hydration of the cements.

The pozzolan portion of pozzolanic cements can not react with water immediately upon the contact. Only the clinker and gypsum portions react with water in a short time. For most pozzolans, to start chemical reactions, one of the requirements is the presence of calcium hydroxide. Until the quantity of it is enough, pozzolanic reactions are not so pronounced. They can not produce C-S-H gels and can not

contribute strength and durability of cement paste. Massazza stated that the pozzolanic reactions of the most of the pozzolans can not be seen in the first 3 days after mixing with water. Particularly at short time periods, mineral admixtures act as filler additives, not reacting chemically. Even if mineral admixtures do not chemically react, they can affect the hydration mechanism in different physical ways as filler materials (Massazza, 2004). The amount of pozzolan can change the characteristics of the heat evolution curve due to the reduction of the clinker content (Dilution effect) (Lawrence et al., 2005). In addition, small replacement causes the hydration to be accelerated due to the increase of nucleation and precipitation sites for the hydration products (Nucleation effect) (Lawrence et al., 2005). Besides these two, filler effect is said to be important in the hydration (Lothenbach et al., 2011).

The amount of pozzolans is significant in the determination of the heat of hydration of cements. Since the pozzolan portion is used as a cement replacement material, the amount of clinker and gypsum, and accordingly, the heat of hydration of the clinker and gypsum decreases. This is named dilution effect. Dilution effect is directly related with the amount of mineral additions. Due to this effect, when the amount of pozzolans is higher, cumulative heat of hydration of the cements containing natural pozzolans for one month period usually has lower values than the ordinary portland cements although pozzolanic reactions produce little amount of heat (Lawrence et al., 2003; Siler et al., 2012; Turanlı et al., 2005).

In the early stages of hydration, most pozzolans cannot show pozzolanic reactions due to the lack of the calcium hydroxide, they act as inert particles. In nucleation effect, filler particles can enhance the hydration process due to double layer theory (Rahhal et al., 2012). During grinding or mixing the cement paste or mortar, the surface of the particle can be negatively or positively charged, and at the very beginning, the surface attracts ions such as  $\text{OH}^-$  and  $\text{Ca}^{2+}$ . The first anion or cation layer developed attracts the ions of the opposite charge and a second layer is formed. This process continues until the surface charge is fully balanced with the counter-ions. The particles of the mineral admixture, which cannot chemically react, act as nucleation locations for the products. Rahhal et al. (2012) concluded that the quantity of the fillers, which begin the double layer process, enhance the hydration process in

two different ways. The former one, direct stimulation, is the increase in hydration due to the pozzolan particles acting as nucleation locations for the hydration products. The latter, non-direct stimulation is explained as the larger number of nucleation sites, in other words the higher amount of mineral addition strengthens the initial electrostatic force. If the electrostatic force of the particle is higher, the thickness of the double layer consisting of hydration products around the particle surface becomes higher therefore, the hydration increases. The factors in the double layer theory are listed as quantity and chemistry of the mineral addition, pH of the pore solution, preparation, mixing and grinding of the cement components (Rahhal et al., 2012). In addition to double layer theory, there can be another explanation about nucleation theory for the enhancement of cement hydration while adding mineral admixture. With mineral additions, the thickness of the hydration products reduces as shown in Figure 2.3 (Lawrence et al., 2003). Therefore, hydration, which is related to diffusion, is enhanced. If the particles of mineral admixture are fine and close enough to the clinker grain, this effect is more visible. Also, it is found that a great amount of mineral admixture reduces the probability of a mineral admixture particle to be close enough to interact a clinker particle. If the quantity is small, this probability increases; therefore, the small addition of mineral admixture enhances hydration (Cyr et al., 2005). In the study conducted by Lawrence et al. (2005), the effects on nucleation effect are listed as fineness, amount and nature of the mineral admixture. Others (Poppe and Schutter, 2005) have concluded that higher amount of mineral additions increase the height of the second rate peak. Moreover, in the study using different fillers like calcite and quartz, Rahhal et al. (2012) shows that the surface texture of the minerals has the ability to change the nucleation effect. It is indicated that calcite is more effective than quartz in enhancing the hydration because texture of calcite is more granulated than that of quartz (Rahhal et al., 2012).

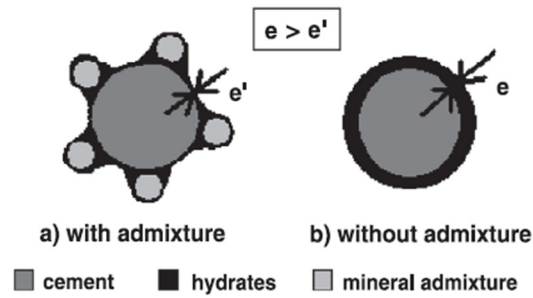


Figure 2.3 Schematic representation of the hypothesis of hydration enhancement by fine admixtures (Lawrence et al., 2003).

Unlike in the nucleation and dilution effects, in filler effect, a different mechanism contributes to the enhancement of hydration. Due to the inert behavior of the pozzolan in the first few minutes, the water available for the hydration of clinker compounds is higher, since the amount of clinker is decreased with the replacement materials. Therefore, the space available for the hydration products increases (Lothenbach et al., 2011; Langan et al., 2002). It is also indicated that the modification of particle size distribution, which depends on fineness and mineral admixture content, can be an important factor for the initial porosity and the available space for hydration products (Lawrence et al., 2003).

The study made by Cyr et al. report that there is an optimum cement replacement amount for the maximum enhancement of cement hydration. Below this optimum amount, there is not sufficient area provided by mineral particles (lack of nucleation effect), so the heat of hydration is lower. Above the optimum amount, heat of hydration is lower due to excess mineral addition (dilution effect) (Cyr et al., 2006).

In addition to these effects, according to Massazza (2004), during the hydration of blended cements, the  $\text{Ca}^{2+}$  ions are adsorbed by the mineral admixtures, and this increases the hydration of  $\text{C}_3\text{S}$ .

### 2.3.3.3 Chemical Composition

Chemical composition is more important factor than the presence of admixtures (Lohtia and Joshi, 1995). Different clinker compounds react with water with different

rates producing different amounts of heat; therefore, the amounts of clinkering oxides are important (Odler, 2004). In addition, they can react with the some hydration products like calcium hydroxide (Odler, 2004). The heat of hydration of different clinker compounds at different ages from the beginning of hydration are given in Table 2.10 (Mehta and Monteiro, 2006; Odler, 2004). Especially, the content of  $C_3S$  and  $C_3A$  is significant (ACI, 2001) since they can produce higher heat in the early stages of hydration. In addition to clinker compounds, impurities that exist in cements can contribute to the cumulative heat of hydration. Moreover, the content of gypsum added to cement to control setting time can affect the rate and cumulative heat of hydration diagrams.

Table 2.10. Heat of hydration of portland cement clinker compounds at the given age (J/g) (Mehta and Monteiro, 2006; Odler, 2004).

<b>Clinker compounds</b>	<b>Hydration Products</b>	<b>3 days</b>	<b>90 days</b>	<b>13 years</b>	<b>Complete Hydration</b>
$C_3S$	C-S-H gel + CH	243	435	510	520
$C_2S$	C-S-H gel + CH	50	176	247	260
$C_3A$	$C_6A\bar{S}_3H_{32}$	886	1300	1355	1670
$C_3A$	$C_4A\bar{S}H_{12}$	-	-	-	1140
$C_3A$	$C_3AH_6$	-	-	-	910
$C_4AF$	$C_6A\bar{S}_3H_{32}$	234	410	427	-

#### 2.3.3.4 Water Amount

Water content can affect the hydration, and correspondingly the heat of hydration. The heat of hydration is increased by increasing w/c ratio (Langan et al., 2002; Siler et al., 2012). Pane and Hansen (2005) reported that the mortars with w/c = 0.35 produced lower heat than w/c = 0.45. The possible reason for that can be the larger available space for hydration products for higher w/c specimens and the cement grains being in better contact with water (Pane and Hansen, 2005; Siler et al., 2012). Moreover, the induction period can be shortened or absent at very high w/c ratios (Odler, 2004).



### **2.3.3.5 Temperature**

Temperature can accelerate not only the hydration, but most of the chemical reactions. Increasing temperature makes the heat of hydration higher initially (Odler, 2004). Pane and Hansen (2005) show that one of the factors in hydration and correspondingly, heat evolution is the temperature. The higher temperature leads to higher heat production rate (Poppe and Schutter, 2005).

### **2.3.3.6 Particle Size Distribution**

The particle size distribution affects heat of hydration of cement. Determination of particle size distribution of a cement is very important for early-age hydration (Irassar et al., 2011). Cumulative heat of hydration is dependent on the particle size distribution (Snellings et al., 2010). In addition, experiments show that distortion of cement particle size distribution curve influences acceleratory period (Mostafa and Brown, 2005). Especially, in pozzolanic cements, in addition to fineness, particle size distribution is a significant factor (Uzal and Turanlı, 2003).

### **2.3.3.7 Chemical Admixtures**

Chemical admixtures added to the concrete to improve some properties during casting, transporting and mixing, can also affect the heat of hydration of cement; depending on the type and the content of chemical admixture. Due to the reduction of cement at a given slump and strength, a water-reducing admixture decreases the temperature of concrete as a result of reduced cement hydration at early ages. Moreover, the time of rapid heat evolution in cement hydration is delayed by water reducing agents (Lohtia and Joshi, 1995). The total heat evolved up to 7 days decreases while the amount of superplasticizer is increasing since it retards the hydration process (Siler et al., 2012). The studies indicating the effects of chemical admixtures on cement hydration kinetics are stated. In the case of the use of retarders, it is shown that the induction period in cement hydration increases and after the acceleration of hydration, the rate of hydration reduces. However, it is also reported that sometimes the opposite effect of the retarders can be seen. If accelerators are used, the induction period is shortened (Cheung et al., 2011).

#### **2.3.4 Methods to Measure Heat of Hydration**

All over the world, different methods are used to measure the heat of hydration, but mainly, heat of hydration of cements is measured by calorimeters and according to Zielenkiewicz (2008), there are many kinds of calorimeters with respect to their dynamic properties and heat transfer exchange conditions with their surroundings. In spite of this, standards refer to only a few of them. It is generally believed that the performance of isothermal calorimeter method is better than the others especially in early ages (Arndt et al., 2007; Siler et al., 2012).

##### **2.3.4.1 Solution Method**

Certain standards like BS EN 196-8 or ASTM C 186 propose to use this type of measurement. According to these standards, first, thermal capacity and thermal leakage coefficient of the calorimeter is calculated, during calibration with a mixture of zinc oxide, hydrofluoric acid and nitric acid. At constant temperature, a known mass of cement is mixed with the acid mixture and over a period of time, the temperature of calorimeter is measured. The increase in corrected temperature is calculated and using the coefficients obtained during calibration, the heat of hydration of the sample is found using the formulas given in standards.

##### **2.3.4.2 Semi-adiabatic Method**

In semi-adiabatic method, also called “Langavant Method” (BS EN 196-9), a mortar sample is prepared using specific amounts of cement, water and a standard sand. According to BS EN 196-9, immediately after mixing operation, the mortar is put in a mortar box which is a cylindrical container, and with the help of a thermometer, the temperature is determined at different times. Using a reference calorimeter, the temperature rise of the sample is found and with the formulas specified in the related standards, the heat of hydration is calculated.

##### **2.3.4.3 Isothermal Calorimeter Method**

Isothermal calorimeters, also called heat conduction or heat flow calorimeters, have two ampoules. One of them is used for the reference material (which does not

produce any heat) and other one for the sample. The calorimeter is monitored by the help of a computer and software. According to ASTM C 1702, before the experiment, an initial baseline should be taken when the temperature difference between environment and calorimeter is below a certain point. Then, the sample is prepared inside (Method A) or outside (Method B) of the calorimeter. In Method B, there can be some data losses which can be important for the experiment. Also, taking the initial base line is more difficult. In Method A, the mixing process is tougher. With software, just the energy produced by chemical reactions is measured and after removing the sample from the calorimeter, the final baseline is taken. In both methods, finally the results are found by considering the sample and reference ampoule.

### **2.3.5 Significance of Determining Heat of Hydration**

It is important to estimate heat of hydration in order to take precautions against the possible damages of excessive temperature rise in concrete due to higher heat of hydration. The measurements of heat of hydration and rate of heat evolution are important since these are functions of temperature, water / cement ratio, particle size and composition (Lohtia and Joshi, 1995). These can be predicted using the curves of heat evolution and rate of heat evolution. Due to the fact that admixtures can affect heat produced, mineral and chemical admixture content may be predicted. In addition, other compounds or impurities of cement can be estimated since they make a small contribution to the heat of hydration with respect to their amounts during hydration process. The peaks on the rate of heat evolution curve are also important in determining the times at which concrete can be placed, or transported (Scrivener and Nonat, 2011).

#### **2.3.5.1 Rate and Degree of Hydration**

Considering the rate of heat evolution, the heat of hydration and the properties depending on rate of hydration can be predicted (Lohtia and Joshi, 1995). A heat of hydration curve can be a good guide for understanding hydration kinetics of a hydraulic cementitious material as specified in ASTM C 1679.

The literature shows that the degree of hydration can be found by using the heat release of the chemical reactions in cement. Poppe and Schutter (2005), the degree of hydration can be found using heat release values. This relation is formulated as follows (Eqn. 2.5) (Poppe and Schutter, 2005).

$$\alpha = \frac{Q(t)}{Q_{max}} = \frac{1}{Q_{max}} \int_0^t q(t) dt \quad (\text{Eqn. 2.5})$$

where,

$\alpha$  = Degree of reaction

t = Time (in h)

Q (t) = Cumulative heat of hydration (in J/g)

$Q_{max}$  = Maximal theoretical cumulated heat of hydration (in J/g)

q(t) = Heat production rate (in J/g.h)

### 2.3.5.2 Temperature

Hydration of cement evolves heat and causes the temperature of cement paste or concrete to increase. This can cause expansion cracks on concrete. The heat of hydration at different ages can be used to predict maximum temperatures of concrete (Najafi and Ahangari, 2013; Mehta and Monteiro, 2006; Binici et al., 2007). From adiabatic tests, the temperature of concrete can be found to be directly proportional to the cumulative heat of hydration. The Eqn. 2.6 shows the relation (Poppe and Schutter, 2005). Furthermore, the strength of a concrete sample can be predicted using the temperature of the concrete, with the maturity method, as given in ASTM C 1074.

$$\theta(t) - \theta_0 = \frac{Q(t) C}{c_c \rho} \quad (\text{Eqn. 2.6})$$

where,

$\theta(t)$  = Temperature of the concrete (in °C)

$\theta_0$  = Initial temperature of the concrete (in °C)

$Q(t)$  = Cumulative heat of hydration (in J/kg)

$C$  = Cement content (in kg/m<sup>3</sup>)

$\rho$  = Concrete density (in kg/m<sup>3</sup>)

$c_c$  = specific heat of concrete (in J/kg/°C)

### 2.3.5.3 Chemical Composition

Chemical composition is the main factor to change the cumulative heat of hydration and rate of heat of hydration evolution (ACI, 2001). The hydrations of different clinker compositions produce different amounts of heat. Using the rate of heat evolution and cumulative heat of hydration, chemical composition can be estimated. According to Mehta and Monteiro (2006), the heat of hydration value of cement at a given time can be found using Eqn. 2.7:

$$H = aA + bB + cC + dD \quad (\text{Eqn. 2.7})$$

where,

A, B, C, D = mass percentages of the four main clinker compounds

a, b, c, d = coefficients representing the contribution of the corresponding clinkering compound (can be obtained from Table 2.10)

The chemical composition of a cement can be estimated if the heat of hydration at a specific time is known.

#### 2.3.5.4 Strength

Chemical properties of cement are related to its strength (Mehta and Monteiro, 2006). It is said that there is relation between the heat release and strength (Bentz, 2010). According to Bentz et al. (2012), the relation between the strength of mortars and the heat of hydration per milliliter of water can be found and using the heat of hydration and 7-day compressive strength values, the 28-day compressive strength can be estimated by using Eqn. 2.8.

$$\sigma_{pred-28\ day} = \sigma_{7\ days} + 0.1179 (HH_{28\ day} - HH_{7\ day}) \quad (\text{Eqn. 2.8})$$

where,

$\sigma_{pred-28\ day}$  = Predicted 28-day compressive strength of mortars (in MPa)

$\sigma_{7\ day}$  = Measured 7-day compressive strength of mortars (in MPa)

$HH_{28\ day}$  = Heat of hydration at 28 days (in J/mL)

$HH_{7\ day}$  = Heat of hydration at 7 days (in J/mL)

#### 2.3.5.5 Setting Time

According to Schindler (2004), the setting time of concrete is a function of the rate of hydration of cement. Therefore, setting times of concrete can be predicted by using rate of the hydration of the cement used as a constituent in the concrete. Eqn. 2.9 and

Eqn. 2.10 have been proposed to find the initial and final setting times (Schindler, 2004).

$$t_{ei} = \tau \left( -\ln \left[ \frac{0.14 w/cm}{\alpha_u} \right] \right)^{-\frac{1}{\beta}} \quad (\text{Eqn. 2.9})$$

$$t_{ef} = \tau \left( -\ln \left[ \frac{0.26 w/cm}{\alpha_u} \right] \right)^{-\frac{1}{\beta}} \quad (\text{Eqn. 2.10})$$

where,

$t_{ei}$ ,  $t_{ef}$  = equivalent age at initial set and final set, respectively (in h)

$\tau$ ,  $\alpha_u$ ,  $\beta$  = hydration parameters determined from semi-adiabatic tests

$w/cm$  = water to cementitious material ratio

### 2.3.5.6 Shrinkage

Shrinkage is dependent on the heat of hydration and rate of heat evolution. A close relationship between rate of heat of hydration evolution and autogenous shrinkage velocity is found (Kim et al., 2009). Considering the rate of the hydration, and the increase in temperature due to hydration reactions in the concrete, the autogenous shrinkage velocity can be predicted by using Eqn. 2.11.

$$ASV = 31.542 HHV - 40.643 \quad (\text{Eqn. 2.11})$$

where,

$ASV$  = Autogenous shrinkage velocity (in  $-1 \times 10^{-6}$  / h)

$HHV$  = Hydration heating velocity (in  $^{\circ}\text{C/h}$ )





## **CHAPTER 3**

### **EXPERIMENTAL PROCEDURE**

#### **3.1 General**

The objective of this experimental study is to determine the effect of pozzolan content and average particle size of cement on the heat of hydration and rate of heat evolution for 48 hours. In addition, the heat of hydration is predicted using clinker content, pozzolan content and the law of mixtures.

First, the materials were ground together with specific ratios using a laboratory ball mill (intergrinding) and pozzolanic cements obtained. Then, using a sonic sifter, the materials were sieved to certain size groups. Finally, using isothermal calorimeter, the heat of hydration and rate of heat evolution were measured for 48 hours, for each specific particle size group.

Except the chemical analyses and particle size distribution measurements, all experiments were performed in the Materials of Construction Laboratory, Department of Civil Engineering, Middle East Technical University. Chemical analyses and particle size distributions were performed at the R&D Laboratories of Turkish Cement Manufacturers Association (TCMA).

### 3.1.1 Materials

The clinker, gypsum, and natural pozzolan (trass) used in the study were obtained from Bursa Cement Factory and all of the materials were obtained unground. Their oxide analyses are shown in Table 3.1 using TSE CEN/TR 196-4.

Table 3.1. Oxide analysis of the materials used in experiments.

	<b>Clinker</b>	<b>Gypsum</b>	<b>Trass</b>
SiO <sub>2</sub>	20.49	1.85	59.26
Al <sub>2</sub> O <sub>3</sub>	4.49	0.05	17.21
Fe <sub>2</sub> O <sub>3</sub>	4.29	0.19	4.65
CaO	66.41	32.40	5.94
MgO	0.97	0.21	1.72
SO <sub>3</sub>	0.77	44.47	0.25
Na <sub>2</sub> O	0.21	< 0.01	3.47
K <sub>2</sub> O	0.80	0.07	1.84
LOI	1.10	20.89	4.58

### 3.2 Grinding of cements

In Turkey, the common grinding method of clinker, gypsum and mineral additions is intergrinding, therefore, this method was performed in this research (Erdoğdu et al., 2009). Four cements (3 of them pozzolanic, and one ordinary portland cement) were produced with specific mass fractions of the materials using laboratory ball mill whose charge properties are given in Table 3.2. The laboratory ball mill used had a length of 465 mm and a diameter of 370 mm. Its volume was about 50 dm<sup>3</sup>.

Table 3.2. Properties of the charge in the laboratory ball mill.

<b>Ball size</b>	<b>50 mm</b>	<b>40 mm</b>	<b>29 mm</b>	<b>22 mm*</b>	<b>16 mm*</b>	<b>Total</b>
Number of balls	15	62	174	160	210	621
Total mass (kg)	7.8	16.9	17.0	10.5	4.9	57.1
* 22 & 16 mm charges are cylindrical. Other ones are spherical.						

For each cement, a total of 2000 g of raw material was put in the mill considering the charge properties. The material proportions are shown in Table 3.3. During grinding process, the Blaine fineness value (ASTM C 204) was measured periodically, until the desired fineness was achieved. Moreover, the total grinding time was measured for each cement group.

Table 3.3. Percentage and mass of the raw materials used in each cement group before grinding process.

	Percentage (%)				Mass (g)			
	Clinker	Gypsum	Trass		Clinker	Gypsum	Trass	Total
Control Group	95.0	5.0	0.0		1900.0	100.0	0.0	2000.0
Group I	89.3	4.7	6.0		1786.0	94.0	120.0	2000.0
Group II	76.8	3.2	20.0		1536.0	64.0	400.0	2000.0
Group III	62.4	2.6	35.0		1248.0	52.0	700.0	2000.0

Each mix was ground until its Blaine surface area reached  $3950 \pm 200 \text{ cm}^2/\text{g}$ . Then, in order to remove the coarse particles, it was sieved through a 2 mm-sieve.

### 3.3 Size Grouping of Cements

In order to obtain different size groups, the cements were further sieved using a sonic sifter separator. The sieves used had sizes of 10  $\mu\text{m}$ , 35  $\mu\text{m}$  and 50  $\mu\text{m}$ . The sieving procedure was applied according to sonic sifter separator's manual. First, the sieve of 50  $\mu\text{m}$  was put above the sieve of 35  $\mu\text{m}$ . The fines collector was placed below the sieves and sample was set above the sieves. A diaphragm was placed on the top of the cone. After putting column lock on the upmost and some spacers, the sample was introduced into the coarsest sieve. Using sonic waves, horizontal and vertical pulse accessory, specific amount of sample were obtained on the sieves. From the sample on the collector, cement is put on the sieve of 10  $\mu\text{m}$ . After the device had been started, the material under 10  $\mu\text{m}$  size was attained. The same procedure was applied for Control Group, Group I, Group II and Group III, total 20 different cements were produced. For each particle size group, a minimum of 13.5 g of cement was obtained.

Between two sieving processes of two different cements, the sieves were washed with ethanol in an ultrasonic bath. Table 3.4 shows the groups and subgroups of the cement produced. The chemical analysis based on TSE CEN/TR 196-4 of cement samples are shown in Tables 3.5 – 3.8. After sieving the cements, the samples were protected from air and moisture in small sealed bottles until the time of test or analysis.

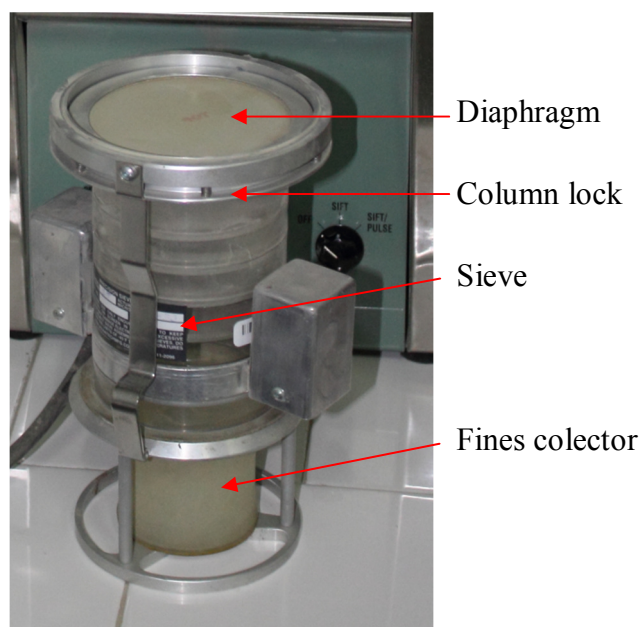


Figure 3.1. Parts of a sieve stack.

Table 3.4. Designation of the subgroups of cements.

	<b>Control Group</b>	<b>Group I</b>	<b>Group II</b>	<b>Group III</b>
Original (0-2000 $\mu\text{m}$ )	0PO	3PO	11PO	22PO
0-10 $\mu\text{m}$	0P0-10	3P0-10	11P0-10	22P0-10
10-35 $\mu\text{m}$	0P10-35	3P10-35	11P10-35	22P10-35
35-50 $\mu\text{m}$	0P35-50	3P35-50	11P35-50	22P35-50
50-2000 $\mu\text{m}$	0P50-2000	3P50-2000	11P50-2000	22P50-2000

Table 3.5. Chemical analysis results of 0P cements.

	<b>0P0</b>	<b>0P0-10</b>	<b>0P10-35</b>	<b>0P35-50</b>	<b>0P50-2000</b>
SiO <sub>2</sub>	19.82	18.45	20.52	20.45	20.29
Al <sub>2</sub> O <sub>3</sub>	4.76	4.73	4.81	5.00	5.08
Fe <sub>2</sub> O <sub>3</sub>	4.65	4.58	4.58	4.75	4.80
CaO	64.78	63.24	65.20	65.07	64.23
MgO	1.09	1.06	1.09	1.11	1.09
SO <sub>3</sub>	1.53	2.54	1.19	1.13	1.89
Na <sub>2</sub> O	0.24	0.22	0.22	0.20	0.20
K <sub>2</sub> O	0.65	0.67	0.57	0.57	0.62
LOI	2.07	4.05	1.69	1.65	1.69

Table 3.6. Chemical analysis results of 3P cements.

	<b>3P0</b>	<b>3P0-10</b>	<b>3P10-35</b>	<b>3P35-50</b>	<b>3P50-2000</b>
SiO <sub>2</sub>	20.33	19.32	20.74	20.84	20.74
Al <sub>2</sub> O <sub>3</sub>	4.95	4.99	4.94	5.18	5.19
Fe <sub>2</sub> O <sub>3</sub>	4.51	4.51	4.45	4.61	4.63
CaO	62.15	59.51	62.64	63.07	61.62
MgO	1.09	1.06	1.08	1.09	1.08
SO <sub>3</sub>	2.52	4.14	2.22	2.19	2.73
Na <sub>2</sub> O	0.33	0.28	0.24	0.22	0.26
K <sub>2</sub> O	0.67	0.67	0.57	0.57	0.63
LOI	2.53	4.80	2.63	2.18	2.39

Table 3.7. Chemical analysis results of 11P cements.

	<b>11P0</b>	<b>11P0-10</b>	<b>11P10-35</b>	<b>11P35-50</b>	<b>11P50-2000</b>
SiO <sub>2</sub>	23.88	24.03	23.81	23.74	24.93
Al <sub>2</sub> O <sub>3</sub>	6.09	6.50	6.02	6.31	6.56
Fe <sub>2</sub> O <sub>3</sub>	4.65	4.75	4.57	4.69	4.67
CaO	58.08	54.21	58.79	60.07	56.47
MgO	1.16	1.16	1.14	1.16	1.17
SO <sub>3</sub>	1.56	2.92	1.58	1.27	1.98
Na <sub>2</sub> O	0.58	0.57	0.47	0.41	0.55
K <sub>2</sub> O	0.70	0.74	0.64	0.62	0.71
LOI	2.79	4.98	2.70	1.71	2.94

Table 3.8. Chemical analysis results of 22P cements.

	<b>22PO</b>	<b>22P0-10</b>	<b>22P10-35</b>	<b>22P35-50</b>	<b>22P50-2000</b>
SiO <sub>2</sub>	28.04	29.19	28.04	27.38	30.28
Al <sub>2</sub> O <sub>3</sub>	7.55	7.99	7.41	7.22	8.05
Fe <sub>2</sub> O <sub>3</sub>	4.59	4.77	4.50	4.59	4.58
CaO	51.74	46.91	52.43	53.77	49.25
MgO	1.21	1.21	1.21	1.23	1.24
SO <sub>3</sub>	1.67	2.69	1.63	1.55	1.89
Na <sub>2</sub> O	0.96	0.92	0.79	0.75	0.98
K <sub>2</sub> O	0.92	0.81	0.69	0.71	0.81
LOI	3.27	5.47	3.25	2.76	2.90

### 3.4 Measurement of the Particle Size Distribution of Cements

The particle size distributions of size groups were measured using a Malvern Mastersizer 2000 laser diffraction device. A laser beam is sent to the particles and the particles scatter the light. With respect to the particle size, the angle of the scattered light changes and the detectors measure the angle of the light scattered.

### 3.5 Measurement of Heat of Reaction of Cements

After starting the software and taking the initial base line, the 3.5 g of sample was put on an ampoule. After an initial base line had been taken, according to ASTM C 1702 – Method A, distilled water was added to cement inside the calorimeter by a syringe. The amount of water was chosen as 1.4 g, so the ratio of water amount to the amount of cementitious material was 0.4. After adding the water, the cement paste was mixed and the measurement was started. After 2 days (48 hours), the experiment was ended. During the whole process of getting heat of hydration curve, the procedure given in the manual (TA Instruments, 2007) was applied.

During hydration process, after adding water, the cement is heated and the temperature of it and hence the temperature of calorimeter increases. The cooling system decreases the temperature of calorimeter and material. A device records the energy spent by the cooling system, as a result of this, the hydration heat and rate of heat evolution can be measured by this device.

The duration when the measurement of heat of hydration of the samples was taken can be determined as 2 days. Because, the time period of 2 day is enough to see the rate of heat of hydration peaks completely and can give an idea about its characteristics.





## CHAPTER 4

### RESULTS AND DISCUSSION

#### 4.1 General

The grinding time and heat evolution properties of interground natural pozzolan-incorporated cements are presented in this chapter. The chemical analysis and particle size distributions of three raw materials (clinker, gypsum and trass) and cements are also studied. The heat evolution values are tried to estimate using clinker compounds and particle size distribution curves.

#### 4.2 Mass fractions of Cement Groups

Though, the mass fractions are designed before the grinding process, the contents of the raw materials in the cement samples change due to the removal of residual coarse particles (  $> 2$  mm) after grinding. Using the chemical analysis of raw materials (clinker, gypsum and trass) and the total mass, the mass percentage of each constituent can be found from Eqn. 4.1, Eqn. 4.2 and Eqn. 4.3. The calculations are based on the total material, total CaO, and total SiO<sub>2</sub> content. The results from the calculations are shown in Table 4.1.

$$CaO_x = \sum_1^i CaO_i \Phi_i \quad (\text{Eqn. 4.1})$$

$$SiO_{2x} = \sum_1^i SiO_{2i} \Phi_i \quad (\text{Eqn. 4.2})$$

$$1 = \sum_1^i \Phi_i \quad (\text{Eqn. 4.3})$$

where,

$CaO_x$  = Lime content fraction in the cement size group

$CaO_i$  = Lime content fraction in the raw material (clinker, trass, gypsum)

$SiO_{2x}$  = Silica content fraction in the cement size group

$SiO_{2i}$  = Silica content fraction in the raw material (clinker, trass, gypsum)

$\Phi_i$  = Mass fraction

i = Raw materials (clinker, trass and gypsum)

Table 4.1. Mass fractions of the raw materials in each cement group after grinding.

	<b>0PO</b>	<b>0P0-10</b>	<b>0P10-35</b>	<b>0P35-50</b>	<b>0P50-2000</b>
Clinker (%)	95.21	90.68	96.44	96.06	93.59
Gypsum (%)	4.79	9.32	3.56	3.94	6.41
Trass (%)	0.00	0.00	0.00	0.00	0.00
	<b>3PO</b>	<b>3P0-10</b>	<b>3P10-35</b>	<b>3P35-50</b>	<b>3P50-2000</b>
Clinker (%)	89.83	82.54	91.42	92.54	89.13
Gypsum (%)	7.15	13.83	5.36	4.43	6.73
Trass (%)	3.02	3.63	3.22	3.03	4.14
	<b>11PO</b>	<b>11P0-10</b>	<b>11P10-35</b>	<b>11P35-50</b>	<b>11P50-2000</b>
Clinker (%)	84.11	75.19	85.70	88.63	81.47
Gypsum (%)	4.82	10.59	3.87	2.01	4.78
Trass (%)	11.06	14.22	10.42	9.35	13.75
	<b>22PO</b>	<b>22P0-10</b>	<b>22P10-35</b>	<b>22P35-50</b>	<b>22P50-2000</b>
Clinker (%)	73.73	63.64	75.35	77.78	70.31
Gypsum (%)	4.59	9.40	3.49	3.00	3.00
Trass (%)	21.68	26.96	21.15	19.21	26.69

As shown in the table, among all the size groups, the clinker content has the lowest value in 0-10  $\mu\text{m}$  size groups. The amounts of the trass and gypsum are higher in

these groups. In the coarser size groups, the quantity of clinker is seen to be higher compared with the two other raw materials. The fact that grindabilities of gypsum and trass are higher than the clinker is the possible reason (Kuleli, 2009; Hoşten and Avşar, 1998).

In the pozzolanic cements, the contents of trass are much less than the desired. 3P cement was produced using 6 % of trass, however the chemical analyses show that the actual content of trass is lower than the desired content. This fact is also true for 11P and 22P cements. The reason for that can be the different particle size of the raw material. The particle size of the trass obtained from Bursa Cement Factory is higher than the one of the clinker. Therefore, the natural pozzolan content may be lower due to this reason.

#### **4.3 Particle Size Distributions of Cement Groups**

The cumulative particle size distributions of the cements are shown in Appendix A. As seen in particle size distribution curves from Fig. 4.1 – 4.5, there is considerable amount of particle sizes which do not belong to the specific size group. In smaller particle size groups like 0-10  $\mu\text{m}$ , there is remarkable content of 10-35  $\mu\text{m}$  cement particles. The exact opposite situation can be considered, also. Coarser cements have some amount of fine particles. The possible reasons can be the attractive forces between the cement particles or the model based on particle size distribution instrument.

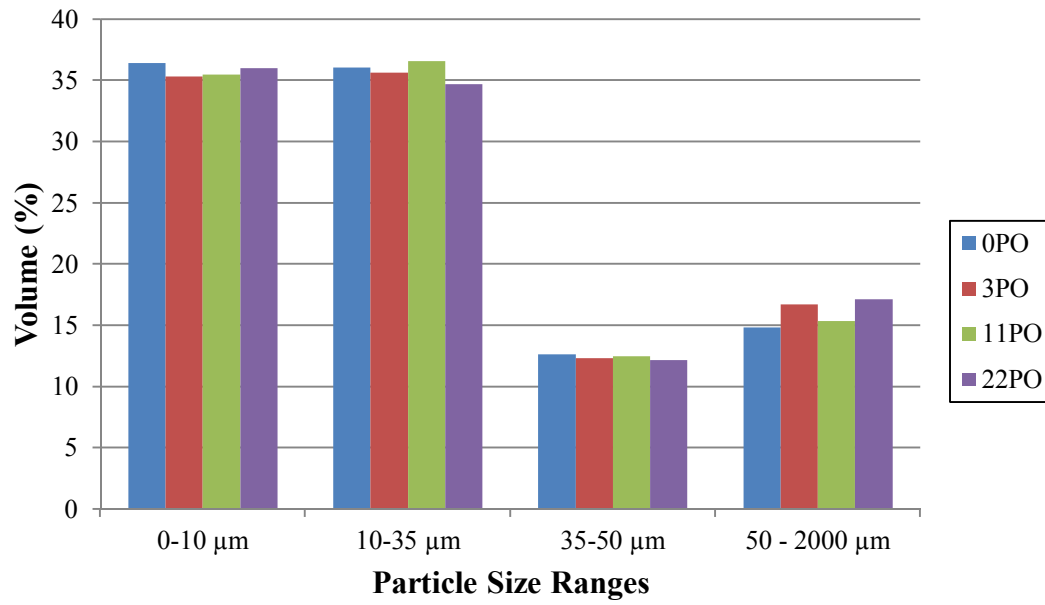


Figure 4.1. Particle size distributions of original groups of cement samples.

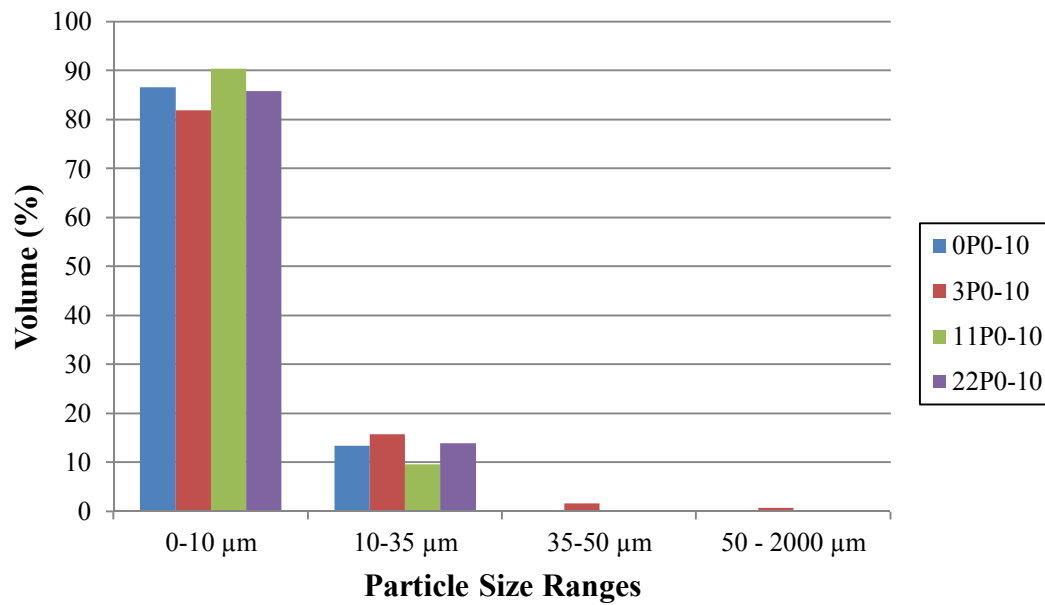


Figure 4.2. Particle size distributions of 0-10 μm size groups of cement samples.

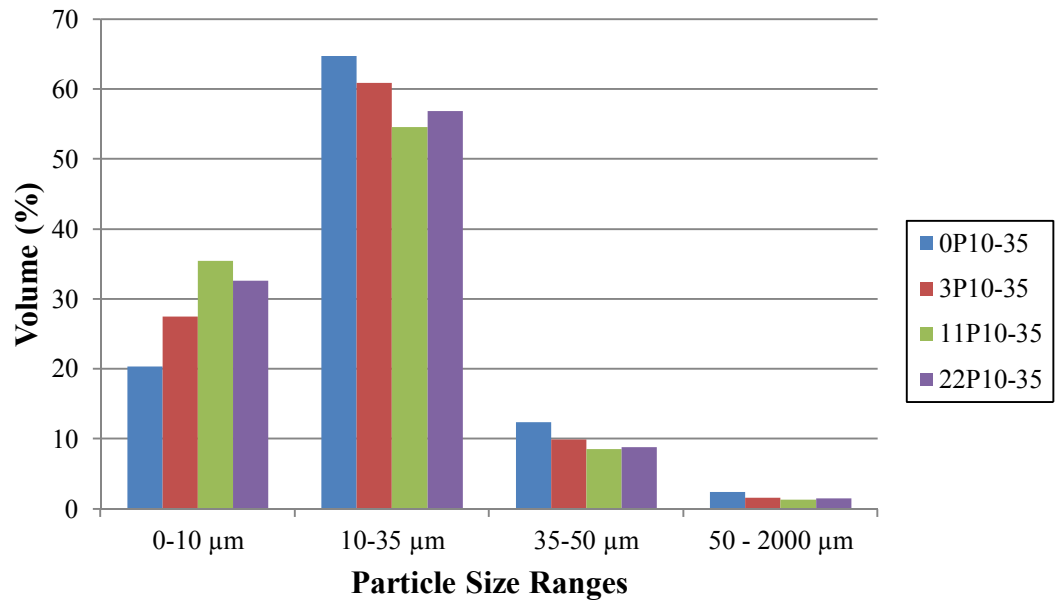


Figure 4.3. Particle size distributions of 10-35 µm sieve groups of cement samples.

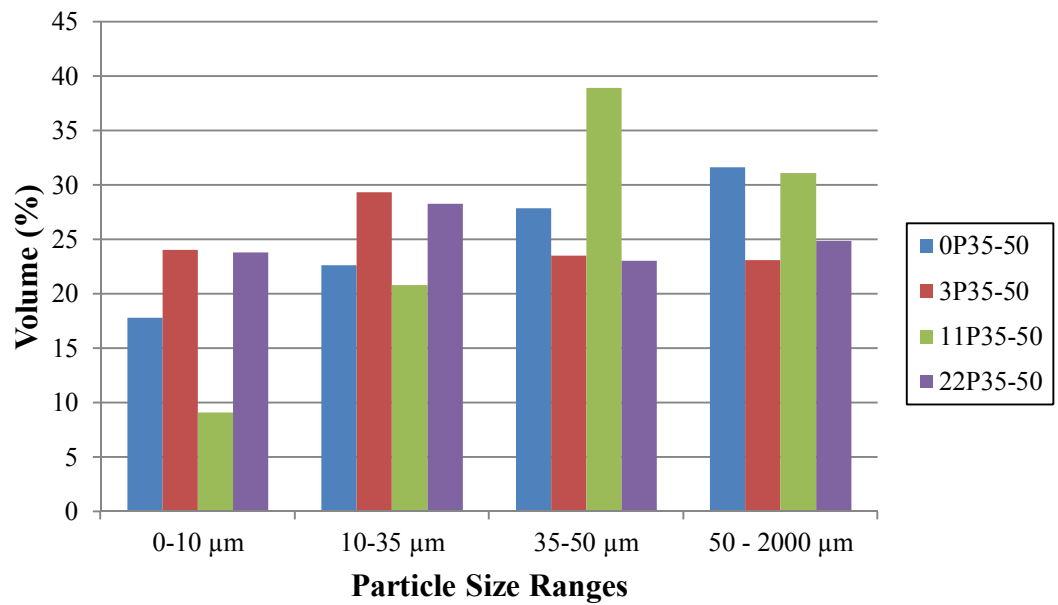


Figure 4.4. Particle size distributions of 35-50 µm sieve groups of cement samples.

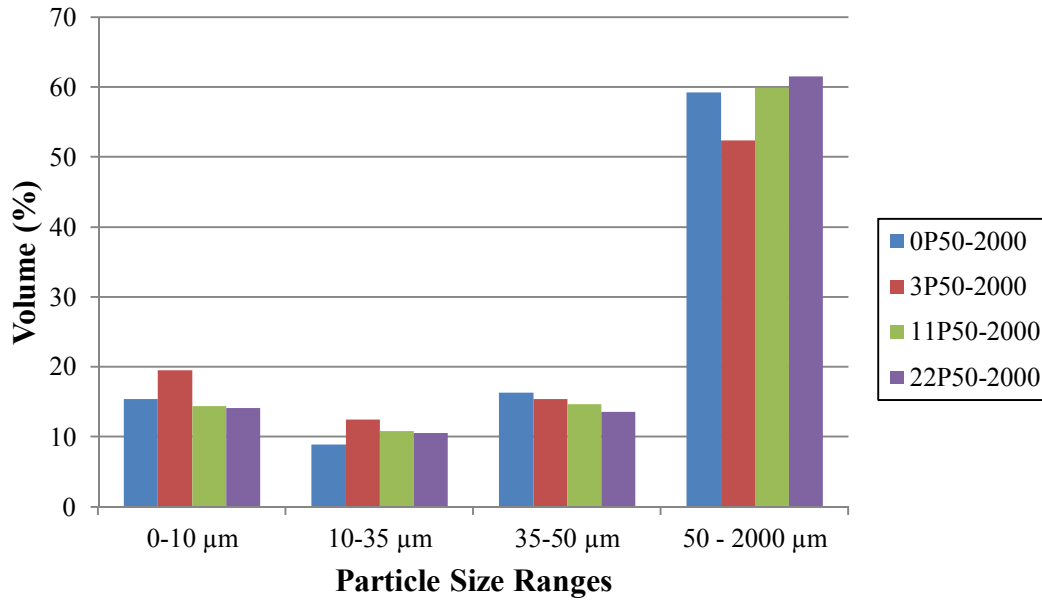


Figure 4.5. Particle size distributions of 50-2000 sieve groups of cement samples.

Particle size distribution instrument uses a laser beam and measures the diffraction images of the particles which are passed in front of the beam by the instrument. Smaller particles and larger particles scatter lights with different properties. The instrument records a thousand of measurements and uses average values of them. The calculations made by the device are based on “Mie’s theory” which assumes that all of the particles are spherical (Stojanović and Marković, 2012). The shape of all the cement particles cannot be perfectly spherical. This assumption causes size determination problems.

The sieving was done by using sonic sifter. The powder can be divided in terms of their particle size. However, ultrasound waves which are used by sonic sifter for the sieving process can not be sufficient to break the attractive forces between colloidal cement particles. Van der Waals forces are developed due to the interaction between the dipoles formed by the electrons orbiting around their nucleus, instantaneously and according to the literature, the forces causing the cement particles to agglomerate can be very important relative to other forces such as gravity or aerodynamic forces

(Lee-Desautels, 2005). Van der Waals forces can be a possible reason for the presence of fine particles in the coarser cement size groups.

Fig. 4.2 – 4.5 show the effectiveness of the sieving of the cements. The cements which were sieved have a great amount of the particles whose average particle sizes are the desired except 35-50  $\mu\text{m}$  size groups. The possible reason can be the coagulation of the particles. During the sieving process, the particles coagulated can not pass the related sieve, so this could reduce the effectiveness of the sieving of the cements. Therefore, the average particle size of the great quantity of the 35-50  $\mu\text{m}$  size cement groups is not between 35 and 50  $\mu\text{m}$ .

#### 4.4 Grinding Time of Cement Groups

During the intergrinding process of cements, the required time values to reach  $3950 \pm 200 \text{ cm}^2/\text{g}$  are shown in Table 4.2.

Table 4.2. For each cement, the grinding time for required specific surface.

	<b>Blaine Specific Surface (<math>\text{cm}^2/\text{g}</math>)</b>	<b>Median Particle Size – d (0.5) (<math>\mu\text{m}</math>)</b>	<b>Grinding Time (min)</b>	<b>Clinker Content Before Grinding (%)</b>	<b>Clinker Content After Grinding (%)</b>
0P	$3950 \pm 200$	17.6	39.0	95.0	95.2
3P	$3950 \pm 200$	18.6	35.0	89.3	89.8
11P	$3950 \pm 200$	18.1	31.0	76.8	84.1
22P	$3950 \pm 200$	18.2	27.5	62.4	73.7

It is clearly seen that increasing clinker content causes an increase in grinding time. It is due to the fact that among the constituents of these cements, clinker is the most difficult material to grind in trass blended cements (Kuleli, 2009; Hoşten and Avşar, 1998).

#### 4.5 48-h Heat of Hydration of Cement Samples

By isothermal calorimetry, the heats of hydration are obtained in the units of J/g for 48 hours. The cumulative heat of hydration of cement groups are shown in Fig. 4.6 – 4.9.

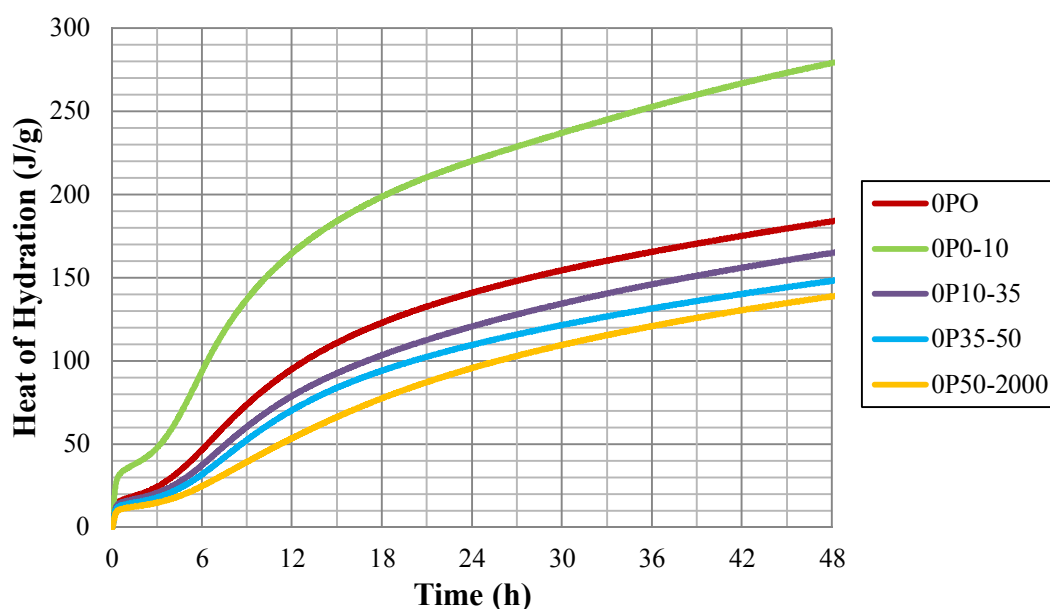


Figure 4.6. 48-hour cumulative heat of hydration of 0P cements.

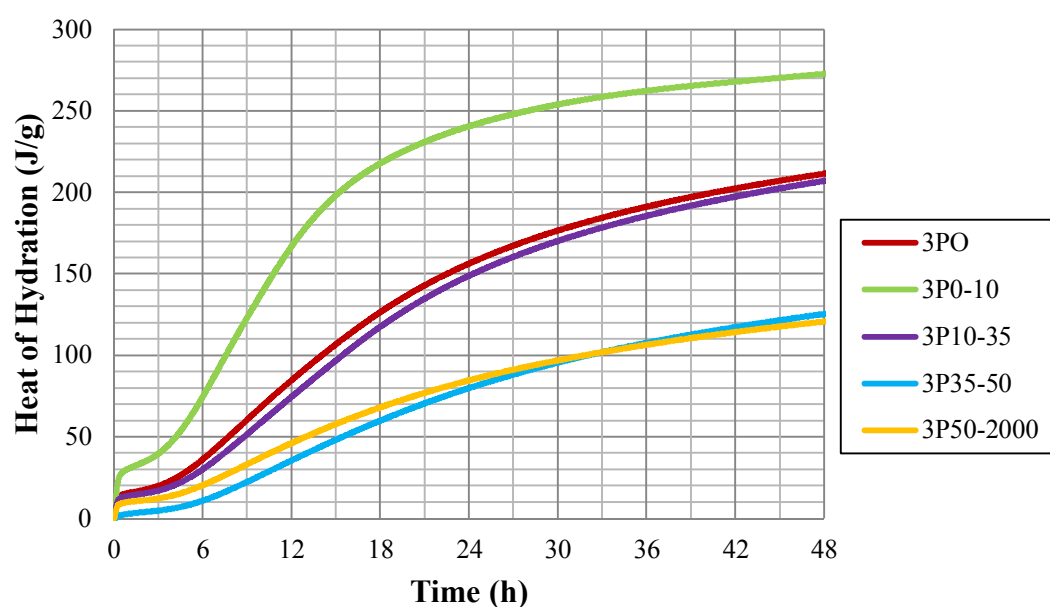


Figure 4.7. 48-hour cumulative heat of hydration of 3P cements.



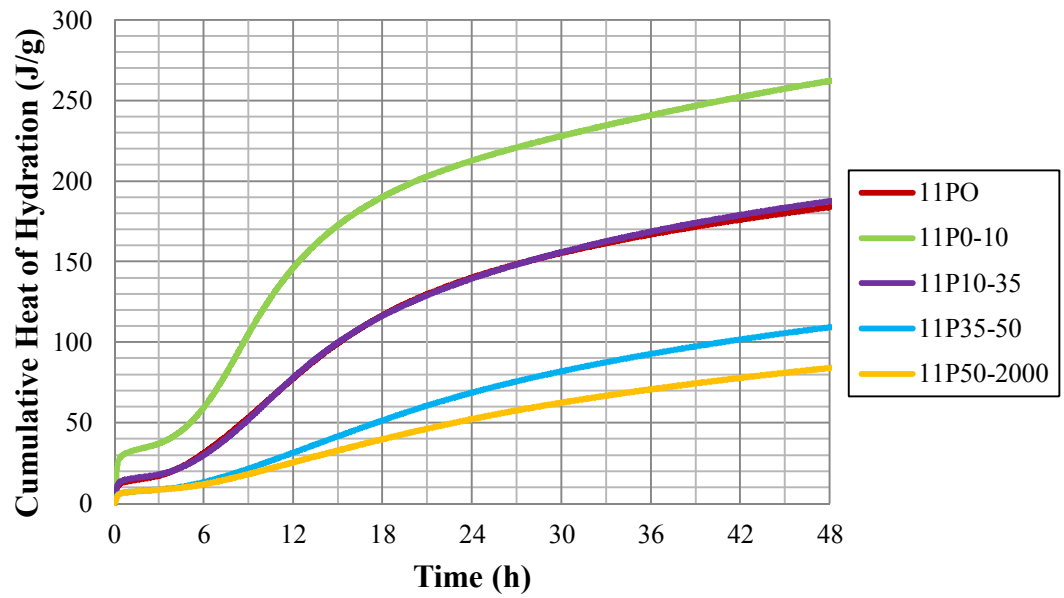


Figure 4.8. 48-hour cumulative heat of hydration of 11P cements.

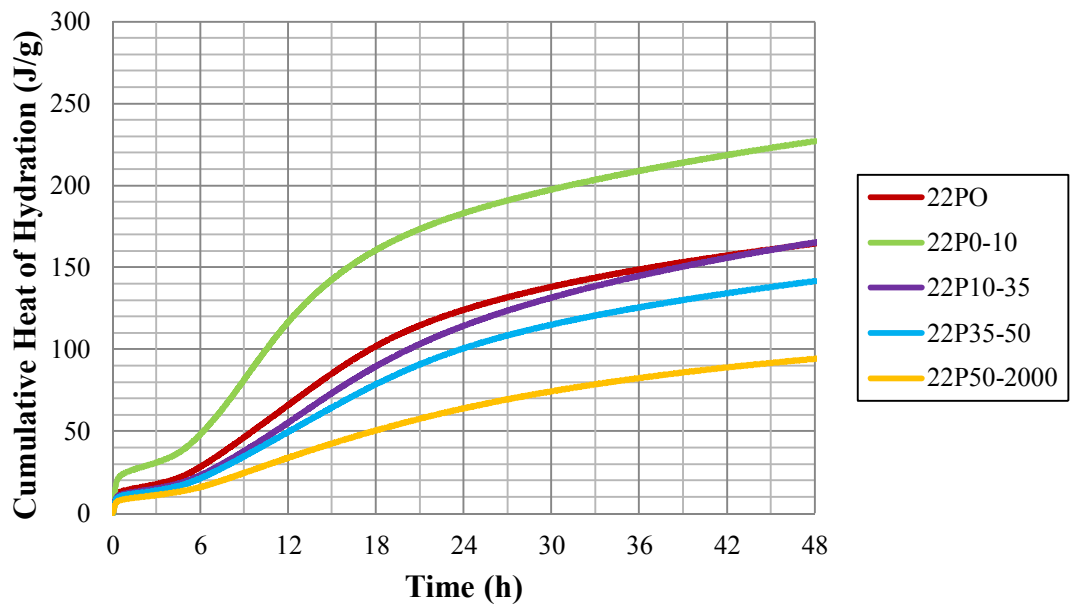


Figure 4.9. 48-hour cumulative heat of hydration of 22P cements.

The heat of hydration of cement samples are shown in Figure 4.10 for the different cement groups. The heats of hydration of cement groups obtained from the experiments are summarized in Table 4.3.

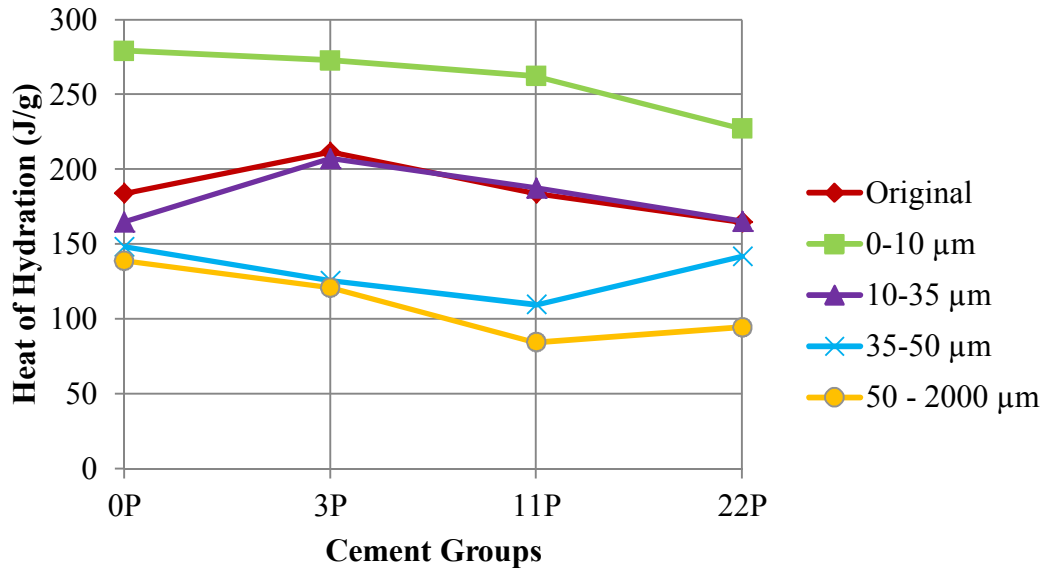


Figure 4.10. 48-hour heat of hydration of cements vs. its size subgroups.

Table 4.3. 48-hour heat of hydration of cements.

Group of Cements	Subgroup of Cements	HH (J/g)	Group of Cements	Subgroup of Cements	HH (J/g)
0P	0PO	184.0	11P	11PO	184.0
	0P0-10	279.1		11P0-10	262.3
	0P10-35	165.0		11P10-35	187.7
	0P35-50	148.3		11P35-50	109.4
	0P50-2000	138.9		11P50-2000	84.2
3P	3PO	211.6	22P	22PO	164.7
	3P0-10	272.8		22P0-10	227.2
	3P10-35	207.2		22P10-35	165.3
	3P35-50	125.5		22P35-50	141.8
	3P50-2000	120.8		22P50-2000	94.4

The heat of hydration of the cements whose size groups are 0-10  $\mu\text{m}$  are the highest and the values of 50-2000  $\mu\text{m}$  size groups are the lowest for each group. For almost all groups, the following sorting can be acceptable:

$$HH_{0-10\mu\text{m}} > HH_{\text{original}} \sim HH_{10-35\mu\text{m}} > HH_{35-50\mu\text{m}} > HH_{50-2000\mu\text{m}}$$

The particles whose sizes are between 0 and 10  $\mu\text{m}$ , are very reactive. Due to their smaller size, their specific surface is very high, and when they are introduced to water, almost all of clinker particles immediately react chemically and produce heat in these size groups. In 2 days, the amount of cement in the finer size groups which has reacted is more than that for other, coarser size groups. The values decrease with increasing particle size due to the same reason. The larger the particle size is, the less reactive the cement is and at a few days, the heat produced is lower.

The underlying reason of identical heat of hydration of original cement and 10-35  $\mu\text{m}$  cement can be their median particle size. For all original cement groups, the median particle size is between 10 and 35  $\mu\text{m}$ . The median particle size of original cement groups can be seen in Table 4.2. Also, as shown in Fig. A.1 – A.4, the particle size distributions of original groups and 10-35  $\mu\text{m}$  are similar. Therefore, the heat produced by original and 10-35 cements in 2 days is similar.

As shown in Table 4.3, for all of the original groups and 10-35  $\mu\text{m}$  size groups, the highest value of heat of hydration is seen in the case of 3P cements due to the fact of possible nucleation effect. In grinding process, the trass is ground more than the clinker phase (Hoşten and Avşar, 1998). The average particle size of trass is less than the average size of a clinker particle. During the hydration process, these smaller pozzolan particles act as a nucleation sites for nascent C-S-H gels and increase the rate of hydration, and correspondingly the heat of hydration. The nucleation effect can be seen in original and 10-35  $\mu\text{m}$  size groups. However, the behavior of 35-50  $\mu\text{m}$  and 50-2000  $\mu\text{m}$  size groups are different. The mineral admixture particles are too large for the nucleation process. To serve nucleation effect, the average particle size of mineral admixtures should be sufficiently small (Lawrence et al., 2003). For these size groups, the nucleation effects cannot be seen. In 0 – 10 size groups, the

behavior is different. The highest value does not belong to the 3P0-10. Since the clinker content is greatly higher in 0P0-10 than 3P0-10 (see Table 4.1).

For the 0P, 3P and 11P cements, 35-50  $\mu\text{m}$  and 50-2000  $\mu\text{m}$  size groups, the values decrease with increasing mineral admixture content. The dilution effect can be a possible reason. An increase in the amount of pozzolan causes the decrease of clinker content and during reactions, less hydrated cement implies less heat of hydration.

The heat of hydration of 22P35-50 is higher than 11P35-50 in spite of the dilution effect. The possible reason can be the remarkable fraction of 0-10  $\mu\text{m}$  and 10-35  $\mu\text{m}$  material present in particle size distribution for 22P35-50 cement group compared with 11P35-50 due to possible ineffectiveness of sieving (see Figure 4.4). While for 11P35-50, the total volume percentage of 0-35  $\mu\text{m}$  is about 30 %, this value for 22P35-50 is about 52 %. This fine fraction can act as nucleation sites in 22P35-50 and can affect the characteristics of heat of hydration curves.

#### 4.6 Rate of Heat Evolution of Cement Samples

The rate of heat evolution curves of the cement groups obtained in this study are shown in Fig. 4.11 – 4.15 with respect to their size groups. In addition, the rate of heat evolution graphs for the pozzolanic groups can be seen in Fig. 4.16 – 4.19.

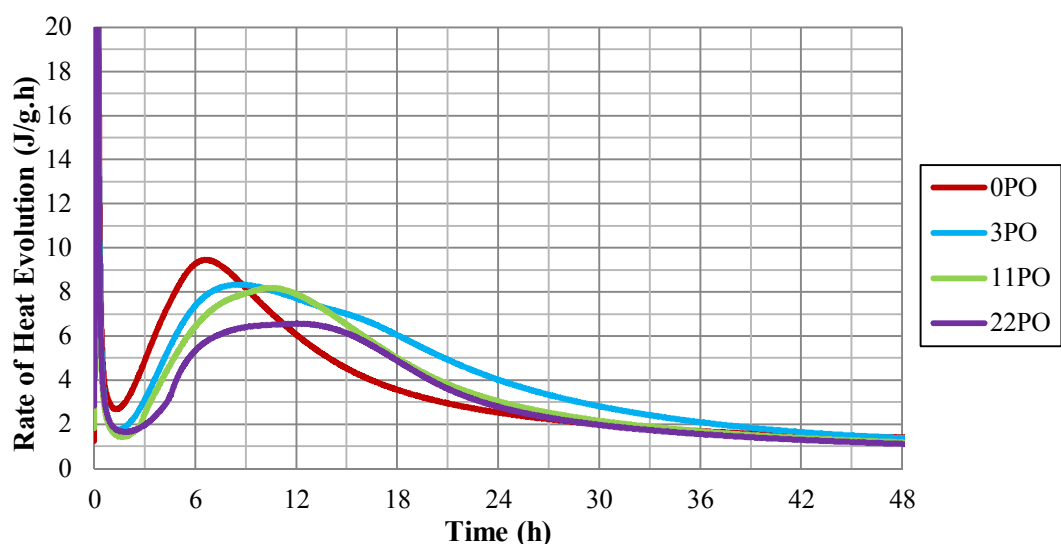


Figure 4.11. Rate of heat evolution of original groups in the 48 hours.

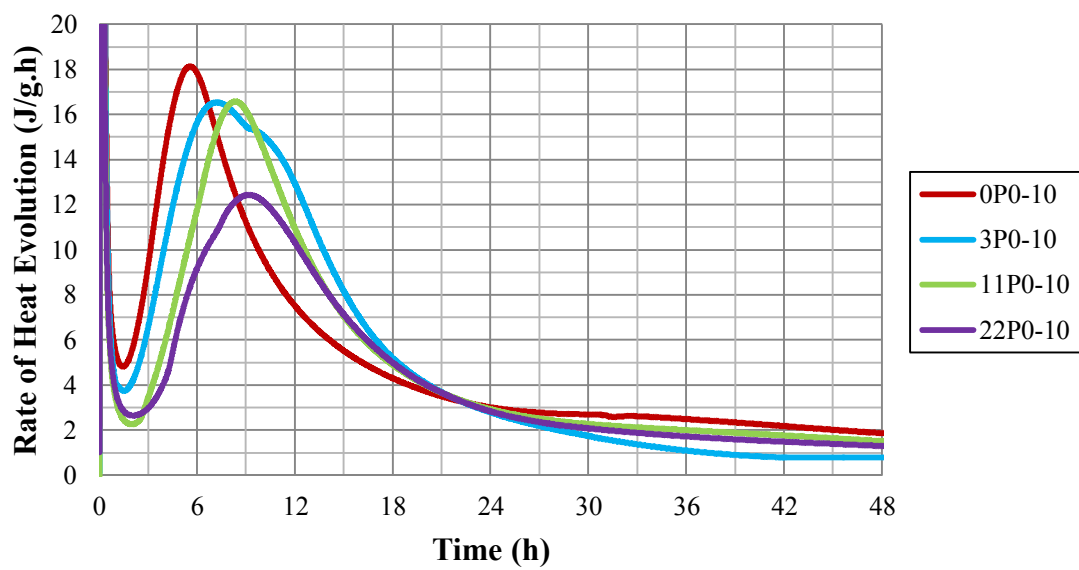


Figure 4.12. Rate of heat evolution of 0-10  $\mu\text{m}$  size groups in the 48 hours.

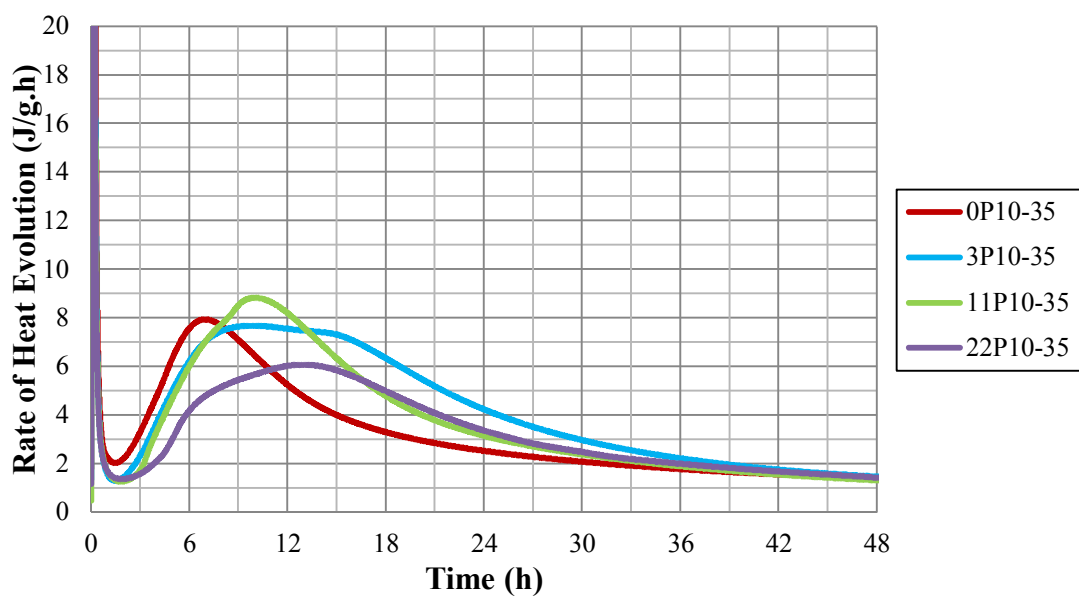


Figure 4.13. Rate of heat evolution of 10-35  $\mu\text{m}$  size groups in the 48 hours.

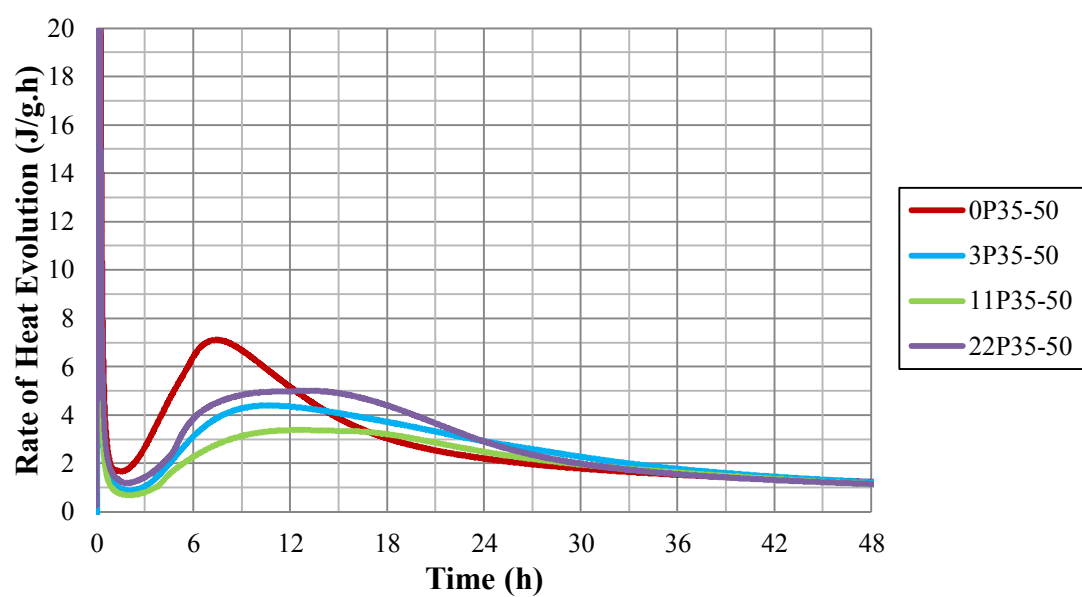


Figure 4.14. Rate of heat evolution of 35-50  $\mu\text{m}$  size groups in the 48 hours.

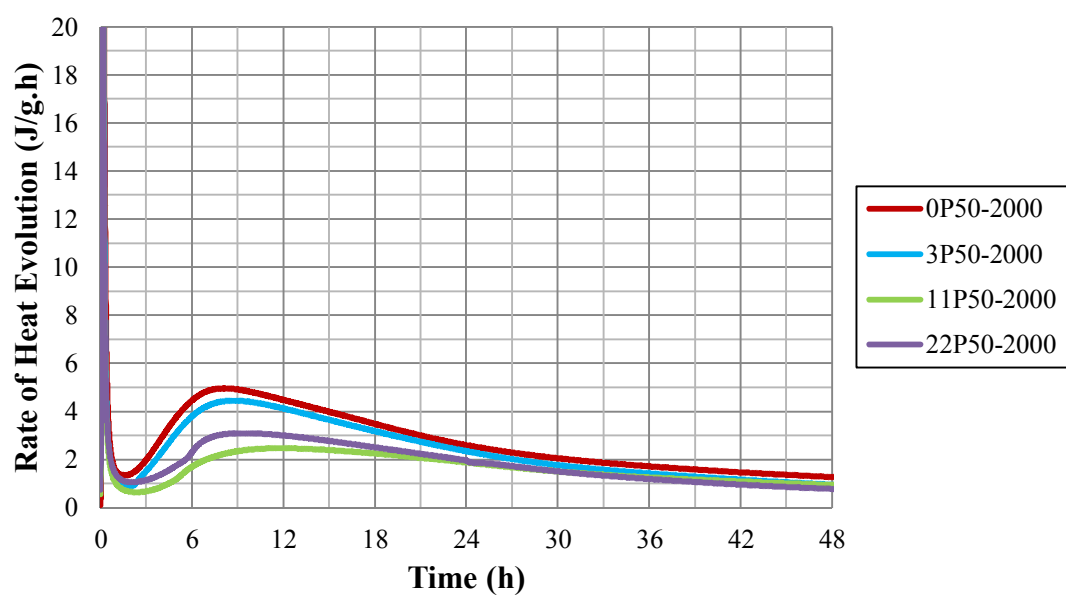


Figure 4.15. Rate of heat evolution of 50-2000  $\mu\text{m}$  size groups in the 48 hours.

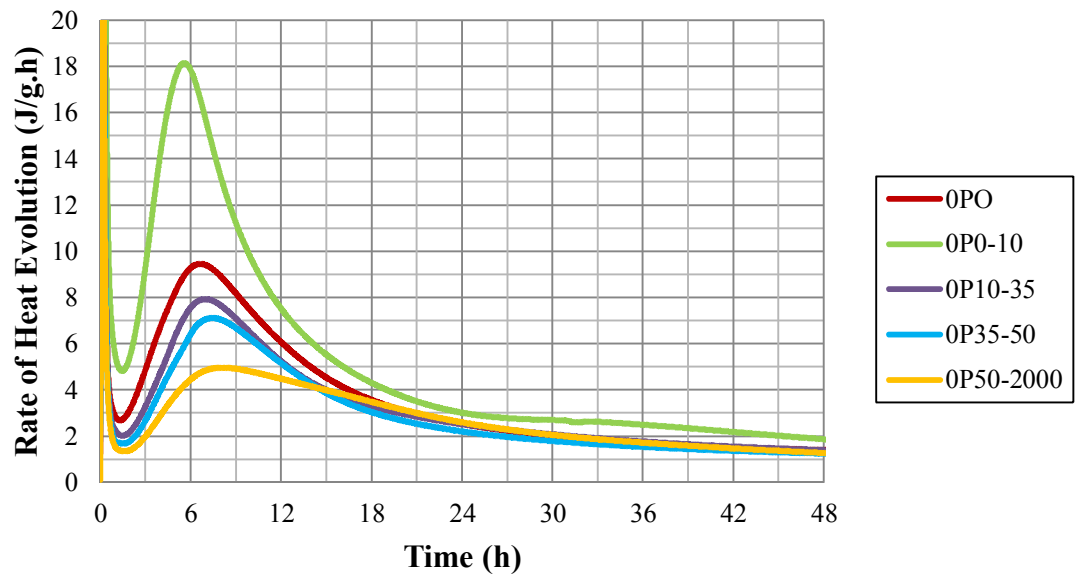


Figure 4.16. Rate of heat evolution of 0P cements in the 48 hours.

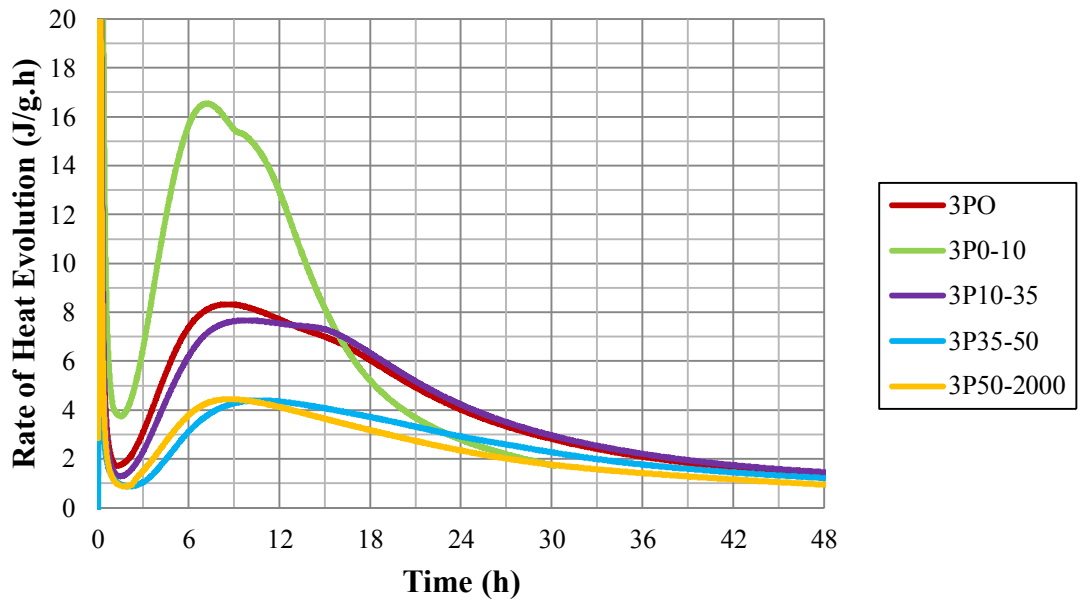


Figure 4.17. Rate of heat evolution of 3P cements in the 48 hours.

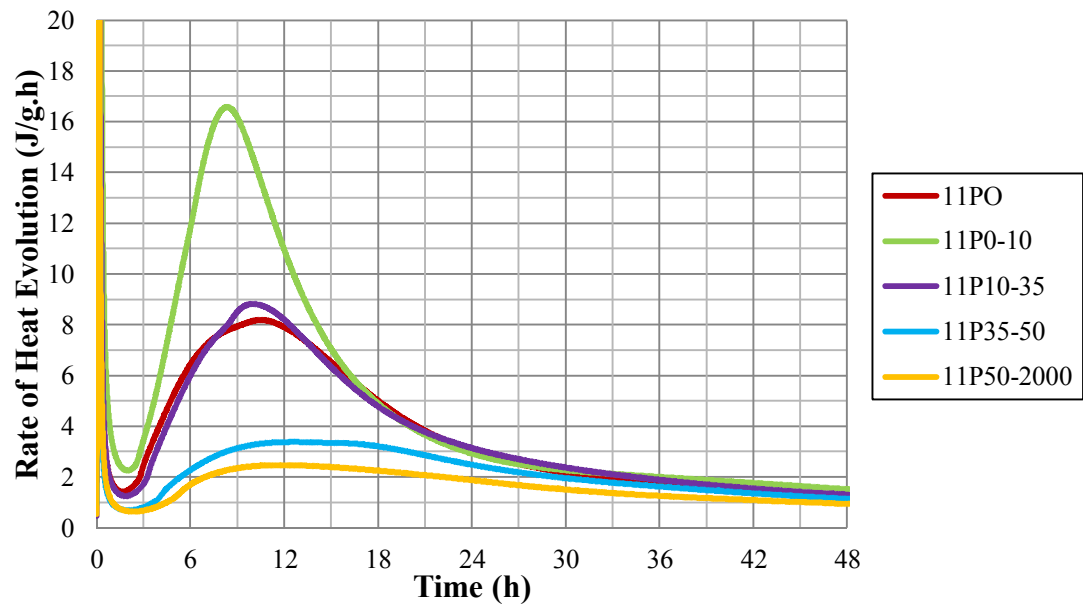


Figure 4.18. Rate of heat evolution of 11P cements in the 48 hours.

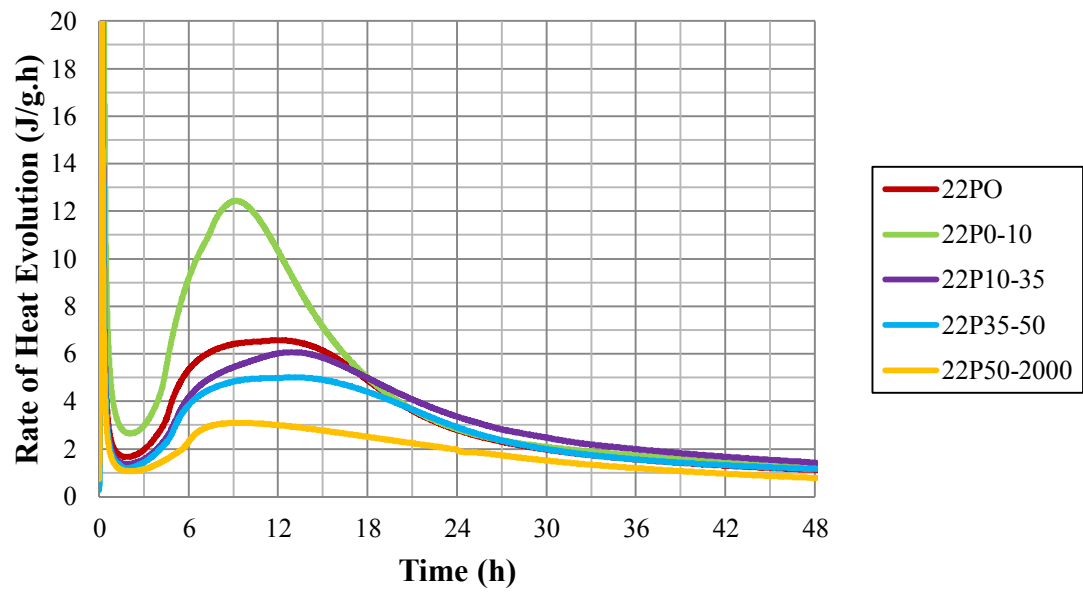


Figure 4.19. Rate of heat evolution of 22P cements in the 48 hours.



#### 4.6.1 First Peaks of Rate of Heat Evolution of Cement Samples

The rate of heat evolution curves are obtained as shown in Fig. 4.20 – 4.23 in first 20 minutes.

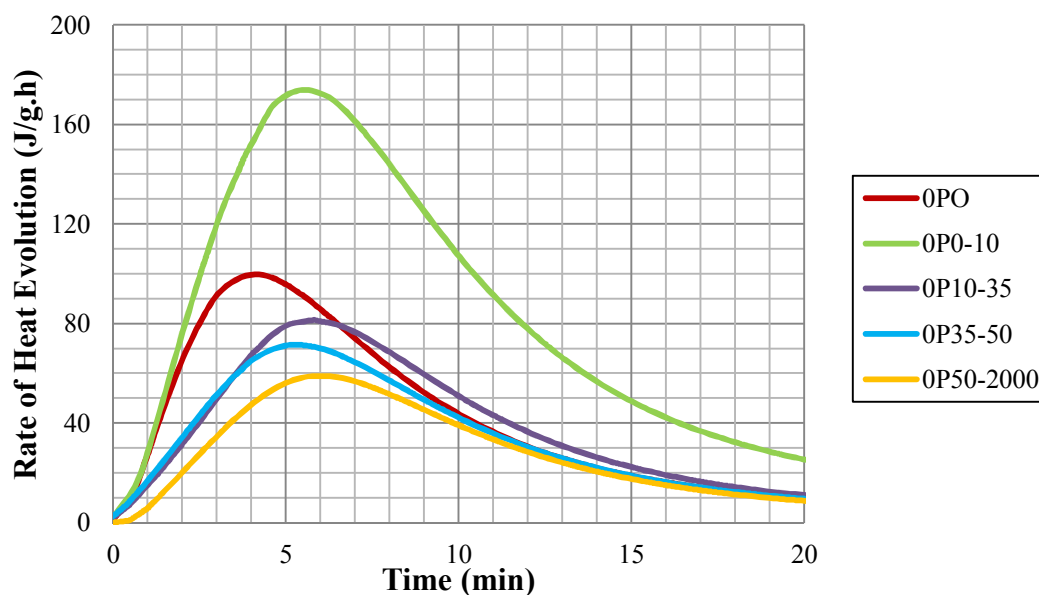


Figure 4.20. Rate of heat evolution of 0P cements in the first minutes.

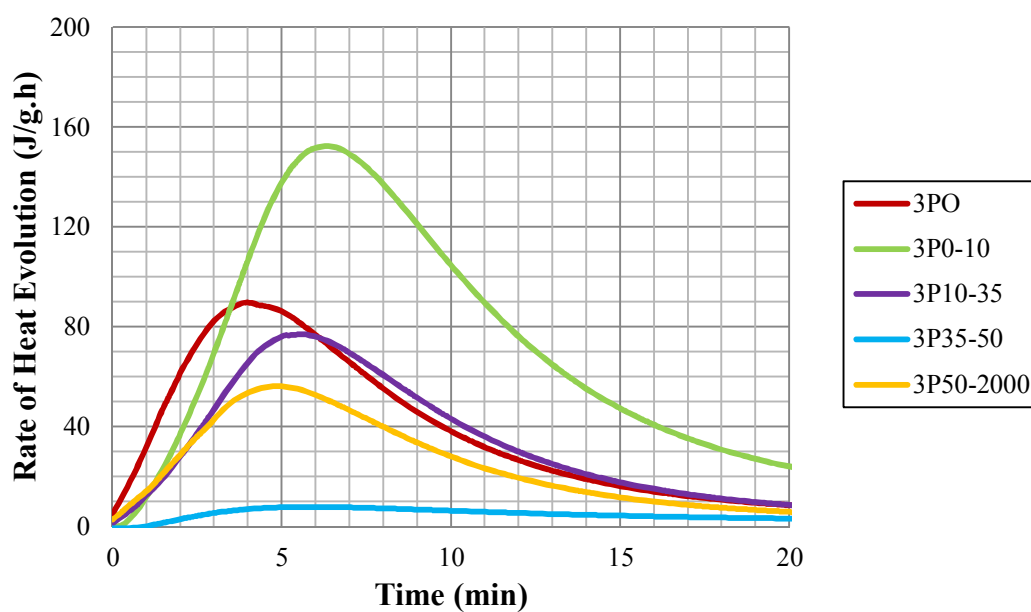


Figure 4.21. Rate of heat evolution of 3P cements in the first minutes.

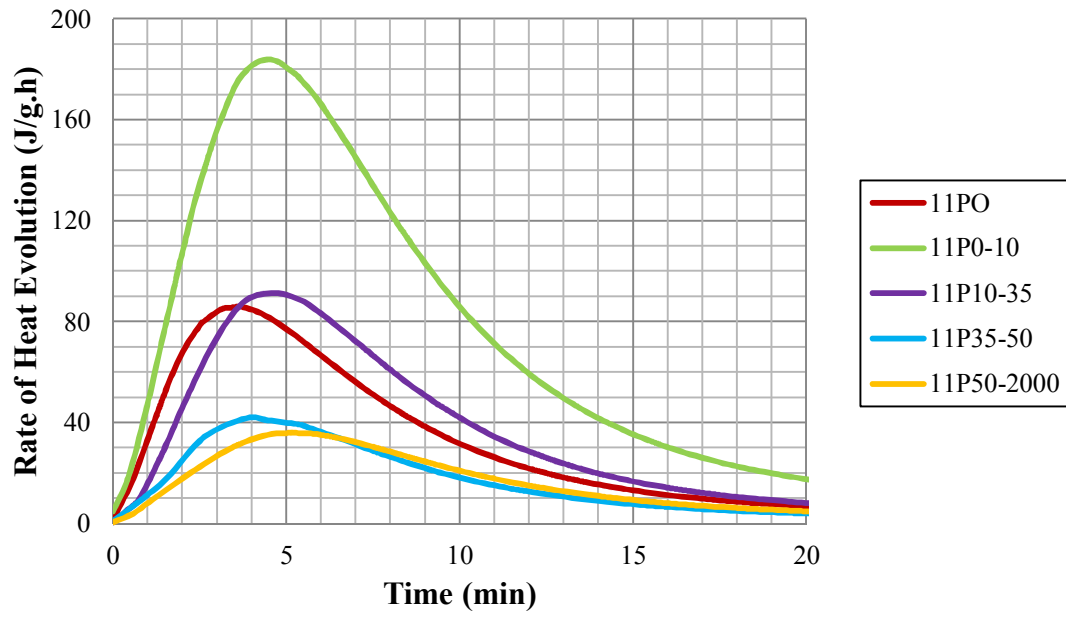


Figure 4.22. Rate of heat evolution of 11P cements in the first minutes.

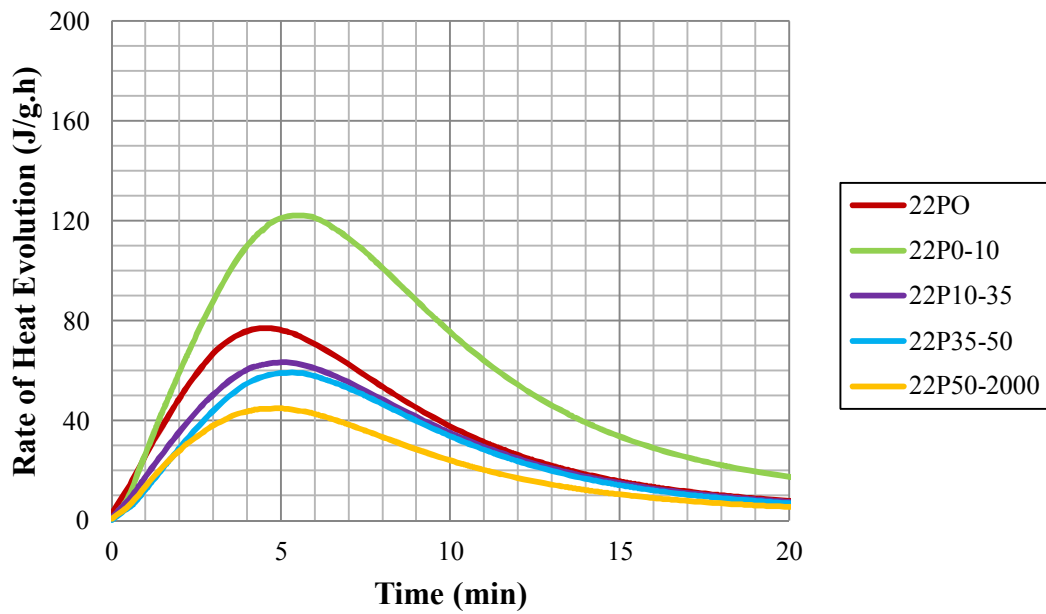


Figure 4.23. Rate of heat evolution of 22P cements in the first minutes.

The time values of the formation of the first peak in very first minutes after starting the experiment are shown in Figure 4.24. In first 20 minutes, the maximum rate of heat evolution values are shown in Figure 4.25.

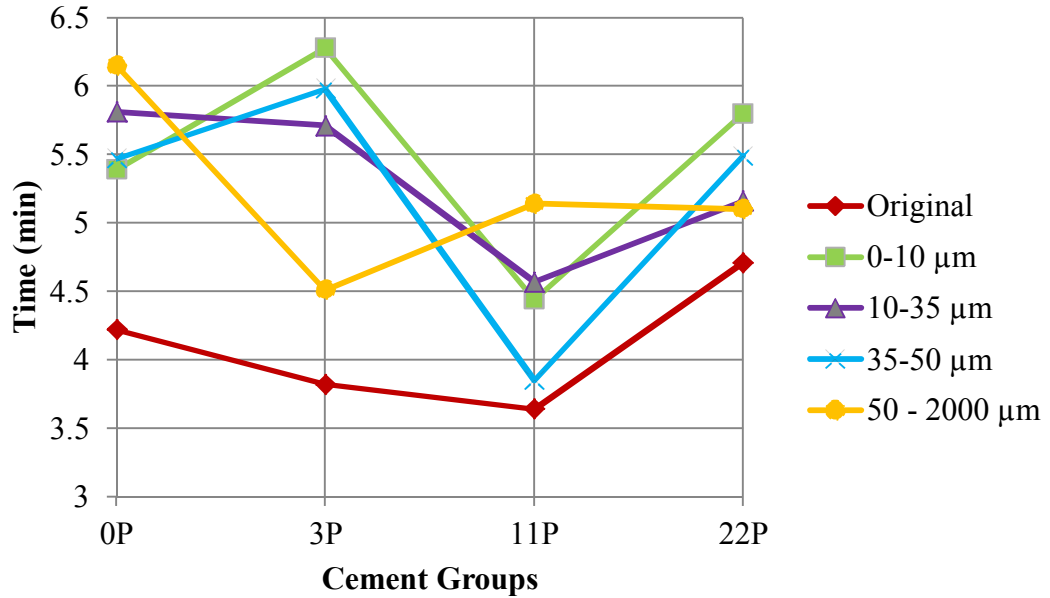


Figure 4.24. The first peak times of cements.

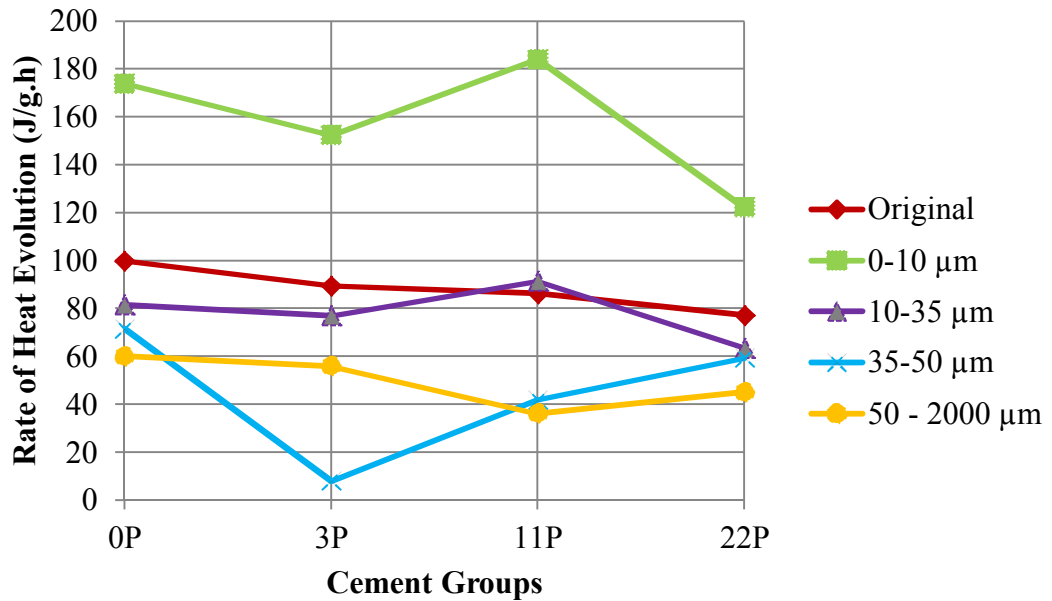


Figure 4.25. Maximum values of rate of heat evolution for the first peak.

0-10  $\mu\text{m}$  size groups have the highest rate of heat evolution values as seen in Figure 4.25. Due to their higher specific surface, in a unit time, water can react with a large amount of cement, therefore, they have the highest rate of heat evolution for first peak. The exact opposite situation can be seen in greater particle size groups.

$$\text{RHE}_{0-10\mu\text{m}} > \text{RHE}_{\text{original}} \sim \text{RHE}_{10-35\mu\text{m}} > \text{RHE}_{35-50\mu\text{m}} > \text{RHE}_{50-2000\mu\text{m}}$$

In Figure 4.25, for the original group, the first peak values decrease with an increasing amount of pozzolan due possibly to the dilution effect. But, the same relation between pozzolan amount and first peak's value can not be found for other size groups due to other possible effects.

It is clearly seen that the time of the occurrence of the first peak is lower for the original groups than the size groups from Figure 4.24. The initial hydration increases with increasing fineness and clinker content in the cement groups. When the two cement groups with higher fine material content are considered, the clinker amounts of the 0-10  $\mu\text{m}$  size groups are lower than original groups. The percentages of clinker in 0PO, 3PO, 11PO and 22PO cement groups are 95.21, 89.83, 84.11 and 73.73 %, respectively. The same values for 0P0-10, 3P0-10, 11P0-10 and 22P0-10 are 90.68, 82.54, 75.19 and 63.64 %, respectively. (The chemical analysis results are shown in Table 4.1) For other cement size groups, in spite of their higher clinker content than original group, their average particle size is higher. Therefore, the first peaks of rate of heat evolution for original cements occur earlier.

Furthermore, for almost all size groups, the first peak of 11P cements occurs earlier than other groups. It can be due to the dispersion effect of the mineral admixture on clinker grains. The first peak in rate of heat evolution of cement is closely related to  $\text{C}_3\text{S}$  hydration (Odler, 2004). According to Dhir (1986), in the very first minutes of hydration, the cement particles are prone to coagulate, forming a non-homogeneous product. Addition of any ultrafine powder can disperse the cement particle groups and increase the total cement surface. Therefore, the  $\text{C}_3\text{S}$  content which is reacted with water and correspondingly, the rate of hydration heat is stimulated. This can be very active in 11P cements because of the higher trass content compared with 0P and 3P cements. However, 22P cements can not show the same effect as 11P, or 3P

cements due to dilution effect. Since the trass content of 22P cements is higher, the amount of clinker hydrated decreases in this group. In other words, the dispersion effect is suppressed by the dilution effect and the reduced  $C_3S$  content in 11P cements results in a slightly longer time to reach the initial peak.

The similarity between the original group and the 10-35  $\mu m$  size groups can be observed like in the case of their heat of hydration curves. This similarity can be originated from the median values of particle sizes. The median particle size values for original cements are between 10 and 35  $\mu m$ . Their particle size distributions are similar also (see Appendix A). Therefore, their behaviors are similar.

#### 4.6.2 Dormant (Induction) Period of Rate of Heat Evolution of Cement Samples

The time until the rate of heat evolution minimum is reached during the dormant period and the rate at this time are given in Table 4.4. The dormant (induction) periods of cement samples' rate of heat evolution with respect to pozzolan amounts are shown in Fig. 4.26 – 4.29.

Table 4.4. The time and rate of heat evolution values of cement samples during dormant period.

<b>Cements</b>	<b>Time (min)</b>	<b>RHE (J/g.h)</b>	<b>Cements</b>	<b>Time (min)</b>	<b>RHE (J/g.h)</b>
0PO	77.7	2.70	11PO	98.1	1.44
0P0–10	85.9	4.83	11P0–10	117.9	2.27
0P10–35	87.9	2.03	11P10–35	109.4	1.26
0P35–50	90.1	1.69	11P35–50	114.9	0.70
0P50–2000	93.6	1.35	11P50–2000	144.4	0.65
3PO	76.0	1.73	22PO	108.8	1.67
3P0–10	90.7	3.76	22P0–10	123.7	2.66
3P10–35	87.9	1.30	22P10–35	109.3	1.37
3P35–50	122.2	0.89	22P35–50	111.0	1.20
3P50–2000	105.6	0.89	22P50–2000	124.0	1.07

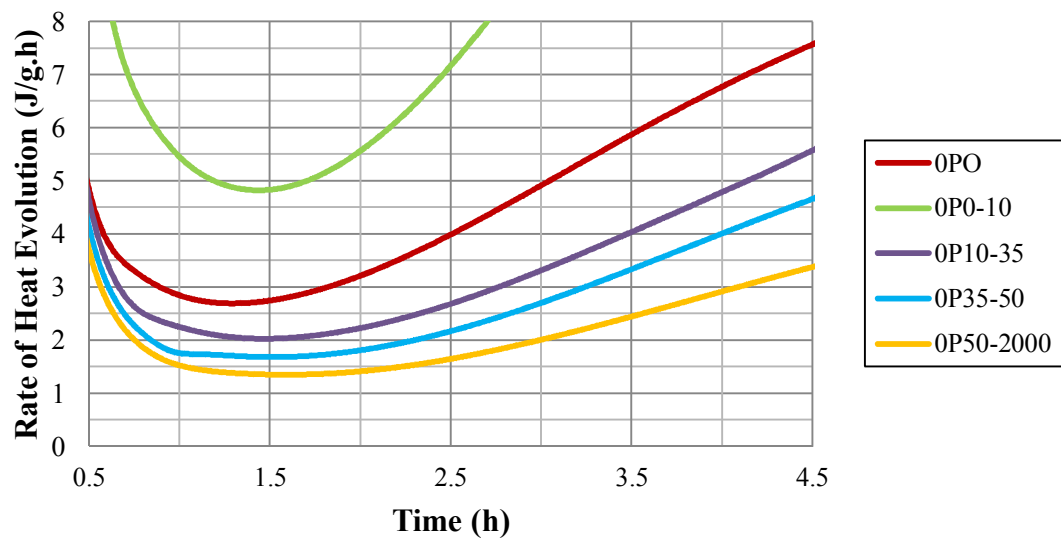


Figure 4.26. Rate of heat evolution of 0P cements during dormant period.

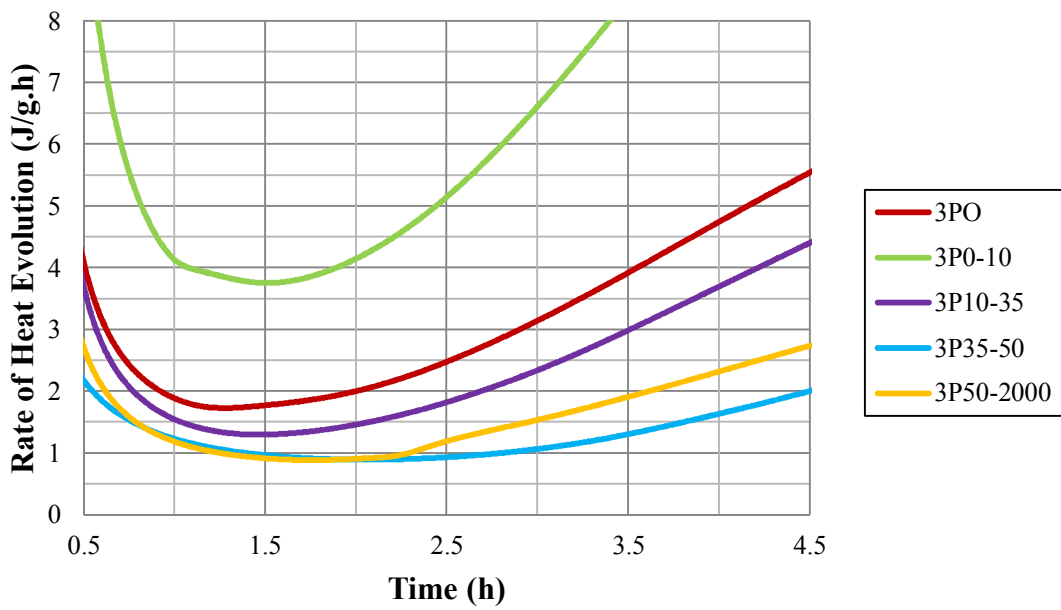


Figure 4.27. Rate of heat evolution of 3P cements during dormant period.

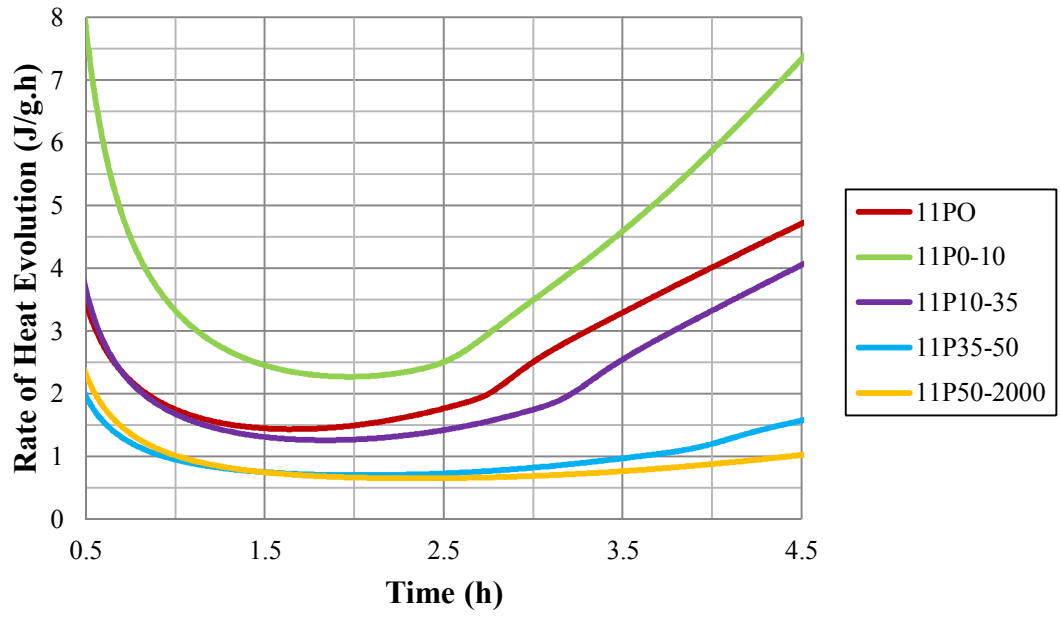


Figure 4.28. Rate of heat evolution of 11P cements during dormant period.

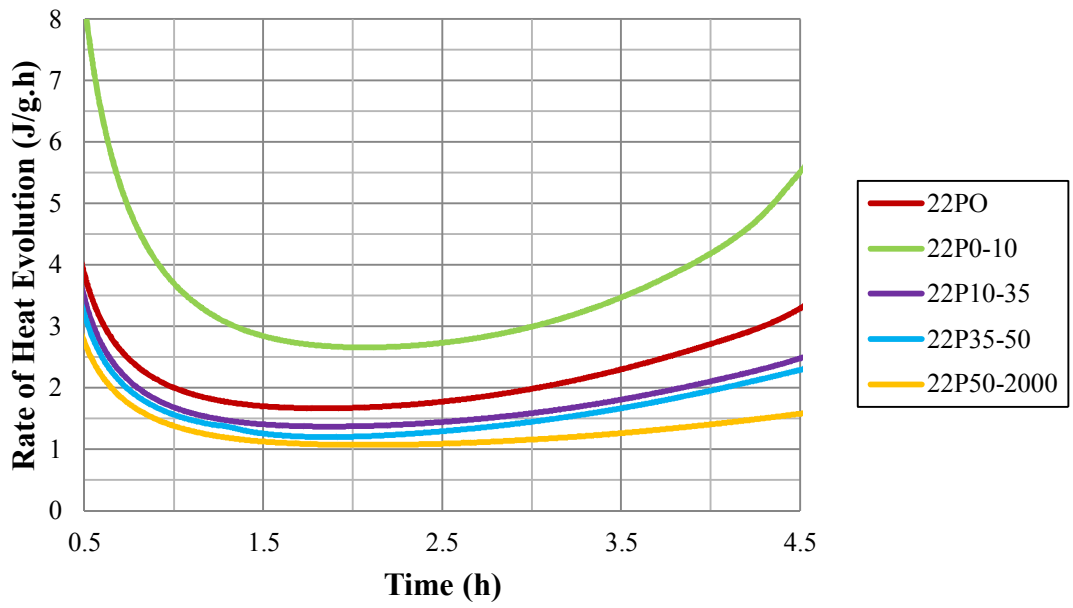


Figure 4.29. Rate of heat evolution of 22P cements during dormant period.

As seen in Table 4.4, the original groups show earlier dormant periods than the size groups due to the earlier occurrence of the first peak of original groups. Since original groups require less time to reach to the first peak, which is followed by the dormant period, the dormant period occurs in original groups earlier than size groups.

$$\text{RHE}_{0-10\mu\text{m}} > \text{RHE}_{\text{original}} > \text{RHE}_{10-35\mu\text{m}} > \text{RHE}_{35-50\mu\text{m}} \sim \text{RHE}_{50-2000\mu\text{m}}$$

The similar behavior to first peak values is due to the fact that the reactivity is increasing with decreasing average particle size.

For original and size groups, the minimum values obtained from 11P cements are lower than other groups during dormant period. Similarly, the values obtained from 0P cements are highest among all the groups as seen in Table 4.4. The possible reason can be the amount of trass particles around the clinker particles reacted during hydration occurring in the first peak. In 11P cements, almost all clinker particles can be surrounded with trass particles, and the initial hydration products can coat the clinker and trass particles. So, the layer on the surfaces of clinker and trass is relatively thinner than the case without any mineral admixtures and the water penetration increases, the heat of hydration is enhanced (Lawrence et al., 2003). In other words, nucleation effect emerges (see sec 2.3.3.2). This fact can be observed in the first few minutes of the rate of heat evolution graph of 11P cements in Figure 4.22. Among all the cement groups, the hydration rate of 11P cements can be distinguished from the first peak of its rate of heat evolution graph, the values of it are usually higher than the others or similar (Figure 4.22 and Figure 4.25). For that reason, due to this large amount of the initial hydration products causing the dormant period around the particles, the amount of the clinker grains still reacting with water chemically is lower during the dormant period. However, the quantity of the initial hydration products forming from the chemical reactions between water and clinker is not high enough to enclose the particles in 0P cements, so a certain part of clinker continues to react with water. In 22P cements, due to the dilution effect, the hydration production content may not be high enough for that effect. Therefore, the minimum rate of heat evolution values for these cement groups are higher.



For the length of the dormant period, visually, the length of minimum peak of 0-10  $\mu\text{m}$  size groups is the lowest for all cement groups as seen in Fig. 4.26 – 4.29. The second one is the original group. However, the sorting of 10-35  $\mu\text{m}$ , 35-50  $\mu\text{m}$  and 50-2000  $\mu\text{m}$  groups is variable with respect to pozzolan content. In general, it can be said that the length of the dormant period is directly related with the average particle size of the cement groups. The more reactive the cement, the shorter the dormant period.

From a pozzolan content point of view, the length of the dormant period of pozzolanic cements is greater for almost every size group than 0P cements, visually. Although this finding contradicts some earlier findings (Erdoğan et al., 2009), the results of this study coincide with a study using fly ash. Due to the pozzolan's inert behavior in the first minutes of the hydration, the decrease in  $\text{Ca}^{2+}$  ion concentration in the solution due to the dilution effect and increase in available water content due to the filler effect can result in longer dormant periods for the super saturation limit for calcium ion concentration (Langan et al., 2002).

#### 4.6.3 Second (Main) Rate of Heat Evolution Peaks of Cement Samples

The time of occurrence of the second peak and the correspondingly rate of heat evolution are given in Table 4.5 and Table 4.6, respectively.

Table 4.5. Time of occurrence of second peak.

Group of Cements	Subgroups of Cements	Time (h)	Groups of Cements	Subgroups of Cements	Time (h)
0P	0PO	6.6	11P	11PO	10.5
	0P0-10	5.6		11P0-10	8.3
	0P10-35	7.0		11P10-35	10.0
	0P35-50	7.4		11P35-50	12.5
	0P50-2000	8.1		11P50-2000	11.5
3P	3PO	8.6	22P	22PO	12.0
	3P0-10	7.2		22P0-10	9.2
	3P10-35	9.9		22P10-35	12.8
	3P35-50	10.8		22P35-50	13.1
	3P50-2000	8.7		22P50-2000	9.5

Table 4.6. Maximum rate of heat evolution values during second peak.

Group of Cements	Subgroups of Cements	RHE (J/g.h)	Groups of Cements	Subgroups of Cements	RHE (J/g.h)
0P	0PO	9.46	11P	11PO	8.20
	0P0–10	18.14		11P0–10	16.59
	0P10–35	7.94		11P10–35	8.83
	0P35–50	7.12		11P35–50	3.39
	0P50–2000	4.97		11P50–2000	2.48
3P	3PO	8.34	22P	22PO	6.58
	3P0–10	16.55		22P0–10	12.44
	3P10–35	7.68		22P10–35	6.07
	3P35–50	4.41		22P35–50	5.02
	3P50–2000	4.46		22P50–2000	3.11

Generally, the main peak seen in rate of heat evolution curves forms in the first 20 hours. The rate of heat evolution curves in 20 hours to observe the second peak are given in Figure 4.30 – 4.34.

According to the graphs, the time required to reach the peak rate is shortest for the smallest size group. The time is expected to be shortened for finer material.

From a pozzolan content point of view, the following order can be reached for almost every size group:

$$\text{Time}_{0P} < \text{Time}_{3P} < \text{Time}_{11P} < \text{Time}_{22P}$$

This result contradicts the findings in the literature (Massazza, 2004; Erdoğan et al., 2009). According to Table 4.6, it is also shown that the 0P heat rate second peak is higher than the others. These behaviors of pozzolanic cements can be due to the decrease in  $\text{Ca}^{2+}$  concentrations in the pore solution. In studies (Langan et al., 2002) with fly ash with similar chemical composition to the natural pozzolan used in this study, this effect was also observed. It is stated that during and before the dormant period, the  $\text{Ca}^{2+}$  ions released from the hydration reactions can be collected by the pozzolan grains and decrease the concentration of calcium ions resulting in a delay of calcium hydroxide and C-S-H gel formation (Langan et al., 2002). Even though that study was conducted with fly ash, the same situation can be seen here since the behaviors of natural pozzolans and fly ashes are similar (Massazza, 2004). This

effect can be more dominant with the increasing quantity of trass and suppress the effect of nucleation.

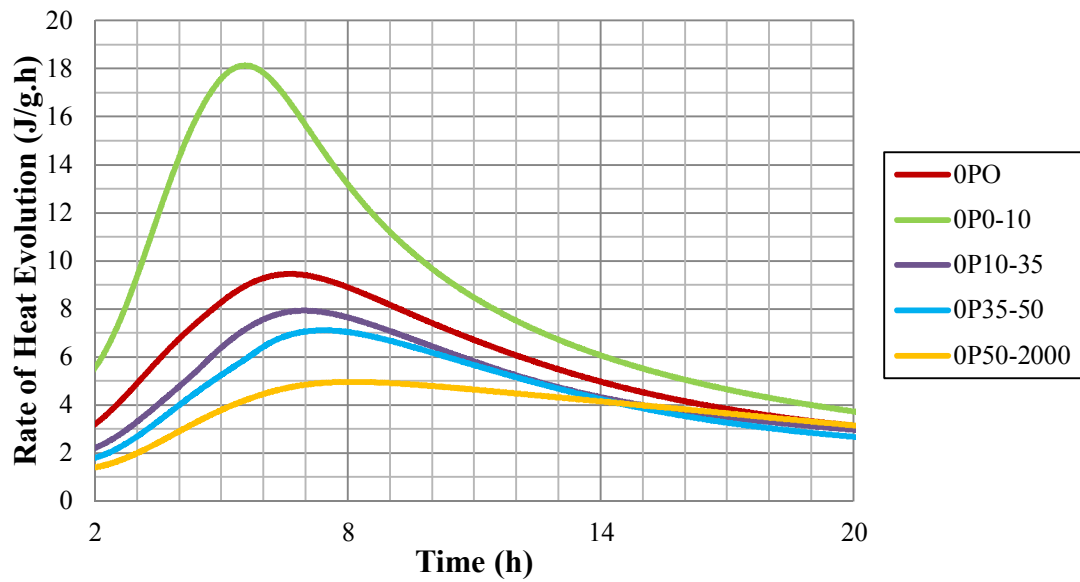


Figure 4.30. Rate of heat evolution of 0P cements during second peak.

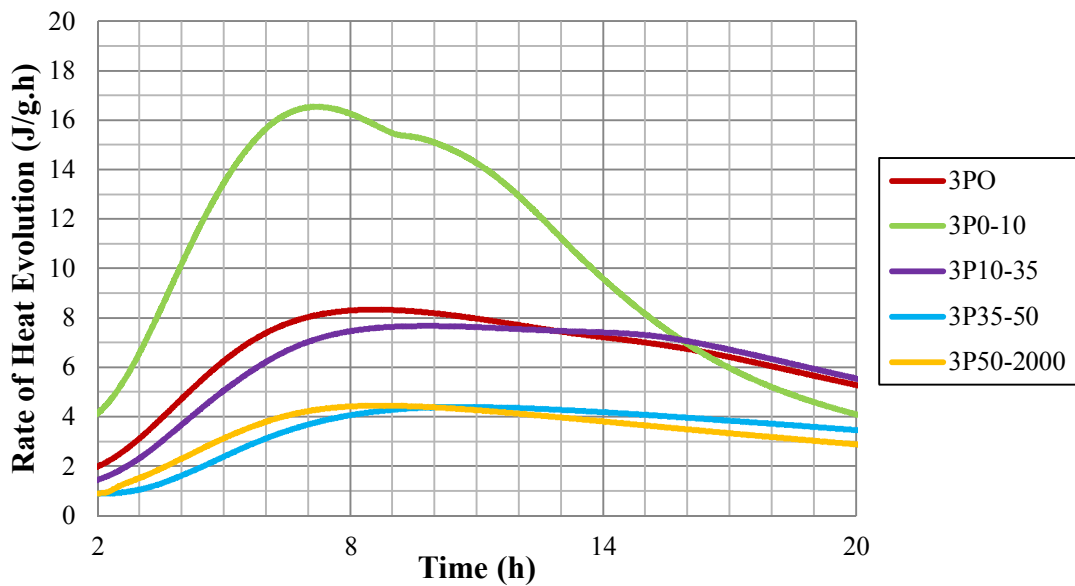


Figure 4.31. Rate of heat evolution of 3P cements during second peak.

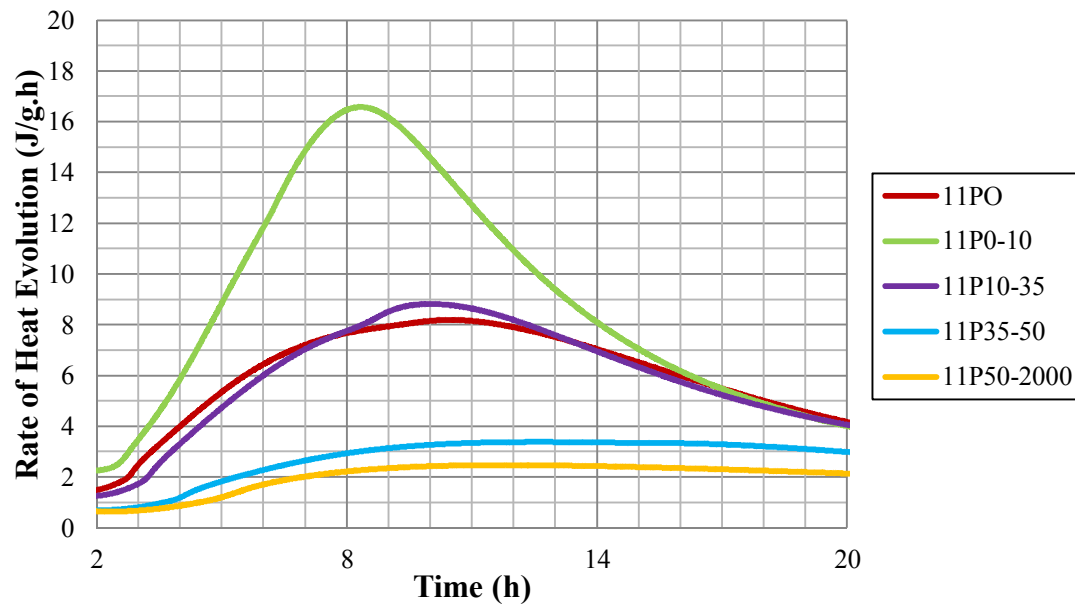


Figure 4.32. Rate of heat evolution of 11P cements during second peak.

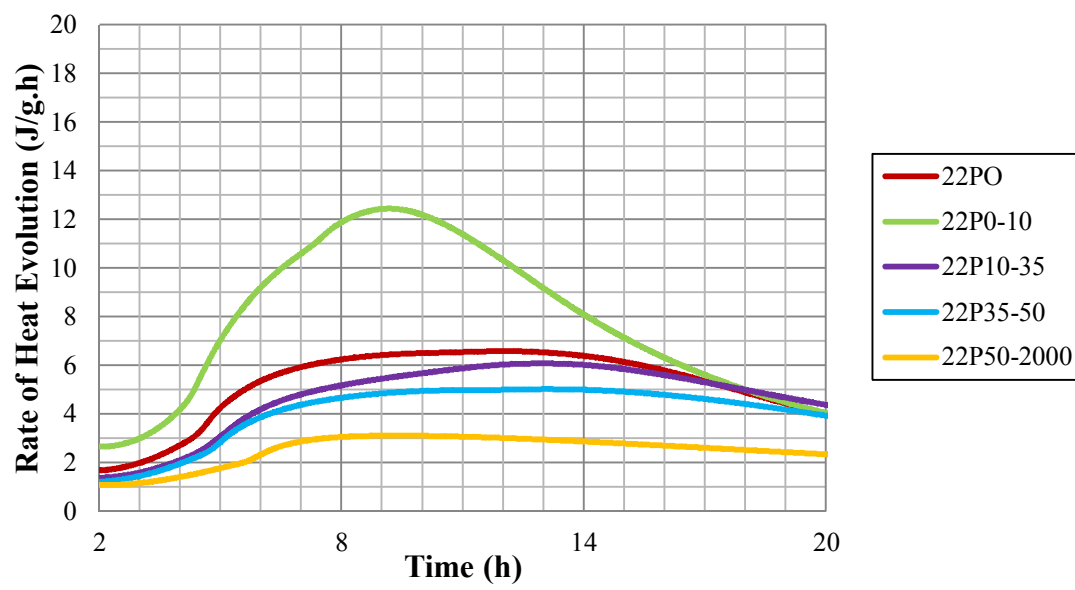


Figure 4.33. Rate of heat evolution of 22P cements during second peak.

The second peaks of the coarsest size groups are lowest for all cement samples. Due to their specific surface areas being the largest, the reaction rate of 0-10  $\mu\text{m}$  cement groups is highest. In unit time, the amount of cement reacting with water is higher than other size groups so the heat evolution is the highest.

It is seen from Figure 4.30 and Table 4.6, that the second peak of 0P cements which do not have any amount of pozzolan are the highest and the values decrease with increasing content of mineral admixtures because of the dilution effect. Although for original size groups, 0-10  $\mu\text{m}$  size groups and 10-35  $\mu\text{m}$  size groups, 22P values are lowest compared with the other corresponding cement groups, the same situation can not be seen for 35-50  $\mu\text{m}$  and 50-2000  $\mu\text{m}$ . One reasonable explanation for this behavior can be the nucleation effect which can increase the rate of heat evolution of 22P cements since there is a considerable amount of fine material in these size groups as shown in Fig. 4.4 – 4.5. The same behavior can be observed for 11P cements, too.

There is a considerable shoulder peak in the rate of heat evolution curve of 3P0-10 cement group in Fig. 4.31 due to its higher gypsum content as shown in Table 4.1. The shoulder peak observed corresponds to the formation of ettringite (Odler, 2004). The excess gypsum reacting with  $\text{C}_3\text{A}$  and  $\text{C}_4\text{AF}$  may form ettringite or ettringite-like products in 3P0-10 to produce the shoulder.

#### **4.7 Estimating the Contribution of Trass Incorporation on Early Heat Evolution of Cement Samples**

Mineral admixtures can make changes in the hydration kinetics (Massazza, 2004). They may accelerate the chemical reactions occurring in cement paste by nucleation effect or cause a reduction in rate of heat evolution peaks due to the dilution effect. Which of these dominates depends on the amount of the additions (Lawrence et al., 2003). The effect of trass in this study can be found by comparing the pozzolanic cements for every size group. However, excluding 0P cements (0P0, 0P0-10, 0P10-35, 0P35-50 and 0P50-2000), all the cements have a mass of trass. Even if the effect is low, all blended cements are exposed to the dilution effect due to the replacement of cement with trass. To estimate the contribution of trass, the dilution effect should

be removed by considering the amount of the clinker, which is the main compound of cement. By using the ratio of clinker amount of 0P cements to that of the cement, the dilution effect can be ignored. Therefore, the effects of the clinker for all pozzolanic cements are equalized by normalizing the mass of the clinker. If there is no effect of mineral additions on hydration kinetics, the values should be similar to each other. The calculation is performed for every cement size group according to Eqn. 4.4. The example of the calculation is shown in Appendix B. The values obtained from the calculations are given in Fig. 4.34 – 4.38.

$$HH_{ix}normalized = \frac{K_{0Px}}{K_{ix}} HH_{ix} \quad (\text{Eqn. 4.4})$$

where,

$HH_{ix}normalized$  = Heat of hydration of the related cement sample (in J/g)

$HH_{ix}$  = Heat of hydration of size groups

$K_{0Px}$  = Clinker content fraction in the 0P size group

$K_{ix}$  = Clinker content fraction in the related cement sample

i = Cement group (3P, 11P, 22P)

x = Size group (O (original), 0-10, 10-35, 35-50, 50-2000)

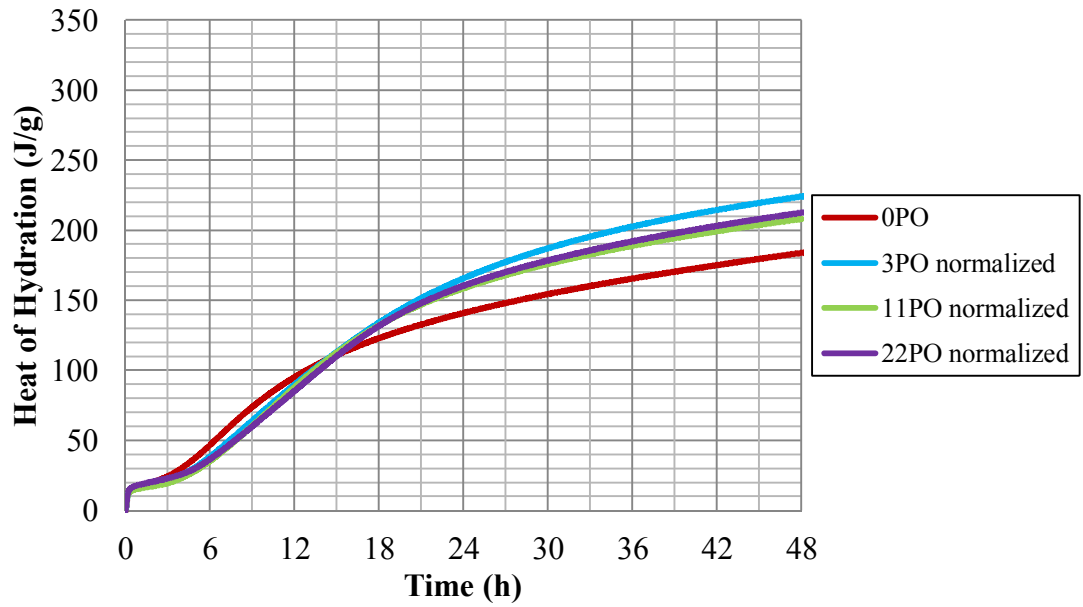


Figure 4.34. Normalized heat of hydration of pozzolanic cement groups and the actual heat of hydration of the non-pozzolanic cement for original groups.

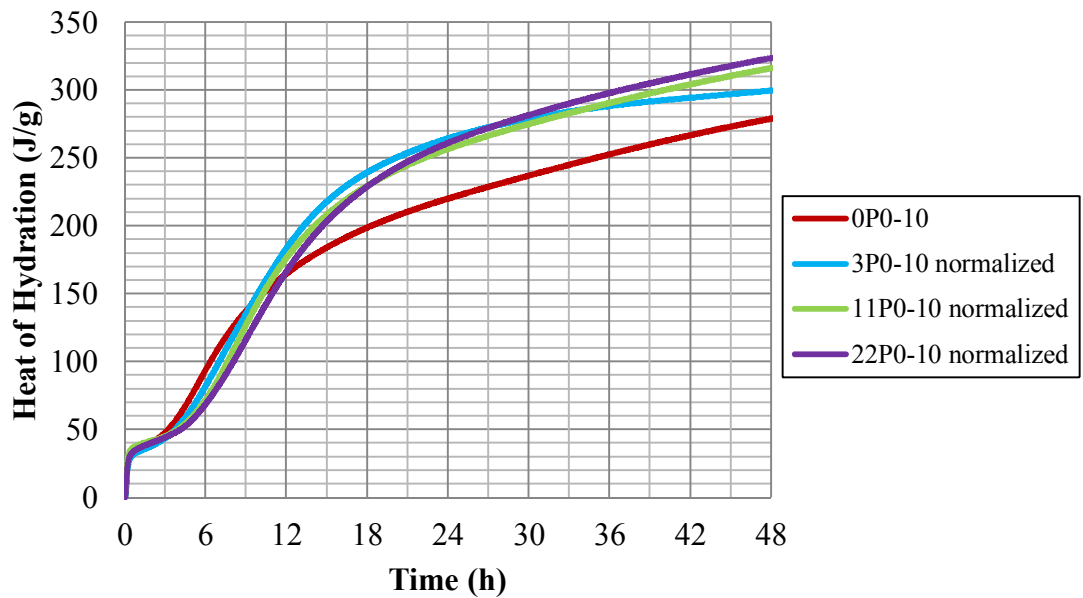


Figure 4.35. Normalized heat of hydration of pozzolanic cement groups and the actual heat of hydration of the non-pozzolanic cement for 0-10  $\mu\text{m}$  size groups.

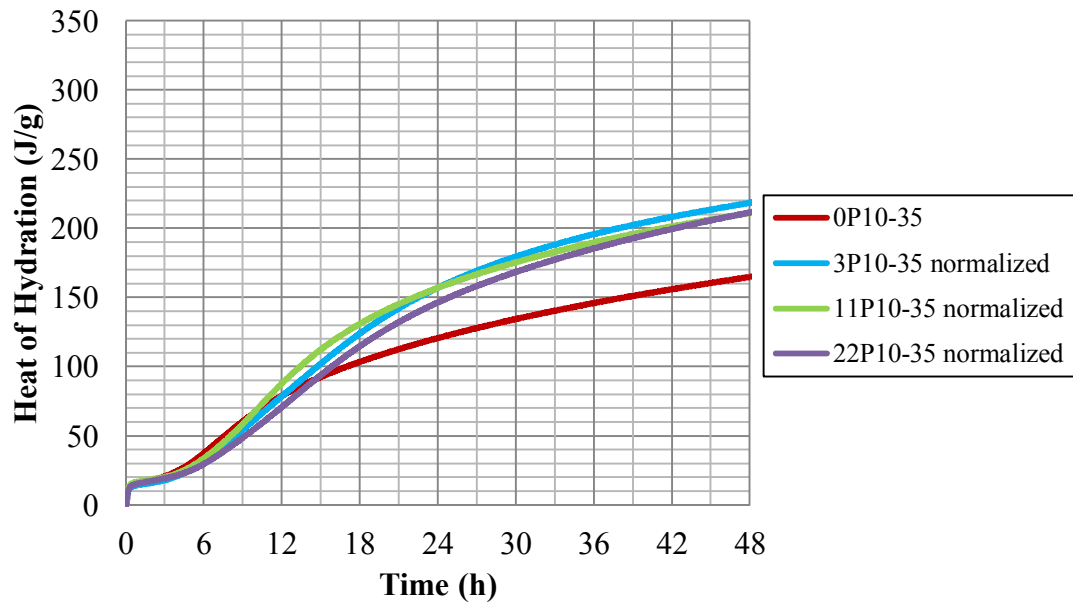


Figure 4.36. Normalized heat of hydration of pozzolanic cement groups and the actual heat of hydration of the non-pozzolanic cement for 10-35  $\mu\text{m}$  size groups.

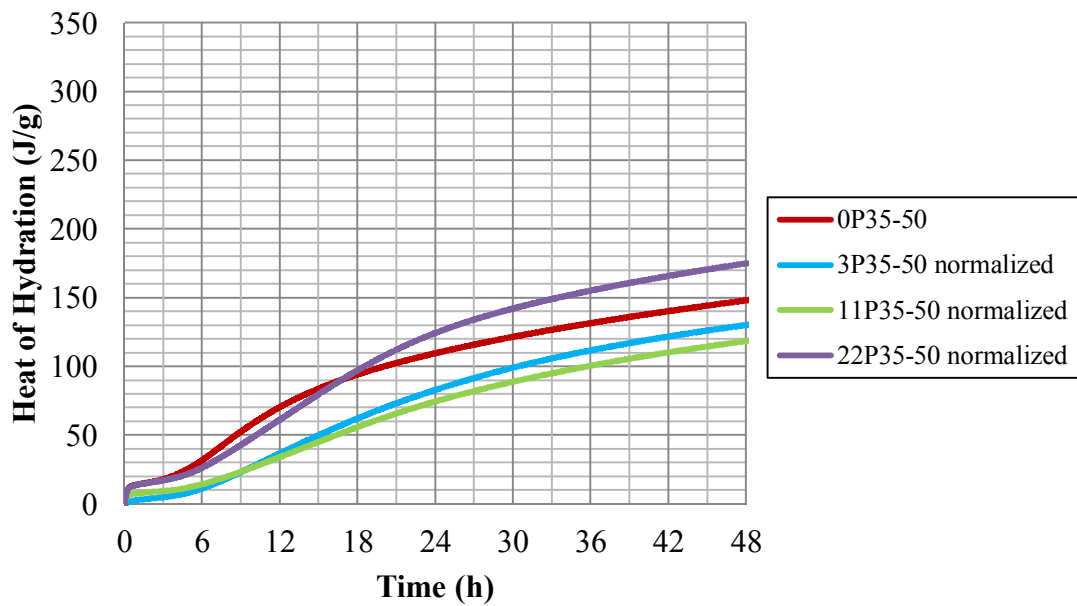


Figure 4.37. Normalized heat of hydration of pozzolanic cement groups and the actual heat of hydration of the non-pozzolanic cement for 35-50  $\mu\text{m}$  size groups.



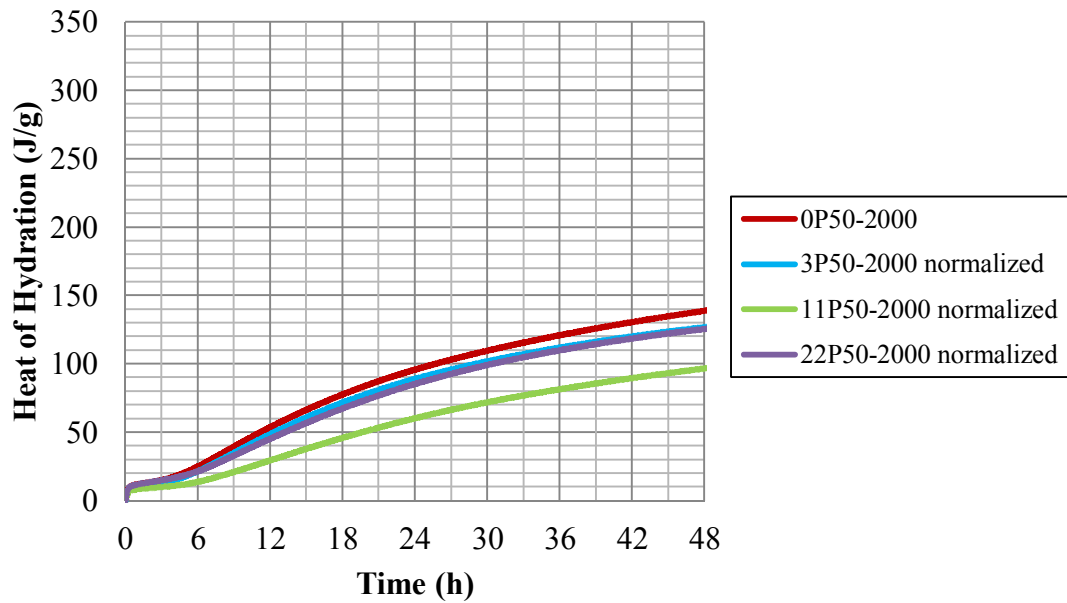


Figure 4.38. Normalized heat of hydration of pozzolanic cement groups and the actual heat of hydration of the non-pozzolanic cement for 50-2000  $\mu\text{m}$  size groups.

In Fig. 4.34 – 4.36, it is obvious that the 48-h heat of hydration of the pozzolanic cements that contain higher amount of finer materials like original groups, or 0-10  $\mu\text{m}$  groups, are higher than the other size groups. The reason may be the nucleation effect. In small size groups, the amount of trass is higher. Even though they can not react chemically with water or any hydration product at the very beginning of the hydration, they can contribute to hydration in physical ways like nucleation effect. Since the hydration products are accumulated by smaller trass particles, the effect of nucleation is greater in smaller size groups. In coarser ones, the effect disappears as seen in Fig. 4.37 – 4.38.

Considering only the clinker fraction, the hydration of 0PO is lower than the pozzolan-containing ones. It coincides with the findings (Massazza, 2004).

Moreover, the hydration heat values decrease with the increasing average particle size due to the reduction in its total surface reacting with water.

#### 4.8 Estimating the Heat Evolution Characteristics of the Original Cement from the Size Groups

The reactivity of cements mainly depends on their fineness (average particle size) (Snellings et al., 2010). At the same time period, more chemical reactions occur in cements with higher fineness than in coarser ones, and they have higher heat of hydration since their total surface areas reacting with water are larger. Heat evolution characteristics of the original (unsieved) group can be predicted using the size groups. But, since the total clinker and gypsum contents of the size groups differ from each other, first they should be normalized. Otherwise the dilution effect can flaw the estimation. For every cement group, with respect to their particle size distribution of the original cements (0PO, 3PO, 11PO and 22PO), the weighted average of the size groups are calculated by using Eqn. 4.5 and Eqn. 4.6. It is assumed that the densities of the different size groups are equal to each other. In Appendix C, an example with actual numbers worked is shown.

$$HH_{iO \text{ calculated}} = \sum_{x=1}^4 \frac{K_{io} + G_{io}}{K_{ix} + G_{ix}} \Phi_{ix} HH_{ix} \quad (\text{Eqn. 4.5})$$

$$RHE_{iO \text{ calculated}} = \sum_{x=1}^4 \frac{K_{io} + G_{io}}{K_{ix} + G_{ix}} \Phi_{ix} RHE_{ix} \quad (\text{Eqn. 4.6})$$

where,

$HH_{iO \text{ calculated}}$  = Calculated heat of hydration (J/g)

$RHE_{iO \text{ calculated}}$  = Calculated rate of heat evolution (J/g.h)

$HH_{ix}$  = Measured heat of hydration of the related cement group (J/g)

$RHE_{ix}$  = Measured rate of heat evolution of the related cement group (J/g.h)

$K_{io}$  = Clinker content fraction in the original group of the related cement group

$K_{ix}$  = Clinker content fraction in the related size group of the related cement group

$G_{io}$  = Gypsum content fraction in the original group of the related cement group

$G_{ix}$  = Gypsum content fraction in the related size group of the related cement group

$\Phi_{ix}$  = Volume fraction of the related cement size group in original group of the related cement group

$i$  = Cement group (0P, 3P, 11P, 22P)

$x$  = Size group (0-10, 10-35, 35-50, 50-2000)

The calculated values for heat of hydration are shown in Fig. 4.39 – 4.42. The comparison between the calculated values and measured values from the experiments is stated in Fig. 4.43 – 4.46. Fig 4.47 shows the graph of the actual (measured) / calculated heat of hydration vs. time.

From Fig. 4.39 – 4.42, it can be concluded that the calculated values for all of the cement groups are approximately equal to each other. The difference is not pronounced. It is possible to estimate the heat characteristics of original groups by using those of the size groups, the clinker and gypsum contents of the groups and their particle size distributions. Also, Fig. 4.43 – 4.46 indicate that the relationship between them is almost linear. The coefficient of determination values are obtained as 0.999, 0.994, 0.998 and 0.999, for 0P, 3P, 11P and 22P, respectively. The values are approximately equal to 1, which indicates the relationship between two variables is nearly a linear function. The more close to 1 the coefficient of determination is, the better the estimation is. In addition, the slopes of the curves are found as 1.058, 0.950, 0.993 and 1.061, respectively. The coefficient of determination value of 3P is relatively smaller than the others and its slope is a little bit different. The possible explanation can be its higher amount of gypsum in 3P0-10. The excess gypsum can cause the shoulder near the second peak in rate of heat evolution of the related cement group and can change the heat characteristics of the combined calculation. As seen in Figure 4.47, the ratios of measured heat of hydration values to the calculated values for all cement groups are less than 10 % in the end of 2 days.

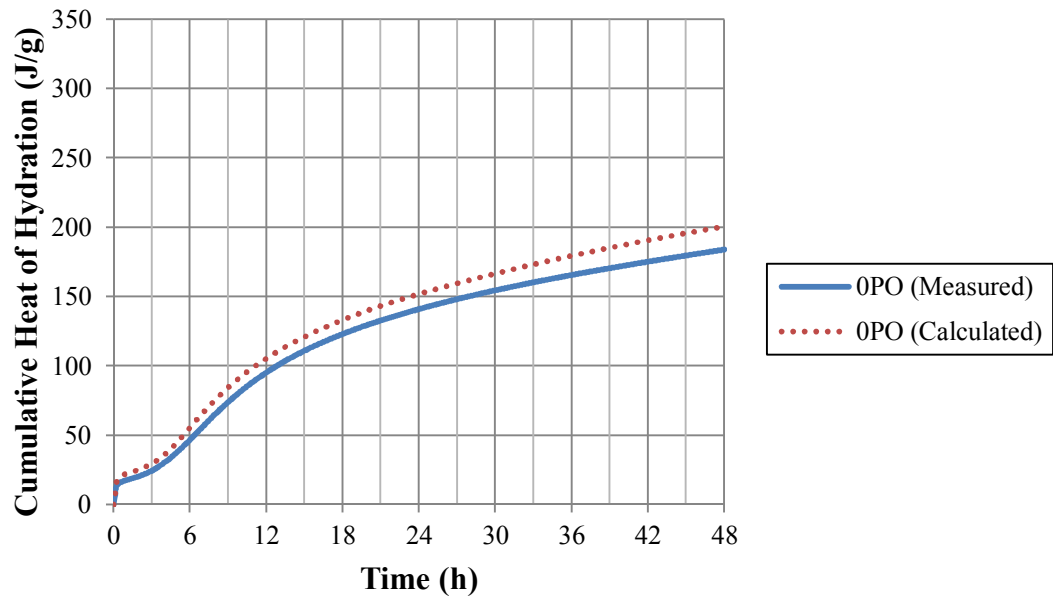


Figure 4.39. Heat of hydration of 0P cements.

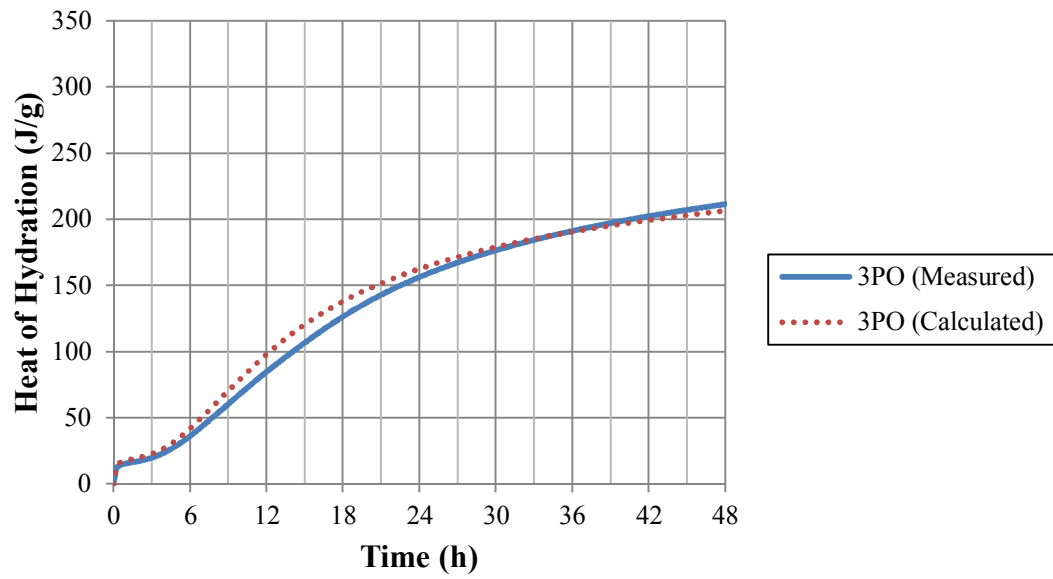


Figure 4.40. Heat of hydration of 3P cements.

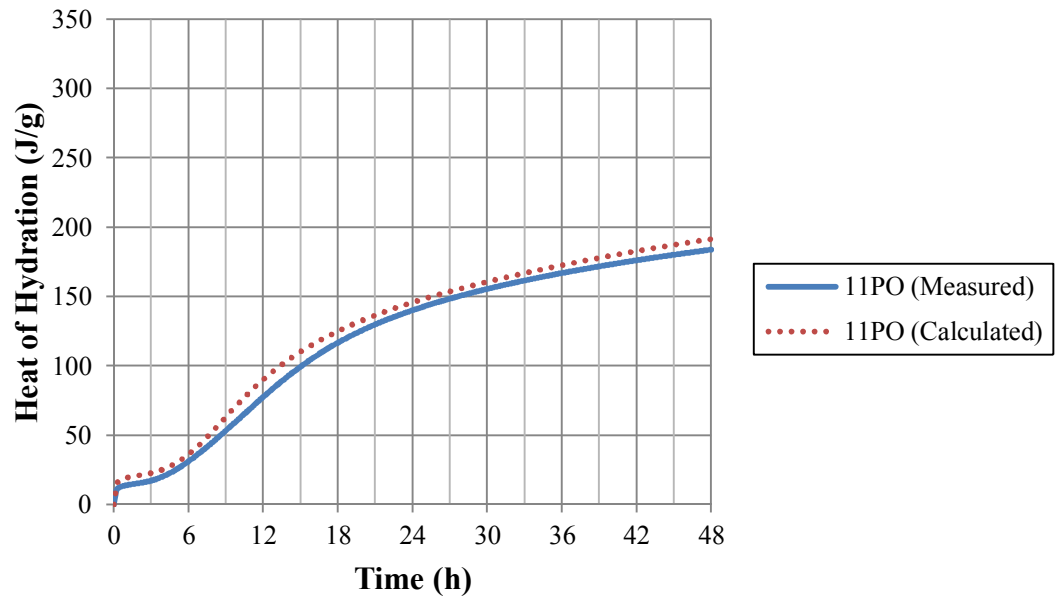


Figure 4.41. Cumulative heat of hydration of 11P cements.

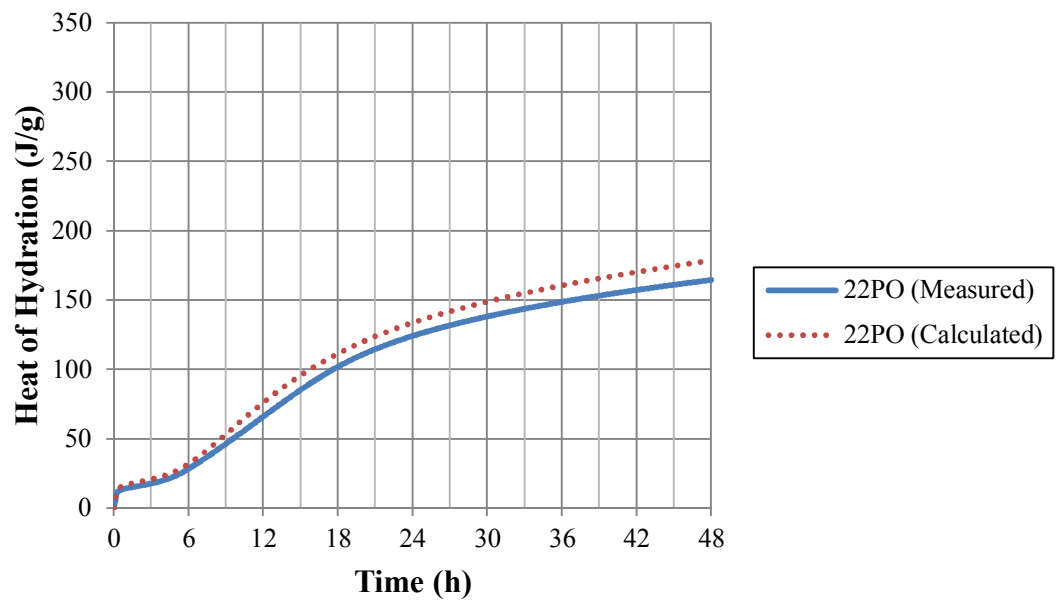


Figure 4.42. Cumulative heat of hydration of 22P cements.

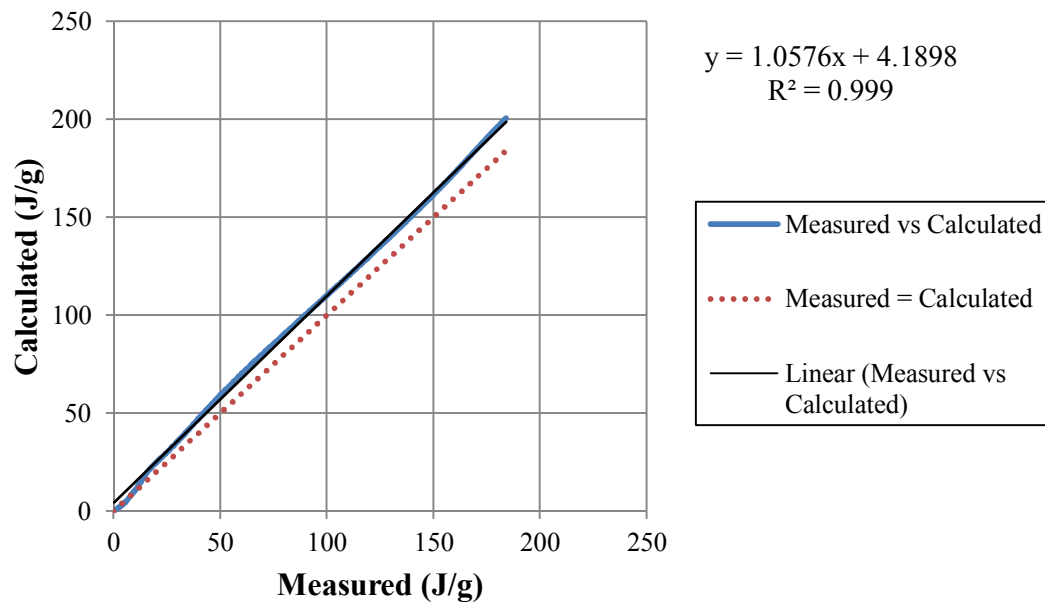


Figure 4.43. Measured vs calculated heat of hydration for 0P cements.

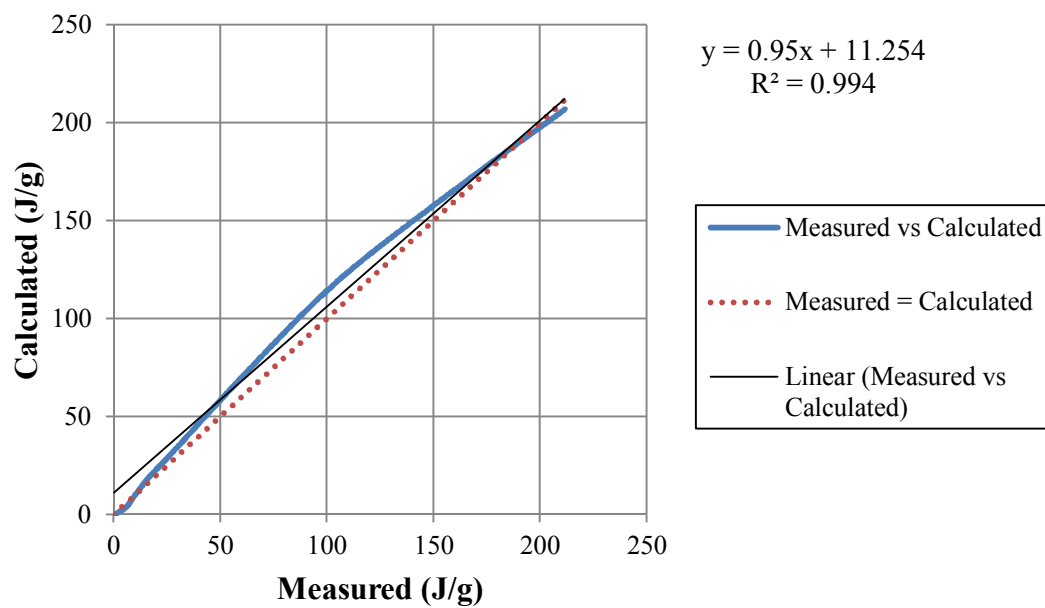


Figure 4.44. Measured vs calculated heat of hydration for 3P cements.

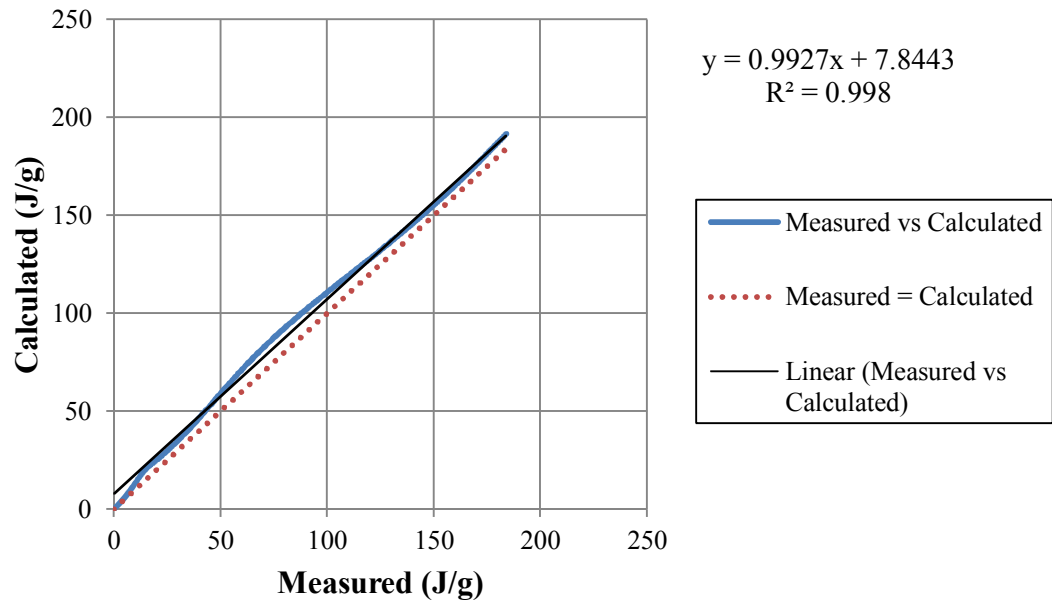


Figure 4.45. Measured vs calculated heat of hydration for 11P cements.

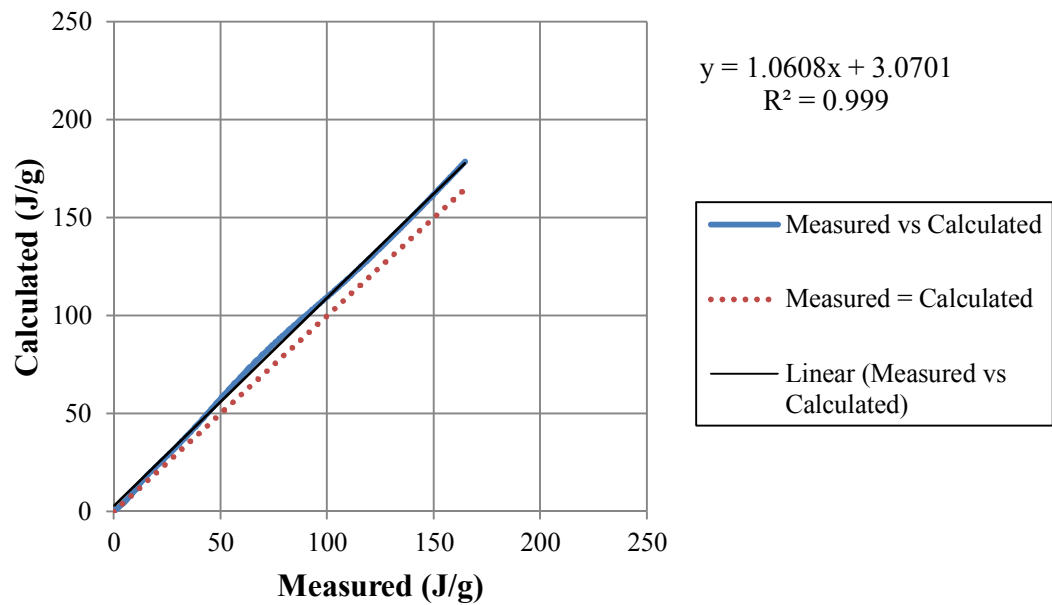


Figure 4.46. Measured vs calculated heat of hydration for 22P cements.

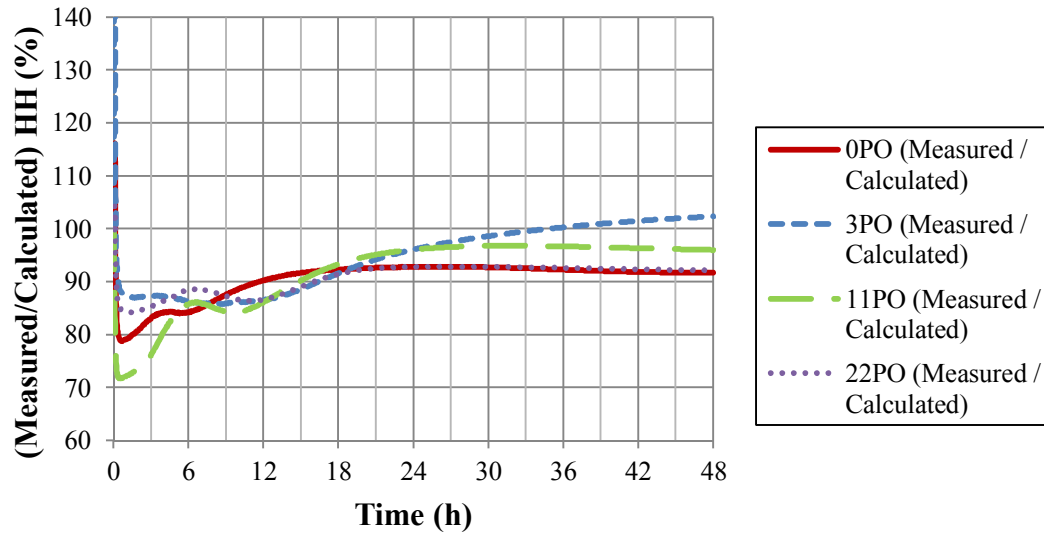


Figure 4.47 Measured / Calculated heat of hydration vs time graph of 0P, 3P, 11P and 22P cements.

The calculated and measured values for rate of heat evolution are indicated in Figure 4.48 – 4.51.

In the rate of heat evolution graphs, the overestimation is noticed. This fact can be clearly seen during the formation of main rate of heat evolution peak. There can be some interactions between particles with different sizes. The interactions between different sizes of particles can be the prevention of water to penetrate by the fine particles due to their higher water absorption capacity. The interactions between different size groups are ignored during the combined calculation. But, in the actual measured case, these interactions can be significant factor changing the heat values. Also, it is assumed that the dividing process of cements into their size groups is successful. However, as shown in Figure 4.1 – 4.5, the success is low. Therefore, both the differences between the rate of heat evolution and heat of hydration can be explained by these facts. Figure 4.52 shows the change in the ratio of measured to calculated rate of heat evolution graphs with time. While after 2 days from the start of the initial hydration, the maximum difference is seen as 25 %, for only 3P



cements, those for other pozzolanic groups is less than 15 %. This estimation can be made for pozzolanic cements.

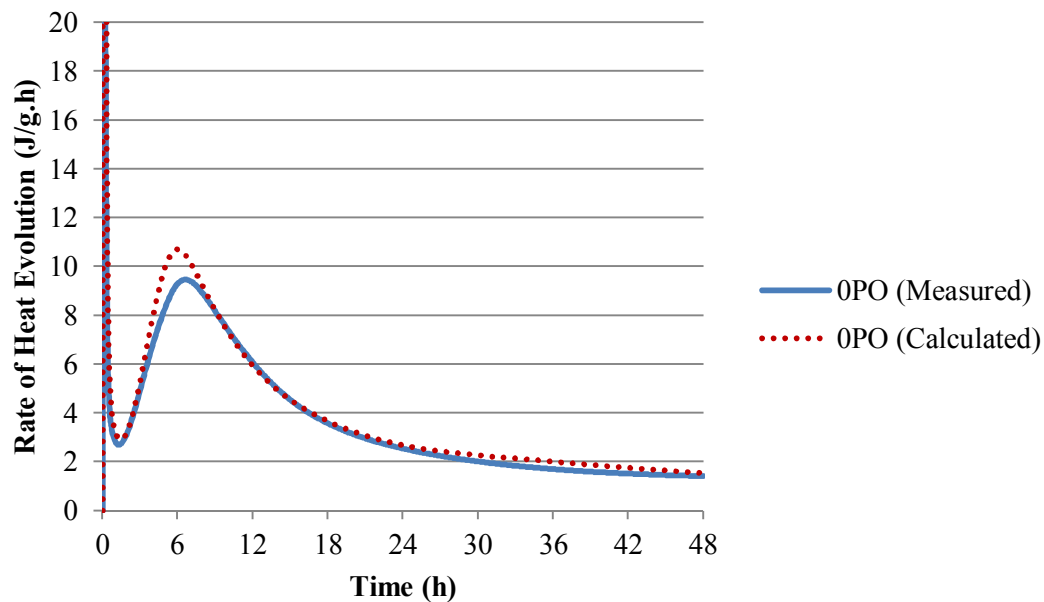


Figure 4.48. Rate of heat evolution for 0P cements.

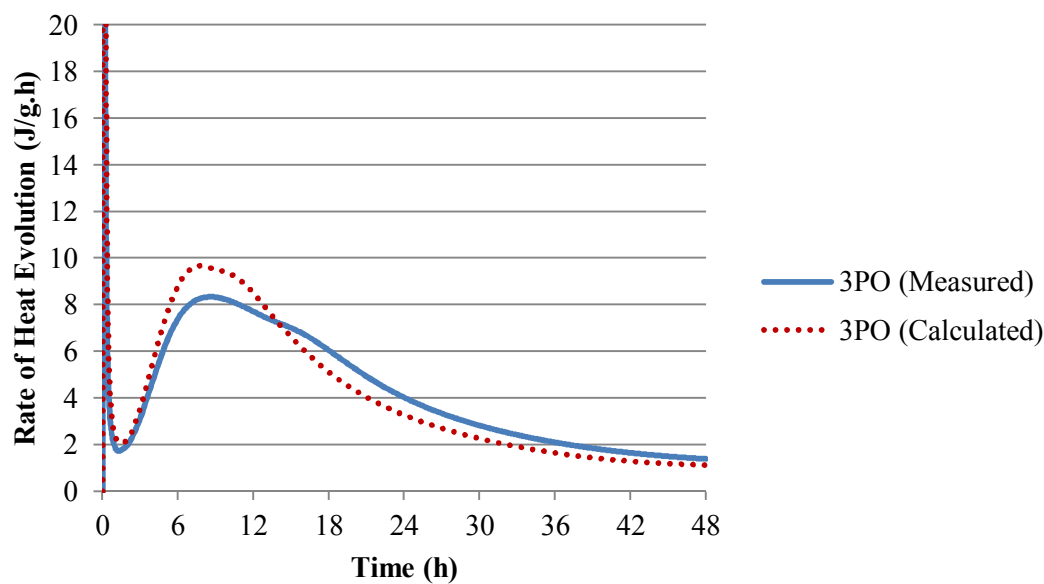


Figure 4.49. Rate of heat evolution for 3P cements.

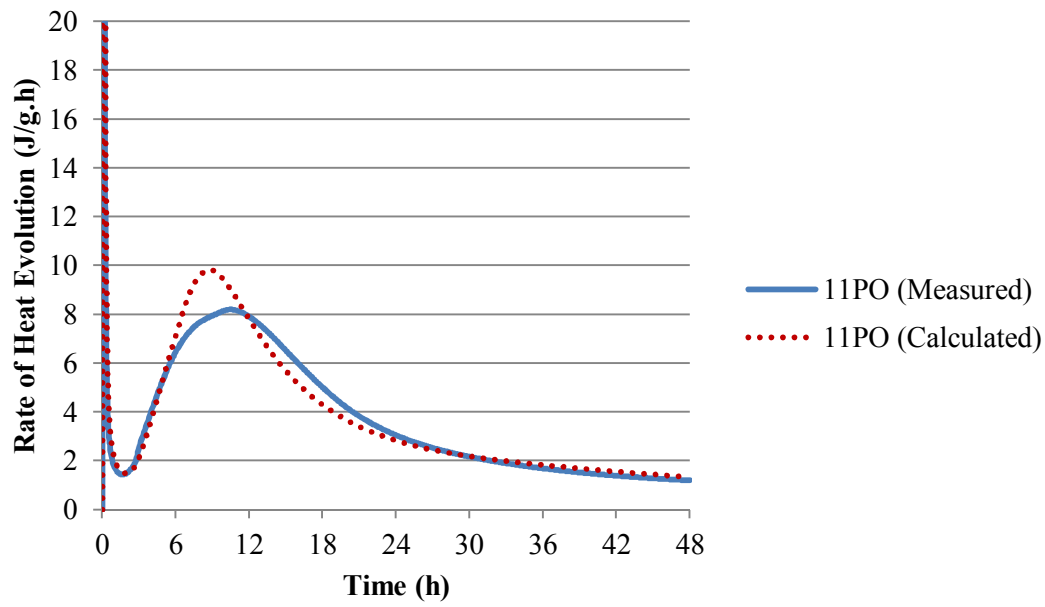


Figure 4.50. Rate of heat evolution for 11P cements.

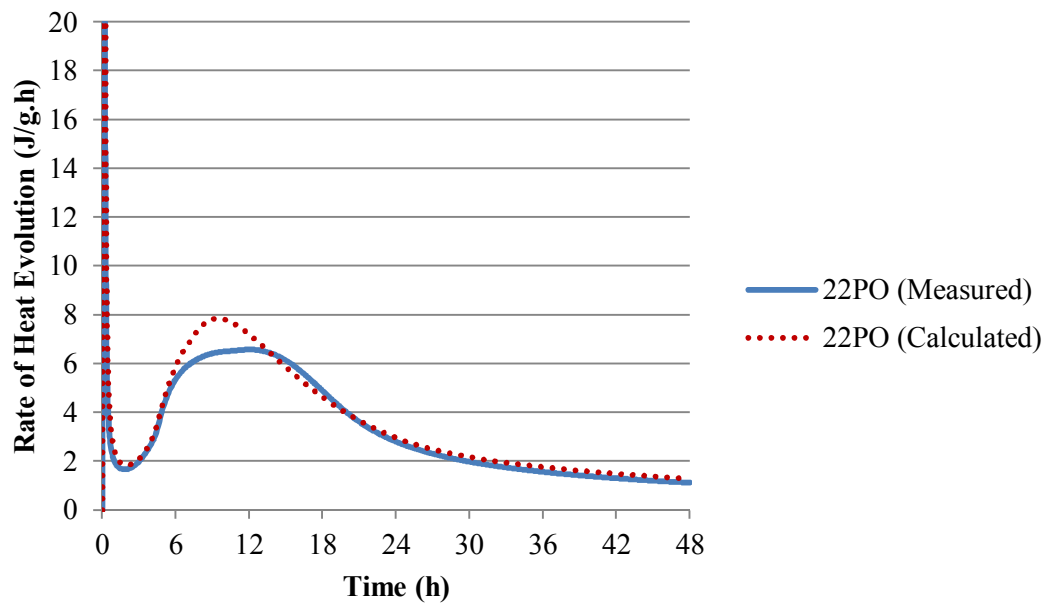


Figure 4.51. Rate of heat evolution for 22P cements.

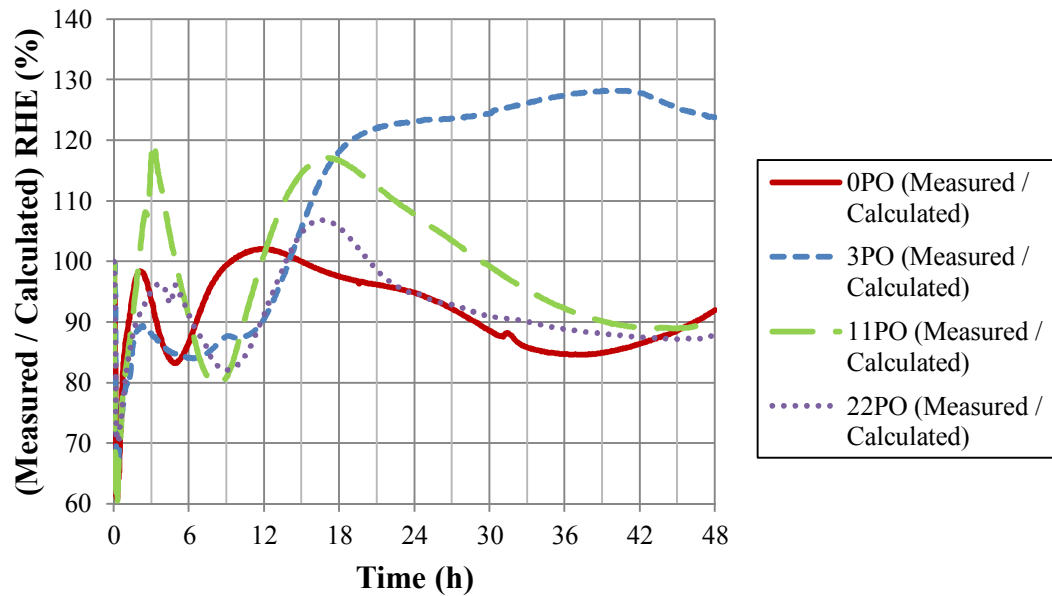


Figure 4.52 Measured / calculated rate of heat evolution vs time graph of 0P, 3P, 11P and 22P cements.

The actual and calculated second peak times are shown in Table 4.7. It can be concluded that the approach does not work very well in estimation of the occurrence time of second peak. Results clearly show that the error seen in Table 4.7 increases with the increasing content of mineral admixtures. It can be stated that this approach can not be applied to estimate the occurrence time of the second peak in rate of heat evolution of blended cements.

Table 4.7. The estimated and actual time values for emergence of second peak.

Cement	Actual time (h)	Estimated time (h)	Difference (%)
0PO	6.61	6.00	10.17
3PO	8.55	7.75	10.32
11PO	10.48	8.75	19.77
22PO	11.98	9.42	27.18

## 4.9 Summary

Zhang et al. (2011) separated an ordinary portland cement into size groups and investigate the hydration characteristics of size groups compared to the original one. Bentz (2010) stated, if the estimation of the properties of the ordinary portland cement is possible by examining the cements with different finenesses produced from the same clinker or not. This approach based on the law of mixtures. Due to the similarities, the findings of this thesis study can be compared with the conclusions of these two papers.

Because of the different grindabilities of the raw materials, the raw material percentage is variable for every size group. In the finer cement group, the contents of gypsum and trass are higher than that in the coarser size groups. This fact can be seen in the grinding process of the cement groups. It is easier to grind the pozzolanic cements to a specific fineness value than the OP, which does not have any mineral admixture, since clinker is harder material to grind than other constituents, trass and gypsum.

The dilution and nucleation effects become alternately dominate in different size groups. It can be stated that in general, in finer size groups, the nucleation effect governs, but in coarser ones, the dominant one is the dilution effect due to their separate amounts of raw material. Furthermore, this variation of clinker, trass and gypsum can cause different effects like dispersion effect, which is the reason of the earlier first peak seen in 11P than in any other cement group, or the difference in  $\text{Ca}^{2+}$  ion concentration in the pore solution, which can induce the longer dormant periods and later second (main) peak in blended cement groups.

Average particle size is important for heat of hydration and rate of hydration since it determines the particle surface reacting with water. In all rate of heat evolution and heat of hydration graphs, the significance of PSD is clearly shown. Due to higher reactivity, the cement groups with smaller average particle size, have higher values for heat evolution and rate of heat evolution curves. Also it is found that the behavior of the original group in rate of heat evolution curve is similar to the cement groups which belong to the size group of 10-35  $\mu\text{m}$ . The possible reason can be the median

particle size of all original group cements are between 10 and 35  $\mu\text{m}$ . These findings agree with the results (Zhang et al., 2011).

Also, from the subgroups of the cement groups, hydration heat values of the original cement groups can be estimated using the particle size distributions and chemical analysis results. But, in rate of hydration, the predicted values overestimated the actual ones (Fig 4.43 – 4.46). In addition to this, according to estimated values, the second peak occurs later than the actual one. In spite of the research showing that the estimation of rate of heat evolution characteristics from the size groups is possible in non-pozzolanic cements (Bentz, 2010), these research findings indicate it is not as straight forward for pozzolan-incorporated cements.



## **CHAPTER 5**

### **CONCLUSIONS**

#### **5.1 General**

In this thesis, the heat of hydration and the rate of heat evolution of sieved (size groups) and unsieved (original) cement samples are compared. The times of occurrence of the first peaks, second peaks and dormant periods are investigated as well as the dormant period heat and rate minima of cement samples. The effects of trass addition and blended cement average particle size on early heat hydration were researched. In addition, an attempt to estimate, the heats of hydration of unsieved groups was made by using their particle size distribution and chemical analysis results.

The following can be concluded:

- For each cement size group, the amounts of the raw materials are not similar due to their grindabilities. This fact is important when considering the effects of the mineral additions on hydration kinetics. In coarser cements, the amount of the clinker, which is one of the hardest constituents among the raw materials, is higher than the finer cements.
- In finer cement, due to higher trass content and lower average particle size, the most dominant effect can be assumed as nucleation effect. The coarser cement groups also have some mineral admixtures, but the average particle

sizes of the mineral additions are not sufficiently small to start the nucleation process. The dominant effect in coarser cement groups can be thought to be the dilution effect due to the reduction of clinker amount. For these reasons, generally, in coarser cement groups, the heat of hydration are decreasing, whereas the hydration heat is firstly increasing and then decreasing with the increasing mineral addition. This implies that there is a certain limit for the maximum amount of mineral addition to enhance the hydration process. Below that limit, the nucleation effect is dominant. Otherwise, the dilution effect governs.

- From the occurrence of the peaks present in rate of heat evolution curves point of view, it can be said that mineral addition amount is a significant factor in rate of heat evolution of blended cements. Mineral addition can cause earlier first peaks because of the dispersion effect which is related with prevention of flocculation of cement particles or can retard the second (main) peak due to the  $\text{Ca}^{2+}$  ion concentration change.
- The rates of heat of hydration are also changed by the mineral admixture content. The groups which have higher mineral admixtures, and correspondingly, greater dilution, have lower rate of heat evolution values. This situation can be seen especially in Fig. 4.11 – 4.15.
- Mineral admixtures can change the length of the dormant period of cements because of the  $\text{Ca}^{2+}$  concentration changed by the incorporation of mineral admixtures.
- As expected, the finer cement groups have higher heats of hydration in 2-day period. Finer cements have higher surface area, so the amount of the cement which reacts with water is higher.
- The length of the dormant period changes with the size groups. It is shown that the most reactive cement size groups, 0P0-10, 3P0-10, 11P0-10 and 22P0-10 have the shortest dormant periods compared with the other size groups (Original group, 10-35  $\mu\text{m}$ , 35-50  $\mu\text{m}$ , 50-2000  $\mu\text{m}$  size groups).
- The rates of heat of hydration are also influenced by the fineness of the cements. The reactivity of the cements is enhanced by the fineness. The rates



of heat evolution of finer cements are greater than the coarser cement groups due to their larger specific surface.

- It is shown that the behavior of the original groups and 10-35  $\mu\text{m}$  groups are similar in heat of hydration and rate of heat evolution graphs due to their close their median particle size seen in their particle size distribution curves.
- Normalizing the clinker content for same size pozzolanic cements and comparing the results with the actual ones of the control groups show the effect of the nucleation, clearly (Fig. 4.34 – 4.38). The effect of the nucleation decreases with increasing average particle sizes of the cement groups.
- The heats of hydration of the control groups are shown to be predicted by normalizing the clinker and gypsum content and using the particle size distributions. But, a similar approach to estimate rate of heat evolution behavior is less successful due to the neglected interactions between the different particle size groups. In addition, this approach can not be applied for the estimation of the occurrence time of the second peak since as seen in Table 4.7, the difference between the actual and estimated values increases with the increasing amount of mineral admixture.

Based on these findings, it can be possible to obtain a specific type of cement arranging the mineral admixture content and particle size distribution without adding any chemical admixture. Not only the heats of hydration, but also the length of the dormant period, the time of occurrence and the values of the peaks seen in rate of heat evolution graph can be changed. Such cements can be used in special environments like hot weather, or cold weather.

## **5.2 Recommendations for Future Studies**

For future studies, the following recommendations can be useful:

- A similar investigation can be performed using different mineral admixtures in order to understand their behavior in interground cements. The mineral admixture used can be a pozzolan or an inert filler material.

- A similar study can be conducted on separately blended cements. A comparison of the results can be useful to detect effects like nucleation.
- Using the same materials and the same levels of replacement, a different (ball) mill can be used to see the differences in the amounts of clinker, trass and gypsum in the sieved cement groups.
- The relationship between early strength and heat of hydration of the interground cements can be investigated. The relation between setting time and heat of hydration can also be investigated.
- Instead of the sonic sifter used, to increase effectiveness and to obtain a better particle size distribution, it is possible to apply different sieving methods like air classifier. Therefore, in coarser samples, the nucleation effect can be ignored.
- In addition to cement groups, clinker, trass and gypsum whose fineness values are similar to those of the cement groups, can be divided into size groups and their rates of reaction with water can be measured. The values obtained from the raw materials and the cement groups can be compared.
- Instead of interground cements, separately-blended cements can be produced and using Bogue's Equations, the clinker compounds can be detected. Investigation of effects of compound composition on heat of hydration can be useful.

## REFERENCES

- ACI E3-01, *Cementitious Materials for Concrete*, USA: American Concrete Institute, 2001.
- Arndt, M., Lipus, K., & Becker, A. (2007, October). Method performance study on heat of hydration determination of cement by heat conduction calorimeter. *The First International Proficiency Testing Conference*, Sinaia, Romania.
- ASTM C 1074, *Standard Practice for Estimating Concrete Strength by the Maturity Method*. ASTM International, 2010.
- ASTM C 1679, *Standard Practice for Measuring Hydration Kinetics of Hydraulic Cementitious Mixtures Using Isothermal Calorimetry*. ASTM International, 2009.
- ASTM C 1702, *Standard Test Method for Measurement of Heat of Hydration of Hydraulic Cementitious Materials Using Isothermal Conduction Calorimetry*. ASTM International, 2009.
- ASTM C 186, *Standard Test Method for Heat of Hydration of Hydraulic Cement*, ASTM International, 2005.
- ASTM C 204, *Standard Test Methods for Fineness of Hydraulic Cement by Air-Permeability Apparatus*. ASTM International, 2011.
- ASTM C 219, *Standard Terminology Relating to Hydraulic Cement*. ASTM International, 2007.
- ASTM C 618, *Standard Specification for Coal Fly Ash and Raw or Calcined Natural Pozzolan for Use in Concrete*. ASTM International, 2012.
- Bentz, D. P. (2010). Blended different fineness cements to engineer the properties of cement-based materials. *Magazine of Concrete Research*, 62, 327-338.
- Bentz, D.P., Barrett, T., De la Varga, I., & Weiss, W.J. (2012). Relating Compressive Strength to Heat Release in Mortars, *Advances in Civil Engineering Materials*, 1 (1), 14 pp.
- Binici, H., Aksoğan, O., Çağatay, I. H., Tokyay, M., & Emsen, E. (2007). The effect of particle size distribution on the properties of blended cements

- incorporating ggbfs and natural pozzolan (np). *Powder Technology*, 177, 140-147.
- Bogue, R. H. (1955). *The chemistry of portland cement*. (2nd ed.). New York: Reinhold Pub. Corp.
- BS EN 196-8, *Methods of testing cement – Part 8: Heat of Hydration – Solution Method*. European Committee for Standardization, 2010.
- BS EN 196-9, *Methods of testing cement – Part 9: Heat of Hydration – Semi Adiabatic Method*. European Committee for Standardization, 2010.
- CEN/TR 196-4, *Methods of testing cement – Part 4: Quantitative determination of constituents*. European Committee for Standardization, 2007.
- Czernin, W. (1962). *Cement chemistry and physics for civil engineers*. (1st ed.). New York: Chemical Pub. Co.
- Cheung, J., Jeknavorian, A., Roberts, L., & Silva D. (2011). Impact of admixtures on the hydration kinetics of Portland cement. *Cement and Concrete Research*, 41, 1289-1309.
- Cyr M., Lawrence, P., & Ringot, E. (2005). Mineral admixtures in mortars: Quantification of the physical effects of inert materials on short-term hydration. *Cement and Concrete Research*, 35, 719-730.
- Cyr M., Lawrence, P., & Ringot, E. (2006). Efficiency of mineral admixtures in mortars: Quantification of the physical and chemical effects of fine admixtures in relation with compressive strength. *Cement and Concrete Research*, 36, 264-277.
- Çavdar, A., & Yetgin, Ş. (2004). Tane inceliğinin traslı çimento özelliklerine etkisi. *Türkiye İnşaat Mühendisliği XVII. Teknik Kongre ve Sergisi*, İstanbul.
- Dhir, R. K. (1986). Pulverized fuel ash. In R. N. Swamy (Ed.), *Cement Replacement Materials* (1st ed.). Surrey University Press.
- Erdem, T. K., Meral, Ç., Tokyay, M., & Erdoğan, T. Y. (2006). Use of perlite as a pozzolanic addition in producing blended cements. *Cement & Concrete Composites*, 29, 13-21.
- Erdoğan, T. Y. (2010). *Beton*. (3rd ed.). Ankara: METU Press Publishing Company.
- Erdoğan, K., Tokyay, M., & Türker, P. (1999). Comparison of intergrinding and separate grinding for the production of natural pozzolan and ggbfs-

- incorporated blended cements. *Cement and Concrete Research*, 29, 743-746.
- Erdođdu, K., Tokyay, M., & Türker, P. (2009). *Traslar ve traslı Çimentolar*. (8th ed., Vol. 1). Ankara: Türkiye Çimento Müstahsilleri Birliđi.
- Gutteridge, W.A., & Dalziel, J.A. (1990). Filler cement: The effect of the secondary component on the hydration of Portland cement Part 2: Fine hydraulic binders. *Cement and Concrete Research*, 20, 853-861.
- Hassett, D.J., & Eyland, K.E. (1997) Heat of hydration of fly ash as a predictive tool. *Fuel*, 76, 807-809.
- Hoşten, Ç., & Avşar, Ç. (1998). Grindability of mixtures of cement and trass. *Cement and Concrete Research*, 28, 1519-1524.
- Irassar, E. F., Violini, D., Rahhal, V. F., Milanesi, C., Trezza, M. A., & Bonavetti, V. L. (2011). Influence of limestone content, gypsum content and fineness on early age properties of portland limestone cement produced by inter-grinding. *Cement & Concrete Composites*, 33, 192-200.
- Kim, G., Lee, E., & Koo, K. (2009). Hydration heat and autogenous shrinkage of high-strength mass concrete. *Journal of Asian Architecture and Building Engineering*, 8, 509-516.
- Kuleli, O. (2009). *Çimento mühendisliđi el kitabı*. (1st ed.). Ankara: Türkiye Çimento Müstahsilleri Birliđi.
- Langan, B. W., Weng, K., & Ward, M. A. (2002). Effect of silica fume and fly ash on heat of hydration of portland cement. *Cement and Concrete Research*, 32, 1045-1051.
- Lawrence, C. D. (2004). Physicochemical and mechanical properties of Portland cements. In P. C. Hewlett (Ed.), *Lea's Chemistry of Cement and Concrete* (4th ed.). Elsevier Science & Technology Books.
- Lawrence, P., Cyr, M., & Ringot, E. (2003). Mineral admixtures in mortars effect of inert materials on short-term hydration. *Cement and Concrete Research*, 33, 1939-1947.
- Lawrence, P., Cyr M., & Ringot, E. (2005). Mineral admixtures in mortars effect of type, amount and fineness of fine constituents on compressive strength. *Cement and Concrete Research*, 35, 1092-1105.

- Lee-Desautels, R. (2005). Theory of van der Waals Forces as Applied to Particulate Materials. *Educational Resources for Particle Technology*. 051Q-Lee.
- Lohtia, R. P., & Joshi, R. C. (1995). Mineral admixtures. In R. V.S. (Ed.), *Concrete Admixtures Handbook Properties, Science, and Technology* (2nd ed.). New Jersey: Noyes Publications.
- Lothenbach, B., Scrivener K., & Hooton R.D. (2011). Supplementary cementitious materials. *Cement and Concrete Research*, 41, 1244-1256.
- Massazza, F. (2004). Pozzolana and pozzolanic cements. In P. C. Hewlett (Ed.), *Lea's Chemistry of Cement and Concrete* (4th ed.). Elsevier Science & Technology Books.
- Mehta, P. K., & Monteiro, P. J. M. (2006). *Concrete microstructure, properties and materials*. (3rd ed.). McGraw-Hill Companies.
- Mostafa, N. Y., & Brown, P. W. (2005). Heat of hydration of high reactive pozzolans in blended cements: Isothermal conduction calorimetry. *Thermochimica Acta*, 435, 162-167.
- Najafi, Z., & Ahangari, K. (2013). The prediction of concrete temperatures during curing using regression and artificial neural network. *Journal of Engineering*, 2013,
- Nanayakkara, S. M. A. (2011). Importance of controlling temperature rise due to heat of hydration in massive concrete elements. *IESL-SSMS Joint International Symposium on Social Management Systems*, Colombo, Sri Lanka.
- Odler, I. (2004). Hydration, setting and hardening of Portland cement. In P. C. Hewlett (Ed.), *Lea's Chemistry of Cement and Concrete* (4th ed.). Elsevier Science & Technology Books.
- Pane, I., & Hansen, W. (2005). Investigation of blended cement hydration by isothermal calorimetry and thermal analysis. *Cement and Concrete Research*, 35, 1155-1164.
- Poppe, A., & Schutter G.D. (2005). Cement hydration in the presence of high filler contents. *Cement and Concrete Research*, 35, 2290-2299.
- Rahhal, V., Bonavetti V., Trusilewicz, L., Pedrajas, C., & Talero, R. (2012). Role of the filler on Portland cement hydration at early ages. *Construction and Building Materials*, 27, 82-90.

- Schindler, A. K. (2004). Prediction of concrete setting. *Rilem International Symposium on Advances in Concrete Through Science And Engineering*, Illinois.
- Scrivener, K., & Nonat, A. (2011). Hydration of cementitious materials, present and future. *Cement and Concrete Research*, 41, 651-665.
- Siler, P., Kratky, J., & De Belie, N. (2012). Isothermal and solution calorimetry to assess the effect of superplasticizers and mineral admixtures on cement hydration. *Thermal Analysis and Calorimetry*, 107, 313-320.
- Snellings, R., Mertens, G., & Elsen, J. (2010). Calorimetric evolution of the early pozzolanic reaction of natural zeolites. *Thermal Analysis and Calorimetry*, 101, 97-105.
- Stojanović, Z., & Marković, S. (2012). Determination of Particle Size Distributions by Laser Diffraction. *Technics – New Materials*, 21, 11-20.
- Sonic Sifter Separator Operation & Set-up Manual*. New Berlin, USA: Advantech, 2001.
- TAM Air Calorimeter Operator's Manual*. New Castle, USA: TA Instruments, 2007.
- TS EN 197-1, *Composition, specifications and conformity criteria for common cements*. European Committee for Standardization, 2011.
- Turanlı, L., Uzal, B., & Bektaş, F. (2005). Effect of large amounts of natural pozzolan addition on properties of blended cements. *Cement and Concrete Research*, 35, 1106-1111.
- Uzal, B., & Turanlı, L. (2003). Studies on blended cements containing a high volume of natural pozzolans. *Cement and Concrete Research*, 33, 1777-1781.
- Wang, J. (2011). Investigation of hydration heat of slag in portland cement environment. *Advanced Materials Research*, 261-263, 431-435.
- Zhang, T., Yu Q., Wei, J., & Zhang, P. (2011). Effects of size fraction on composition and fundamental properties of Portland cement. *Construction and Building Materials*, 25, 3038-3043.
- Zielenkiewicz, W. (2008). Towards classification of calorimeters. *Thermal Analysis and Calorimetry*, 91, 663-671.





## APPENDIX A

### CUMULATIVE PARTICLE SIZE DISTRIBUTIONS OF CEMENTS

The cumulative particle size distributions of OP and pozzolanic cements are shown in Fig. A.1 – A.4.

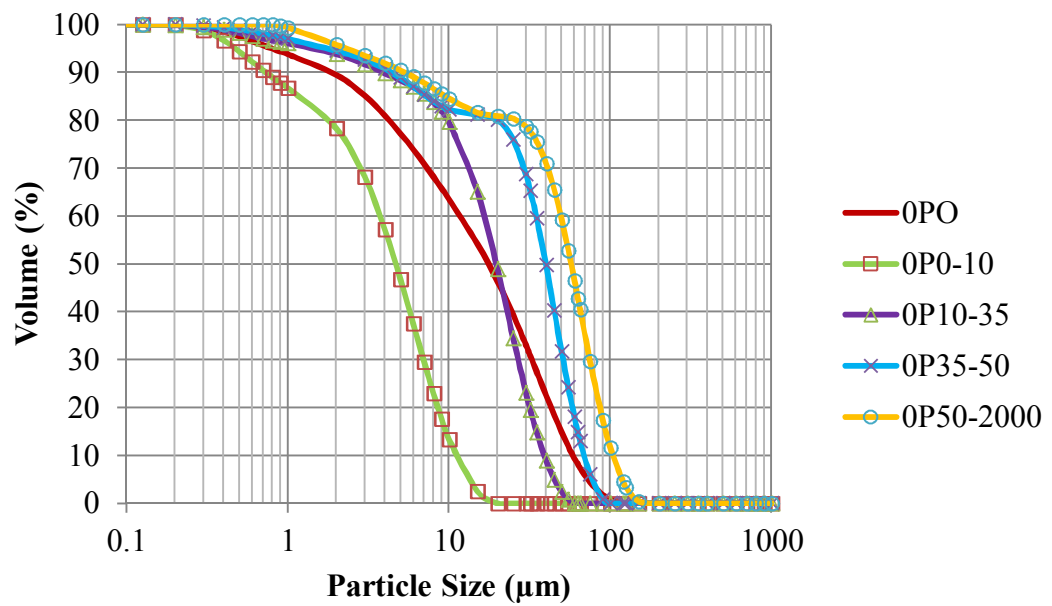


Figure A.1. The cumulative particle size distribution of OP cements.

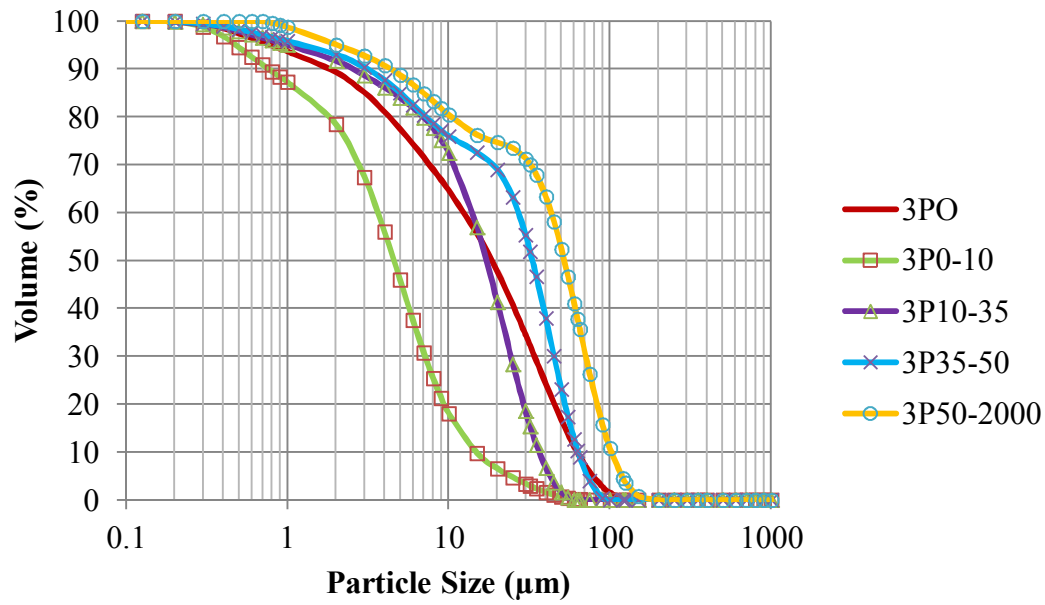


Figure A.2. The cumulative particle size distribution of 3P cements.

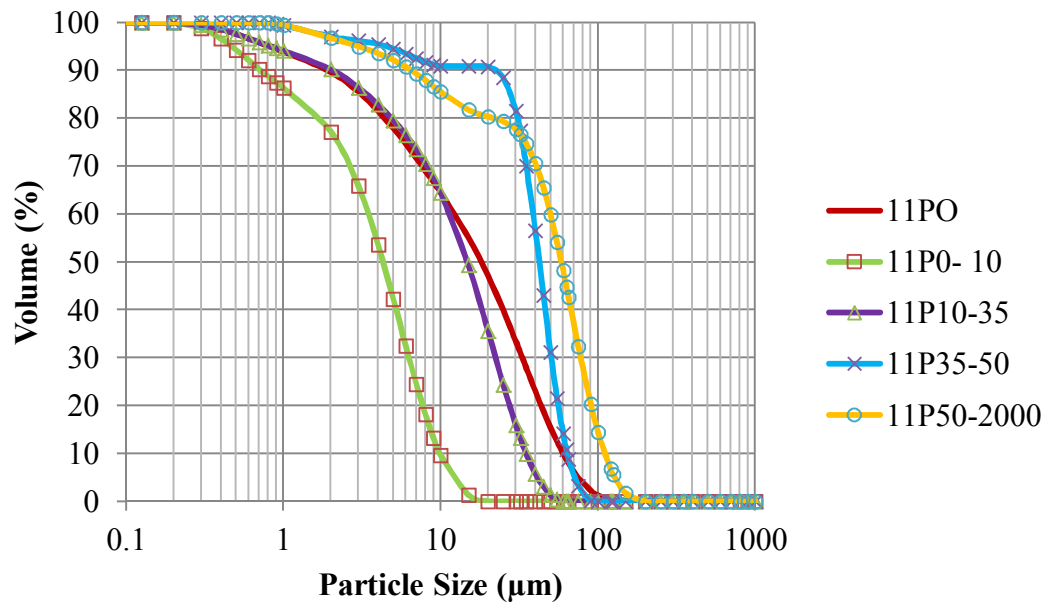


Figure A.3. The cumulative particle size distribution of 11P cements.

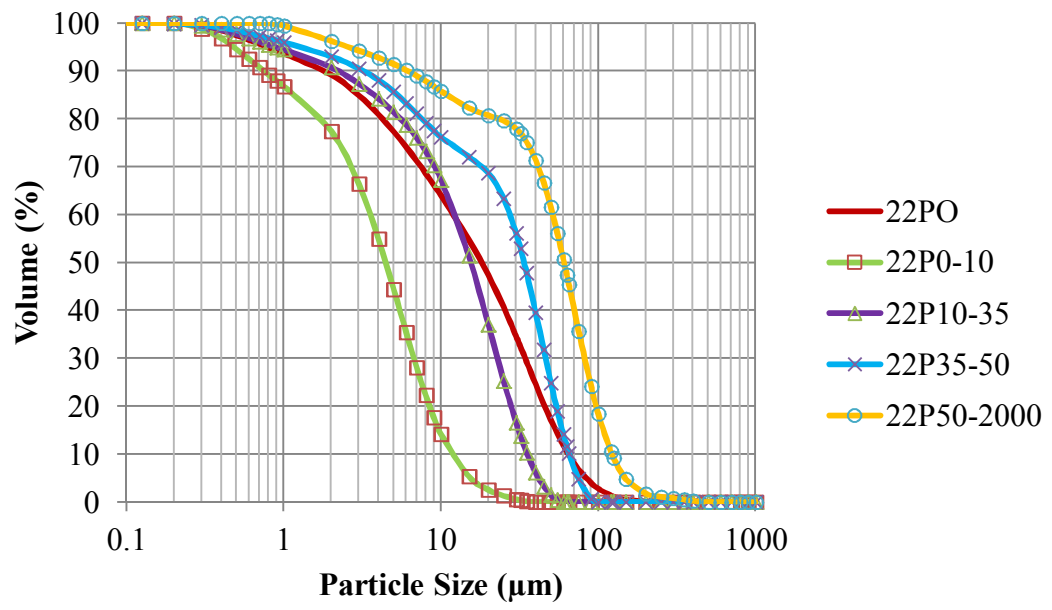


Figure A.4. The cumulative particle size distribution of 22P cements.



## APPENDIX B

### A CALCULATION EXAMPLE ABOUT ESTIMATING THE CONTRIBUTION OF TRASS INCORPORATION ON EARLY HEAT EVOLUTION

The heat of hydration of 3P0-10 at 48 hours is 272.84 J/g (see Table 4.3). The clinker contents of 0P0-10 and 3P0-10 are about 90.68 % and 82.54 %, respectively (see Table 4.1).

$$HH_{ix}normalized = \frac{K_{0Px}}{K_{ix}} HH_{ix}$$

$$HH_{3P0-10}normalized = \frac{90.68}{82.54} \times 272.84$$

$$HH_{3P0-10}normalized = 299.75 J/g$$



## APPENDIX C

### A CALCULATION EXAMPLE ABOUT ESTIMATING THE HEAT EVOLUTION CHARACTERISTICS OF THE ORIGINAL CEMENT FROM THE SIZE GROUPS

The 48-hour hydration heat values of the size groups of 3P and their 24-hour rates of heat evolution are also given in Table C.1. The table also shows the clinker and gypsum contents. The particle size distribution of the original (unsieved) group is shown in Table C.2.

Table C.1. The 48-h heats of hydration, 24-h rates of heat evolution and clinker and gypsum contents observed in 3P cements.

	<b>3PO</b>	<b>3P0-10</b>	<b>3P10-35</b>	<b>3P35-50</b>	<b>3P50-2000</b>
HH <sub>48h</sub> (J/g)	211.63	272.84	207.21	125.52	120.83
RHE <sub>24h</sub> (J/g.h)	4.03	2.80	4.24	2.93	2.36
Clinker content (%)	89.83	82.54	91.42	92.54	89.13
Gypsum content (%)	7.15	13.83	5.36	4.43	6.73

Table C.2. The particle size distribution of 3PO.

	<b>0-10 µm</b>	<b>10-35 µm</b>	<b>35-50 µm</b>	<b>50-2000 µm</b>
3PO (%)	0.35	0.36	0.12	0.17

$$HH_{iO \text{ calculated}} = \sum_{i=1}^4 \frac{K_{io} + G_{io}}{K_{ix} + G_{ix}} \Phi_{ix} HH_{ix}$$

$$HH_{3PO \text{ calculated}}$$

$$\begin{aligned} &= \frac{K_{Group \text{ I O}} + G_{Group \text{ I O}}}{K_{Group \text{ I O-10}} + K_{Group \text{ I O-10}}} \Phi_{Group \text{ I O-10}} HH_{Group \text{ I O-10}} \\ &+ \frac{K_{Group \text{ I O}} + G_{Group \text{ I O}}}{K_{Group \text{ I 10-35}} + K_{Group \text{ I 10-35}}} \Phi_{Group \text{ I 10-35}} HH_{Group \text{ I 10-35}} \\ &+ \frac{K_{Group \text{ I O}} + G_{Group \text{ I O}}}{K_{Group \text{ I 35-50}} + K_{Group \text{ I 35-50}}} \Phi_{Group \text{ I 35-50}} HH_{Group \text{ I 35-50}} \\ &+ \frac{K_{Group \text{ I O}} + G_{Group \text{ I O}}}{K_{Group \text{ I 50-2000}} + K_{Group \text{ I 50-2000}}} \Phi_{Group \text{ I 50-2000}} HH_{Group \text{ I 50-2000}} \end{aligned}$$

$$HH_{3PO \text{ calculated}}$$

$$\begin{aligned} &= \frac{89.83 + 7.15}{82.54 + 13.83} \times 0.35 \times 272.84 + \frac{89.83 + 7.15}{91.42 + 5.36} \times 0.36 \times 207.21 \\ &+ \frac{89.83 + 7.15}{92.54 + 4.43} \times 0.12 \times 125.52 + \frac{89.83 + 7.15}{89.13 + 6.73} \times 0.17 \times 120.83 \end{aligned}$$

$$HH_{3PO \text{ calculated}} = 206.69 \text{ J/g}$$



$$RHE_{iO \text{ calculated}} = \sum_{i=1}^4 \frac{K_{io} + G_{io}}{K_{ix} + G_{ix}} \Phi_{ix} RHE_{ix}$$

$$\begin{aligned} & RHE_{3PO \text{ calculated}} \\ &= \frac{K_{Group I O} + G_{Group I O}}{K_{Group I 0-10} + K_{Group I 0-10}} \Phi_{Group I 0-10} RHE_{Group I 0-10} \\ &+ \frac{K_{Group I O} + G_{Group I O}}{K_{Group I 10-35} + K_{Group I 10-35}} \Phi_{Group I 10-35} RHE_{Group I 10-35} \\ &+ \frac{K_{Group I O} + G_{Group I O}}{K_{Group I 35-50} + K_{Group I 35-50}} \Phi_{Group I 35-50} RHE_{Group I 35-50} \\ &+ \frac{K_{Group I O} + G_{Group I O}}{K_{Group I 50-2000} + K_{Group I 50-2000}} \Phi_{Group I 50-2000} RHE_{Group I 50-2000} \end{aligned}$$

$$\begin{aligned} & RHE_{3PO \text{ calculated}} \\ &= \frac{89.83 + 7.15}{82.54 + 13.83} \times 0.35 \times 2.80 + \frac{89.83 + 7.15}{91.42 + 5.36} \times 0.36 \times 4.24 \\ &+ \frac{89.83 + 7.15}{92.54 + 4.43} \times 0.12 \times 2.93 + \frac{89.83 + 7.15}{89.13 + 6.73} \times 0.17 \times 2.36 \end{aligned}$$

$$RHE_{3PO \text{ calculated}} = 3.282 \text{ J/g.h}$$